Takeru Yanagi

LECTURE NOTES IN EARTH SCIENCES

136 LNES

Arc Volcano of Japan

Generation of Continental Crust from the Mantle

Springer

Lecture Notes in Earth Sciences 136

For further volumes:
http://www.springer.com/series/772

Takeru Yanagi

Arc Volcano of Japan

Generation of Continental Crust from the Mantle

Springer

Takeru Yanagi
Fukuoka
Japan
yanagi.takeru.818@m.kyushu-u.ac.jp

ISSN 0930-0317
ISBN 978-4-431-53995-7 e-ISBN 978-4-431-53996-4
DOI 10.1007/978-4-431-53996-4
Springer Heidelberg Dordrecht London New York

Library of Congress Control Number: 2011933221

Cover design: SPi Publisher Services

Printed on acid-free paper

Springer is part of Springer Science+Business Media (www.springer.com)

Preface

This book presents an analysis of our current knowledge on the origin of the Earth's continental crust. There are two aspects to consider: tectonic and igneous processes. Tectonic aspects include sedimentary accretion, terrane accretion, and continental collision at continental margins, in association with plate subduction. These processes result in the formation of large mountain belts, the building up of which literally grows the continents. However, these tectonic aspects are concerned with material recycling within the crust, and hence do not contribute to volumetric growth of continental crust. Igneous processes concern separation of continental crust from the mantle and result in the volumetric growth of continental crust. Therefore, the main focus of this book is to systematically examine why and how the Earth's continental crust forms, by evaluating magmatic processes at island arcs where new continental crust forms.

Over years of research, it has been discovered that the chemical composition of the upper continental crust provides clues to the mechanism by which the Earth's continental crust develops from the primitive mantle. Although rock configurations are complex, the chemical composition of the upper continental crust has been uniform following the Archean, regardless of which continent or their ages. Through my research, and that of many colleagues, the structure of magma chambers have come to be understood, and we have recognized their functional similarities to island arc volcanoes. This is evident because continental crust is born beneath island arc volcanoes. This book outlines the research directions that have allowed us to reach this conclusion.

Chapters 1–3 constitute an introduction to the topic. Chapter 1 addresses tectonic sites where continental crust forms from the mantle; Chap. 2 presents chemical compositions of both continental crust and the primitive mantle from which continental crust separates; and Chap. 3 is a brief introduction to the history of igneous petrology relevant to genesis of continental crust. Chapters 4–7 present explanations regarding how the origin of continental crust has been elucidated. Chapter 8 shows how the geology and topography of island arcs are related to the formation processes for continental crust.

The construction of a consistent theory on the origin of continental crust is well underway. It is, however, still incomplete. I hope that the research process that is presented in this short book may stimulate future research development in this field. It would give me great pleasure if this is achieved, even just a little.

This book is the English version of one entitled “Island Arc Volcanoes and the Earth’s Continental Crust”, which was written in Japanese and published by Kyushu University Press in 2008. Chapter 9 of the original book is not included here, which described the crust of the Moon and terrestrial planets. In addition, minor changes have been made to this version, and the references updated.

Fukuoka, Japan Takeru Yanagi

Acknowledgments

The main part of this book is a summary of research conducted with my colleagues at Kyushu University from 1971 to 2004. They are I. Hirano, H. Kawano, S. Maeda, S. Hirahara, H. Arikawa, Y. Ichimaru, S. Yamada, M. Ogata, M. Tanaka, H. Matsushita, T. Ishida, J. Sato, T. Nagano, T. Takahashi, H. Mashima, K. Yamashita, T. Ide, H. Matsuyama, T. Sugimoto, T. Myogan, H. Isshiki, Y. Uehara, H. Ishibashi, R. Makiyama, T, Matsushita, R. Aoki, S. Kosono, and S. Goto. K. Ishizaka collaborated with me in constructing the differentiation mechanism for volcanic rocks of the Myoko volcanic group. In this study, K. Hayatsu offered rock samples and geologic maps of the Myoko volcanic group. Many data were compiled from the literature and used for the construction of relevant diagrams. K. Suwa gave me invaluable opportunities and support to study Archean and Proterozoic geology in Africa. R. Hamamoto, S. Nakada, T. Nishiyama, T. Ikeda, and T. Miyamoto assisted me in many ways during the course of my work. E. Abe also helped with drawings and in preparation of drafts throughout my research. I want to express my sincere thanks to all these people. I am also deeply grateful to my wife Misao Yanagi for her understanding and continuing support.

Contents

Chapter 1
Continental Crust and Granitic Plutons

1.1 Growth of Continental Crust

It is well known that the solid Earth is wholly covered by a thin rock layer called the crust. The Earth's crust is made up of two parts. One is oceanic crust and the other is continental crust. Oceanic crust occupies about 60% and continental crust occupies the remaining 40% of the solid Earth's surface. Oceanic crust is generally believed to form at oceanic ridges by cooling and solidification of basaltic magma that forms from mantle convection. However, the origin of continental crust has not yet been clearly elucidated. Today, most researchers have come to think that continental crust has been separated from the mantle throughout the Earth's history. However, there remains a wide range of opinions on the processes of its formation.

When we start thinking about the origin of continental crust, we must first study how it has grown throughout Earth history. Rocks which give the oldest age on Earth are faux-amphibolites and gabbros in the 3.8 Ga Nuvvuagittuq greenstone belt on the eastern shore of Hudson Bay, northern Quebec, Canada. Isotopic analyses of these rocks yielded 4.28 Ga (O'Neil et al. 2008, 2009). This greenstone belt represents a part of ancient mafic crust (O'Neil et al. 2007) trapped within the North American continent. The oldest felsic rock on Earth is the Acasta Gneiss Complex in the Slave craton in the Northwest Territories, Canada. This complex is a fragment of ancient continental crust and has been dated at 4.03 Ga (Bowring and Williams 1999). However, there are much older ages among individual recycled minerals. The oldest measured at present is a zircon grain that has been dated at 4.4 Ga (Wilde et al. 2001). This grain seems to have formed about 100 million years after the birth of the Earth. It is a single crystal grain found among 200 zircon grains that were separated from a 3.0 Ga conglomerate sample collected from the Yilgarn craton, Western Australia. There were a considerable number of zircon grains that had been dated to between 4.3 and 4.1 Ga. They contain much uranium, suggesting they crystallized from granitic magmas rich in potassium. At present, however, there are no such old rock outcrops on Earth. They probably have been completely

T. Yanagi, *Arc Volcano of Japan*, Lecture Notes in Earth Sciences 136,
DOI 10.1007/978-4-431-53996-4_1,

destroyed by heavy meteorite bombardments or were incorporated back into the mantle in association with plate subduction.

Although the occurrence of zircons older than 4.0 Ga is limited to Western Australia, 4.0–3.8 Ga zircons have been reported from North America, East Asia and Antarctica. With regard to ancient rocks, the Itsaq Gneiss Complex on the southern coast of West Greenland has been known for a long time, and was dated at 3.9–3.6 Ga (Nutman et al. 1996; Nutman 2006). During the Archean, continental crust grew at high rates. In particular, the crust that had formed by the end of the Archean (2.5 Ga) is believed by some researchers to exceed half of the present continental crust area (Reymer and Schubert 1986; Abbott et al. 2000). Thus, continental crust appears to have grown with time after the birth of the Earth.

1.2 Orogeny and Continental Crust

If continental crust has grown with time, then the question remains as to from whence it came. There exists a spectrum of arc crust, ranging from the oceanic type of immature arcs to the continental type of mature arcs. This suggests that continental crust has evolved from oceanic crust at island arcs. This idea may be confirmed by examining the crustal evolution of an island arc on an oceanic plate beneath which another oceanic plate subducts. The Aleutian arc has been built on the oceanic part of the North American plate, along the convergent zone from which the Pacific Plate has continuously subducted since about 50 million years ago. Its crust is now 25–30 km thick. However, its P-wave velocity exceeds the velocity profile of average continental crust at any depth, and suggests that the crust is basaltic (Holbrook et al. 1999; Lizarralde et al. 2002).

On the other hand, the Izu-Bonin arc is an island arc that has been built on the Philippine Sea Plate by subduction of the Pacific Plate since about 50 million years ago. Its crust is 20–22 km thick, which is rather thin for its age. However, its P-wave velocity profile clearly indicates the existence of a granitic layer in the middle of the crust (Suehiro et al. 1996). This is an important fact demonstrating the genesis of continental crust at this arc, although neither granitic plutons nor regional metamorphic rocks have yet been found at the surface of this arc.

The Japanese archipelago comprises two arcs, the northeast and southwest Japan arcs. The northeast Japan arc runs in parallel with the Japan Trench along which the Pacific Plate subducts beneath the Eurasian Plate. The southwest Japan arc runs in parallel with the Nankai Trough along which the Philippine Sea Plate subducts beneath the Eurasian Plate. These two arcs have grown along subduction zones formed at the eastern margin of the Eurasian Plate for over about 300 million years. The crust is now 32–35 km thick, and hosting a thick granitic layer (Zhao et al. 1992). Its surface geology contains abundant granitic batholiths, high and low P/T regional metamorphic rocks, and accretionary sedimentary complexes. The volcanism is characterized by extrusion of calc-alkaline volcanic rocks. Thus, we can say that the crust of these arcs has geophysical and geological characteristics that define continental crust.

Since continental crust now seems to be generated at island arcs, the next step is to identify how the island arcs are geologically recorded. We have a geotectonic concept that includes all geological phenomena that occur at subduction zones, such as formation of accretionary complexes, metamorphism, magmatism, tectonic deformation, terrane accretion and continental collision. This concept is collectively called orogeny, because a large mountain belt, such as the Cordillera or Himalayas, forms as a result of the orogeny. Orogenic belts generally have characteristic rock configurations. Accordingly, orogenic belts of the geological past are well recognized even after they have lost their heights through erosion. Through detailed geological surveys, continents have been found to be assemblages of orogenic belts of varied ages. Even the 3.9–3.6 Ga geology of the southern part of West Greenland has been found to be an example of such orogenic belts (Nutman et al. 1996; Komiya et al. 1999). Therefore, orogeny seems to have been acting since a time soon after the birth of the Earth.

Materials that characterize continental crust are granitic plutons, and sedimentary and metamorphic rocks of granitic compositions. I use "granite" here as a generic name for igneous plutonic rock types, mainly made of quartz and feldspars. Granite as a rock species is written herein as granite (in the strict sense). Since sedimentary and metamorphic rocks have their sources in continents, the formation of these rocks has no relation to the growth of continental crust with respect to volume. In other words, these rocks are recycled. By contrast, since granitic plutons and volcanic rocks are originally derived from the mantle, the emplacement of granitic plutons and extrusion of volcanic rocks result in volumetric growth of continental crust. Volcanic rocks are ultimately lost from the land surface by erosion over geologic time. However, granitic plutons progressively become well exposed at the land surface owing to erosion. Accordingly, the global study of exposure areas of granitic plutons of varied ages seems to give us an indication as to how the continental crust has grown throughout Earth's history. Such studies make it clear that the emplacement frequency of granitic plutons of varied ages has not been steady, but instead varied with time, showing peaks and valleys (Condie 1998; Rino et al. 2004). For instance, granitic emplacement in the Japanese Islands occurred only within a few short periods of time, although the growth history has a span of about 300 million years. Granitic emplacement seems to have occurred episodically and repeatedly throughout Earth's history.

1.3 Growth Theory *versus* Steady-State Theory

The fact that all granitic plutons are not derived directly from the mantle makes the problem much more complex. For instance, there are granitic plutons that are included in metamorphic complexes. These plutons were formed under such conditions that rock temperatures exceeded their melting points during regional metamorphism. This extensive rock melting in these cases eventually led to the melts gathering and solidifying to form plutonic rocks. These plutons are similar to

those formed from granitic magmas derived from the mantle. However, granitic plutons of this metamorphic type have nothing to do with growth of continental crust. Therefore, they need to be distinguished from those derived from the mantle. However, the chemical and mineralogical compositions of these two groups are essentially the same. As a result, the problem remained as to how to distinguish these two groups of plutons. The research group at the Massachusetts Institute of Technology first answered this question (Hurley et al. 1962). Their argument is presented below, although through a slightly different proof than the route they followed.

Rubidium comprises two isotopes, ^{85}Rb and ^{87}Rb, of which ^{87}Rb is radioactive and decays to stable ^{87}Sr. Strontium comprises four stable isotopes—^{84}Sr, ^{86}Sr, ^{87}Sr and ^{88}Sr. Accordingly ^{87}Sr/^{86}Sr ratio increases with time depending on the Rb/Sr ratio of a rock. The Rb/Sr ratios of the mantle and of metamorphic rocks of sedimentary origin are about 0.02 and 1, respectively. Therefore, the ^{87}Sr/^{86}Sr ratio of the metamorphic rocks increases at a rate of about 50 times the rate of the mantle. Hence, ^{87}Sr/^{86}Sr ratios are generally much higher in granitic plutons derived from metamorphic rocks than in those derived from the mantle. This is because in most cases, much time has elapsed before the melting occurs in metamorphic rocks. Presently, ^{87}Sr/^{86}Sr ratios in the mantle are known to be 0.702–0.705 based on measurements of young oceanic basalts derived from the mantle. Furthermore, a mantle ^{87}Sr/^{86}Sr ratio at the time of the birth of the Earth has been estimated from ^{87}Sr/^{86}Sr ratios of meteorites. From these data, the ^{87}Sr/^{86}Sr ratio has been found to have increased in the mantle from 0.699 at 4.5 Ga to 0.702 to 0.705 at present. Hurley et al. (1962) analyzed granitic plutons from North America and found that many of them had initial ^{87}Sr/^{86}Sr ratios lying within or close to the evolution band of the ^{87}Sr/^{86}Sr ratio of the mantle. Based on this information, they suggested that the continental crust has grown by accretion of granitic plutons from the mantle.

However, we cannot simply conclude that the continents have progressively grown. The reason is as follows: Hurley and Rand (1969) collected global age data for rocks from the world's continents and found that rocks of younger ages have the tendency to occupy more extensive areas. Based on this evidence, they suggested that the growth rate of continental crust has accelerated with time. However, Armstrong and Hein (1973) and Armstrong (1981) argued that older rocks have been more lost because of exposure to erosion for longer periods of time, and also because of their rapid destruction caused by continental collisions. On the other hand, new crust has continued to be formed in orogenies, resulting in exposure of relatively narrow surface areas for older rocks and wider surface areas for younger rocks. Furthermore, they argued that since sediments have been considered to have been continuously recycled on a global scale into the mantle, in association with plate subduction at a rate of 1–3 km^3 per year, and this rate almost corresponds to the global production rate of arc crust, the total amount of continental crust has probably been constant over time. In addition, they argued that since there were no distinctions in ^{87}Sr/^{86}Sr ratios between granites derived from the primitive mantle and those derived from the hybrid mantle, produced by mixing of subducted

sediments and the depleted mantle, the proof for the derivation of granitic plutons from the mantle using $^{87}Sr/^{86}Sr$ ratios does not always mean growth of continental crust. They concluded that the total volume of continental crust has probably remained constant through most of Earth's history. It is likely that the amount of continental crust has not simply grown, but has been determined by the competition between recycling rate into the mantle, and derivation rate from the mantle.

1.4 Continental Growth and Breakup

A comprehensive view of the topic necessitates an examination of how the present continents are related to the genesis of continental crust. The Indian continent has continued to move northwards since the breakup of Gondwana at 120 Ma, and has finally collided with the Eurasian continent. According to Taira and Tashiro (1987), continental collisions have been recurring for about 300 million years from the Late Paleozoic up to the present, during which time the eastern part of the Eurasian continent has grown to attain its present configuration. The collision of the Indian subcontinent and the Eurasian continent is but just one of such events. That is, the present configuration of the eastern Eurasian continent has been attained by collisions of many arcs and continental masses, and successive accretions of sediments and oceanic plateaux, to the eastern and southern margins of the Siberian craton (Fig. 1.1). This view has now been reconfirmed and developed by Metcalfe (2006, 2009) for the southeastern part of the Asian continent.

The idea of continental growth by terrane accretion was put forth by Coney et al. (1980) through study of the growth history of the Cordilleran orogenic belt in Canada. The Cordilleran mountain belt has grown through accretion of more than 200 terranes to the western margin of the North American continent, in association with plate subduction that started at the end of the Paleozoic. The growth of this mountain chain is not only due to terrane accretion, but also to violent igneous activity. The mountains are represented by the emplacement of batholithic granitic plutons in a belt, which intermittently extends for about 5,500 km from Baja California to Alaska with a width of about 100–300 km. Granitic plutons of the same age range also occur along the eastern margin of the Eurasian continent from southern China to Sikhote Alin.

The growth of continents takes place through sedimentary accretion and continental collisions, in association with oceanic plate subduction. In addition, supercontinents break up into fragmental continents of various sizes and sea water invades the openings growing between them. Examples include the separation of the North American continent from the Eurasian continent at about 170 Ma, the separation of the South American continent from the African continent at about 130 Ma, and the simultaneous opening of the Atlantic Ocean between the North and South American continents and the Eurasian and African continents. The supercontinents so far confirmed are Gondwana, Pangea, and Rodinia. However, it is possible that older supercontinents existed.

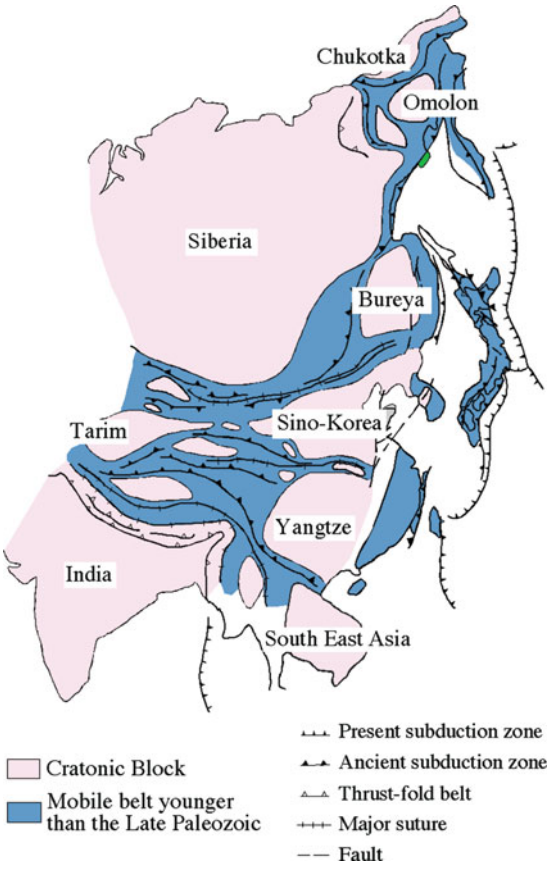

Fig. 1.1 Growth of the East Asian continent since the Late Paleozoic by sedimentary accretion and continental collisions (Modified from Taira and Tashiro (1987))

Since the continents, as discussed above, have experienced repeated growth and breakup through Earth's history, the growth of continents and the growth of continental crust are discriminated in this book. Thus, the growth of continents is defined as growth of individual continents by sedimentary accretion and by collisions of continental masses and island arcs. On the other hand, the growth of continental crust is defined as the growth of the total amount of continental crust on Earth by the accretion of continental materials from the mantle.

References

Abbott D, Sparks D, Herzberg C, Mooney W, Nkishin A, Zhang YS (2000) Quantifying Precambrian crustal extraction: the root is the answer. Tectonophysics 322:163–190

Armstrong RL (1981) Radiogenic isotopes: the case for crustal recycling on a near-steady-state no-continental-growth Earth. Philos Trans R Soc Lond A 301:443–472

Armstrong RL, Hein SM (1973) Computer simulation of Pb and Sr isotope evolution of the Earth's crust and upper mantle. Geochim Cosmochim Acta 37:1–18

Bowring SA, Williams IS (1999) Priscoan (4.00-4.03 Ga) orthogenesis from northwest Canada. Contrib Miner Petrol 134:3–16

Condie KC (1998) Episodic continental growth and supercontinents: a mantle avalanche convection? Earth Plane Sci Lett 163:97–108

Coney PJ, Jones DL, Monger JWH (1980) Cordilleran suspect terranes. Nature 288:329–333

Holbrook WS, Lizarralde D, McGeary S, Bangs N, Diebold J (1999) Structure and composition of the Aleutian island arc and implications for continental crustal growth. Geology 27:31–34

Hurley PM, Rand JR (1969) Pre-drift continental nuclei. Science 164:1229–1242

Hurley PM, Hughes H, Faure G, Fairbairn HW, Pinson WH (1962) Radiogenic strontium-87 model of continental formation. J Geophys Res 67:5315–5334

Komiya T, Maruyama S, Masuda T, Nohda S, Okamoto K (1999) Plate tectonics at 3.8-3.7 Ga; Field evidence from the Isua accretionary complex, West Greenland. J Geol 107:515–554

Lizarralde D, Holbrook WS, McGreary S, Bangs N, Diebold JB (2002) Crustal construction of volcanic arc, wide-angle seismic results from the western Alaska Peninsula. J Geophys Res 107. doi:10.1029/2001JB000230

Metcalfe I (2006) Palaeozoic and Mesozoic tectonic evolution and palaeogeography of East Asian crustal fragments: the Korean Peninsular in context. Gondwana Res 9:24–46

Metcalfe I (2009) Late Palaeozoic and Mesozoic tectonic and palaeogeographical evolution of SE Asia. Geol Soc Spec Pub 315:7–22

Nutman AP (2006) Antiquity of the oceans and continents. Elements 2:223–227

Nutman AP, McGregor VR, Friend CRL, Bennet VC, Kinny PD (1996) The Itsaq Gneiss Complex of southern West Greenland: the world's most extensive record of early crustal evolution (3900-3600 Ma). Precamb Res 78:1–39

O'Neil J, Maurice C, Stevenson RK, Larocque J, Cloquet C, David J, Francis D (2007) The geology of the 3.8 Ga Nuvvuagittuq (Porpoise Cove) greenstone belt, Northeastern Superior Province, Canada. In: Martin J, Kranendonk V, Smithies RH, Bennett VC (eds) Earth's oldest rocks, Condie KC (Series ed) Developments in Precambrian Geology 15, 219–250

O'Neil J, Carlson RW, Francis D, Stevenson RK (2008) Neodymium-142 evidence for Hadean mafic crust. Science 321:1828–1831

O'Neil J, Carlson RW, Francis D, Stevenson RK (2009) Response to comment on "Neodymium-142 evidence for Hadean mafic crust". Science 325:267

Reymer A, Schubert G (1986) Rapid growth of some major segments of continental crust. Geology 14:299–302

Rino S, Komiya T, Windley BF, Katayama I, Motoki A, Hirata T (2004) Major episodic increases of continental crustal growth determined from zircon ages of river sands; implications for mantle overturns in the early Precambrian. Phys Earth Planet Inter 146:369–394

Suehiro K, Takahashi N, Ariie Y, Yokoi Y, Hino R, Shinohara M, Kanazawa T, Hirata N, Tokuyama H, Taira A (1996) Continental crust, crustal underplating, and low-Q upper mantle beneath an oceanic island arc. Science 272:390–392

Taira A, Tashiro M (1987) Late Paleozoic and Mesozoic accretion tectonics in Japan and eastern Asia. In: Taira A, Tashiro M (eds) Hisrtorical biogeography and plate tectonic evolution of Japan and Eastern Asia. Terra Scientific Publishing Company,Tokyo, pp 1–43

Wilde SA, Valley JW, Peck WH, Graham CM (2001) Evidence from detrital zircons for the existence of continental crust and oceans on the Earth 4.4 Gyr ago. Nature 409:175–178

Zhao D, Horiuchi S, Hasegawa A (1992) Seismic velocity structure of the crust beneath the Japan Islands. Tectonophysics 212:289–301

Chapter 2
Chemical Composition of Continental Crust and the Primitive Mantle

2.1 Continental Crust

To study the origin of continental crust, we need to first know its structure and chemical composition, as well as the chemical composition of the primitive mantle that is the source of continental crust.

The Earth's continental crust comprises large continents, such as Eurasia and Africa, and islands with continental crust such as Greenland and New Guinea. This definition also includes mature island arcs, such as the Japanese islands and the Sunda arc, as well as submarine plateaus, such as the Seychelles plateau. The total area of continental crust is 2.1×10^8 km^2, covering 41.2% of the solid Earth's surface (Cogley 1984). Its mass is 2.09×10^{22} kg, corresponding to 0.52% of the mass of the mantle (Taylor and McLennan 1985). Its thickness ranges from 14 to 80 km, averaging 41.1 km (Christensen and Mooney 1995).

Continental crust differs from oceanic crust in origin, chemical composition and structure. Oceanic crust comprises three layers (Raitt 1963). Layer 1 represents a sedimentary cover of the crust. Layer 2 has P-wave velocities from 4.5 to 5.6 km/s, and comprises pillow basalts and underlying sheeted dikes. This layer ranges in thickness from 1.5 to 2 km. Layer 3 represents a gabbroic layer with P-wave velocities from 6.5 to 7.0 km/s. It ranges in thickness from 4.5 to 5.0 km. The boundary between this third layer and the underlying hartzburgite is the Mohorovičić discontinuity, or Moho, which separates the crust from the mantle.

However, based on a characteristic P-wave velocity profile, two to four layers are recognized within the continental crust. The four-layer model of Rudnick and Fountain (1995) is presented here to explain its structure. The first is a surface layer with P-wave velocities of less than 5.7 km/s. It consists mostly of sedimentary and volcanic rocks. The second layer ranges in P-wave velocities from 5.7 to 6.4 km/s, and consists of granitic plutons and low-grade metamorphic rocks. The third layer has P-wave velocities ranging from 6.4 to 7.1 km/s, and is made of gabbroic cumulate with small amounts of intercalated pelitic metamorphic rocks of the granulite facies. P-wave velocities of the fourth layer vary from 7.1 to 7.6 km/s.

T. Yanagi, *Arc Volcano of Japan*, Lecture Notes in Earth Sciences 136,
DOI 10.1007/978-4-431-53996-4_2,

In most cases, this layer is either very thin or missing. Accordingly, in the latter case, the third layer directly lies on the mantle. However, the second and third layers always are present in continental crust. The boundary between these two layers commonly lies at a depth of 20–28 km beneath the surface of shields, platforms, Mesozoic to Cenozoic orogenic belts and mature island arcs. Since clastic sedimentary and metamorphic rocks are, on average, both granitic in composition, the first and second layers together represent the granitic upper crust. The third layer represents the gabbroic lower crust. It ranges in thickness from 9 to 21 km. The granitic layer is seismologically transparent, while the third layer has many parallel reflectors, suggesting stratification of materials of different physical properties.

2.2 Chemical Composition of Continental Crust

Oceanic crust is chemically homogeneous and basaltic (Table 2.1). Accordingly, its bulk chemical composition can be determined rather easily. On the other hand, it is not easy to estimate the bulk chemical composition of continental crust, because it consists of various types of rocks with different compositions. Estimation of the bulk chemical composition of continental crust of today's definition was made first by Poldervaart (1955). Based on both average chemical compositions and seismic velocities of individual different rock types, he determined chemical composition from rock configuration estimated from the seismic velocity structure model of continental crust. His estimation has since been improved with the same approach by Ronov and Yaroshevsky (1969), and recently by Wedepohl (1995) (Tables 2.2–2.4).

Unlike these estimates, average chemical compositions at the surface of the continental crust (Tables 2.2 and 2.3) were determined by analyzing composite samples produced by mixing of rocks collected from intersections of a lattice network laid over different regions in Canada (Fahrig and Eade 1968; Shaw et al. 1986). In China, similar work was conducted by Gao et al. (1998). They collected

Table 2.1 Chemical composition of the oceanic crust

	Taylor and McLennan (1985) (wt.%)	Condie (1997) (wt.%)
SiO_2	49.5	50.5
TiO_2	1.5	1.6
Al_2O_3	16.0	15.3
T.FeO	10.5	10.4
MgO	7.7	7.6
CaO	11.3	11.3
Na_2O	2.8	2.7
K_2O	0.15	0.2
Total	99.5	99.6

T.FeO Total iron as FeO

Table 2.2 Chemical composition of the upper continue crust

	Shields	Ukrainian-Baltic shield	Upper continental crust	Canadian shield surface	Canadian shield surface	Upper continental crust	Upper continenetal crust [a] before restoration	Upper continenetal rust[a] after restoration	Surface of continental crust of Central East China[b]
	Poldervaart (1955)	Ronov and Yaroshevky (1969)	Ronov and Yaroshevky (1969)	Fahrig and Eade (1968)	Shaw et al. (1986)	Taylor and McLennan (1985)	Condie (1993)	Condie (1993)	Gao et al.(1998)
SiO_2	66.4	66.0	65.2	66.1	66.71	66.0	66.86	67.80	67.81
TiO_2	0.6	0.6	0.6	0.5	0.53	0.5	0.64	0.59	0.67
Al_2O_3	15.5	15.3	15.6	16.1	15.03	15.2	15.26	15.11	14.14
Fe_2O_3	1.8	1.9	2.1	1.4	1.40				2.43
FeO	2.8	3.1	2.8	3.1	2.83	4.5	4.90	4.52	3.13
MnO	0.1	0.1	0.1	0.1	0.07	0.1			0.10
MgO	2.0	2.4	2.3	2.2	2.30	2.2	2.26	1.98	2.61
CaO	3.8	3.7	4.7	3.4	4.23	4.2	3.57	3.25	3.43
Na_2O	3.5	3.2	3.1	3.9	3.55	3.9	3.34	3.36	2.85
K_2O	3.3	3.5	3.3	2.9	3.18	3.4	3.01	3.26	2.67
P_2O_5	0.2	0.2	0.2	0.2	0.15		0.14	0.13	0.16
Total	100.0	100.0	100.0	99.9	99.98	100.0	99.98	100.0	100.0

[a] 2.5 ~ 1.8 Ga.(wt. %)

[b] H_2O and CO_2 were eliminated

Table 2.3 Incompatible element composition of the upper continental crust

	Upper continental crust	Surface of Canadian shield	Upper continental crust[a] before restoration	Upper continental crust[a] after restoration	Upper continental crust	Surface of continental crust Central East China[b]
	Taylor and McLennan (1985)	Shaw et al. (1986)	Condie (1993)	Condie (1993)	Wedepohl (1995)	Gao et al. (1998)
Rb (ppm)	112	110	92	99	110	85
Sr (ppm)	350	316	287	280	316	276
Y (ppm)	22	21	30	32	20.7	18
Zr (ppm)	190	237	174	180	237	195
Nb (ppm)	25	26	11.2	12.1	26	12
Cs (ppm)	3.70				5.80	3.67
Ba (ppm)	550	1070	684	700	668	702
La (ppm)	30	32.3	28.8	30.9	32.3	36.0
Pb (ppm)	20	17	17	18	17	19
Th (ppm)	10.7	10.3	9.2	10.4	10.3	9.27
U (ppm)	2.8	2.45	2.40	2.6	2.5	1.61

[a]2.5 ~ 1.8 Ga
[b]H_2O and CO_2 were eliminated

Table 2.4 Compositions of the lower continental crust and bulk composition of the continental crust

	Lower continental crust	Lower continental crust	Continental crust	Continental crust	Continental crust
	Taylor and McLennan (1985) (wt.%)	Rudnick and Fountain (1995) (wt.%)	Taylor and McLennan (1985) (wt.%)	Rudnick and Fountain (1995) (wt.%)	Wedepohl (1995) (wt.%)
SiO_2	54.4	52.3	57.3	59.1	61.5
TiO_2	1.0	0.8	0.9	0.7	0.68
Al_2O_3	16.1	16.6	15.9	15.8	15.1
T.FeO	10.6	8.4	9.1	6.6	6.28
MgO	6.3	7.1	5.3	4.4	3.7
CaO	8.5	9.4	7.4	6.4	5.5
Na_2O	2.8	2.6	3.1	3.2	3.2
K_2O	0.34	0.6	1.1	1.88	2.4
Total	100.04	97.80	100.1	98.08	98.36
Rb (ppm)	5.3	11	32	58	78
Sr (ppm)	230	348	260	325	333
Y (ppm)	19	16	20	20	24
Zr (ppm)	70	68	100	123	203
Nb (ppm)	6	5	11	12	19
Cs (ppm)	0.1	0.3	1.0	2.6	3
Ba (ppm)	150	259	250	390	584
La (ppm)	11	8	16	18	30
Pb (ppm)	4.0	4.2	8.0	12.6	14.8
Th (ppm)	1.06	1.2	3.5	5.6	8.5
U (ppm)	0.28	0.2	0.91	1.42	1.7

Total iron as FeO

rock samples from different sites of individual tectonic regions in China, and then mixed them to form composite samples, which were analyzed to obtain average compositions for the individual different tectonic regions.

Instead of analyzing composite samples, sedimentary rocks can also be measured to estimate average composition of surface layers of continental crust. Elements insoluble to water are generally included in clastic particles, while they are carried by river water from continental source areas to submarine depositional sites. Since the smallest particles are least fractionated during transport, fine sediments such as shale maintain the insoluble-element ratios of the source areas. If La content of a shale sample is 30 ppm, then Th content of the source area is estimated at 10.7 ppm, since La/Th ratio averages 2.8 ± 0.2 at the surface of continental crust. The average value of 3.8 for Th/U ratios at the surface of continental crust yields 2.8 ppm as the U content of the source area. Furthermore, the average value of 1.0×10^4 for K/U ratios gives 2.8% by weight as the K content of the source. Based on this method, Taylor and McLennan (1985) determined average abundances of 62 metal elements in the upper continental crust (Tables 2.2 and 2.3).

In addition to these average abundances of elements, we need to identify the effect of erosion on composition at the surface of the upper continental crust. Condie (1993) noticed that the geological configuration at the surface of the continental crust changes systematically in such a way that the surface area of plutonic rocks increases and exposure of sedimentary rocks decreases with advancing erosion. Thus, it is reported that 5–10 km of erosion at the surface does not significantly affect composition at the surface of the upper continental crust (Tables 2.2 and 2.3).

Because surface geology of the analyzed regions consists mostly of metamorphic rocks and granitic plutons, and the second layer of the seismological model of continental crust is thought to be made of low grade metamorphic rocks and granitic plutons, these reported compositions probably represent bulk composition of the second layer and/or a combination of the first and second layers of the seismological model of continental crust.

Estimation of lower crustal composition is much more difficult. Poldervaart (1955) provided the first estimations, and assigned an average composition of basalts that had seismic velocities corresponding to those of the lower crust. His estimation was improved by Ronov and Yaroshevsky (1969). Unlike these estimates, Taylor and McLennan (1985) used a combination of the average mass ratio between upper and lower crust, and the composition of upper continental crust. Their work was based on the assumption that the bulk composition of continental crust is identical to the average composition of arc andesites (andesite model of Taylor and McLennan 1981). The compositions estimated by Taylor and McLennan (1985) are listed in Table 2.4.

In addition, Rudnick and Fountain (1995) determined the lower crust composition by selecting rocks with seismic properties corresponding to those of the lower crust from rocks produced under physical conditions equivalent to those of the lower crust. There are two types of these corresponding rocks. One consists of

metamorphic rocks of orogenic belts, and the other comprises xenoliths carried by basaltic lavas from depth. Rudnick and Fountain (1995) assumed that granulite-facies rocks in cratons that have isobaric cooling histories might represent the lower crust. They are mostly basaltic in composition, although they have a few pelitic intercalations. In the estimation of lower crustal composition, they combined xenoliths and granulite-facies metamorphic rocks to explain P- and S-wave velocities of the lower crust. Then, they added some pelitic rocks sufficient to explain terrestrial heat flow rates in continental crust. Their estimated composition is listed in Table 2.4.

2.3 Chemical Composition of the Primitive Mantle

The primitive mantle is defined as the mantle before segregation of the crust. Its chemical composition has been estimated from chemical compositions of chondrites, primitive basalts, peridotites from orogenic belts, and peridotite inclusions in basalts. These peridotites are materials that represent the upper mantle. Except for gaseous elements, the average elemental abundances in CI chondrites are identical to those in the chromosphere of the sun. Therefore, the average composition of the CI chondrites has been considered to represent the chemical composition of solar nebulae.

There are two estimation methods, one mainly from peridotites (e.g., Ringwood, 1991; McDonough and Sun, 1995) and the other from chondrites (e.g., Anderson 1983; Taylor and McLennan, 1985) Ringwood assumed that the combination of primitive basalts and peridotites might represent the primitive mantle (Ringwood, 1991), and he called it pyrolite. The composition as reported in 1991 is presented in Table 2.5. McDonough and Sun (1995) found that peridotite samples were arranged in a line on rectangular coordinates having axes of two refractory element ratios. Based on these findings, they assumed that the chemical composition of primitive mantle might be estimated by reconstituting the peridotite compositions so as to have the same refractory element ratios as those of the chondrites. The titanium abundance in the primitive mantle, for instance, was estimated at 1,200 ppm by extrapolating the linear array of peridotite samples on the coordinates, until the ratio of the linear array became the average value of chondrites. The coordinates had axes of titanium abundance and a refractory element ratio, such as Sc/Yb, Ca/Yb and Sm/Yb. As estimated by the same method, the abundance of any refractory element in the primitive mantle was found to be 2.75 times the abundance of the element in the chondrites. This fact made it possible to estimate abundances of volatile elements in the primitive mantle using various element ratios of the mantle. For instance, since uranium abundance in CI chondrites was 7.4 ppb, the uranium content of the primitive mantle was estimated at 20.3 ppb by multiplying its abundance in the chondrites by 2.75. The U/K ratio of 1.2×10^4 of the mantle gave 240 ppm of potassium content, and the K/Rb ratio of 400 of the mantle yielded 0.6 ppm of the rubidium content of the primitive mantle. Since strontium is a

Table 2.5 Primitive and depleted mantle compositions

	Primitive mantle	Primitive mantle	Primitive mantle	Primitive mantle	Depleted mantle
	Anderson (1983) (wt.%)	Taylor and McLennan (1985) (wt.%)	Ringwood (1991) (wt.%)	McDonough and Sun (1995) (wt.%)	Condie (1997) (wt.%)
SiO_2	49.3	49.90	44.78	45.0	43.6
TiO_2	0.21	0.16	0.21	0.201	0.134
Al_2O_3	3.93	3.64	4.46	4.45	1.18
FeO	7.86	8.0	8.40	8.05	8.22
MgO	34.97	35.1	37.22	37.8	45.2
CaO	3.17	2.89	3.60	3.55	1.13
Na_2O	0.27	0.34	0.34	0.36	0.02
K_2O	0.018	0.02	0.029	0.029	0.008
Total	99.73	100.05	99.04	99.44	99.49
Rb (ppm)	0.39	0.55	0.635	0.60	0.12
Sr (ppm)	16.2	17.8	21.05	19.9	13.8
Y (ppm)	3.26	3.4	4.55	4.30	2.7
Zr (ppm)	13	8.3	11.22	10.5	9.4
Nb (ppm)	0.97	0.56	0.713	0.658	0.33
Cs (ppb)	20	18	33	21	
Ba (ppb)	5220	5100	6989	6600	
La (ppb)	570	551	708	648	330
Pb (ppb)	120	120	185	150	
Th (ppb)	76.5	64	84.1	79.5	18
U (ppb)	19.6	18	21	20.3	3

refractory element, the combination of 7.25 ppm of strontium content of CI chondrites and of 0.03 of the Rb/Sr ratio of the mantle again gave 0.6 ppm for rubidium content of the primitive mantle. Furthermore, since barium also is a refractory element, the combination of 2,410 ppb of barium content of CI chondrites and of 11 for the Ba/Rb ratio of the mantle yielded 0.6 ppm for rubidium content of the primitive mantle, indicating that all these estimates were internally consistent. The primitive mantle composition estimated in this manner by McDonough and Sun (1995) is listed with other estimates in Table 2.5.

2.4 Mass of Primitive Mantle Necessary for Formation of Continental Crust

As already stated, the Earth's continental crust has a two-layer structure and is chemically characterized by the composition of the upper crust. Herein, the amount of primitive mantle necessary to form the present total mass of the upper crust is estimated based on its chemical composition and the composition of the primitive

mantle. For this purpose, we will adopt the composition estimated by Taylor and McLennan (1985) for the upper continental crust, and the composition estimated by McDonough and Sun (1995) for the primitive mantle. Potassium, rubidium, cesium, lead, thorium, and uranium are concentrated in the upper continental crust by 118, 187, 176, 133, 135, and 138 times those contents of the primitive mantle, respectively. We may adopt 150 times as a rough enrichment ratio by taking the median. Since all these elements now in the upper continental crust were originally contained in the primitive mantle, this enrichment ratio gives a minimum amount of primitive mantle necessary to produce the present mass of the upper continental crust. If the upper 20 km of the continental crust of an area of 2.1×10^8 km^2 is assumed to approximately represent a total amount of the present upper continental crust, then the minimum amount necessary to produce it may amount to a volume corresponding to a ~1,600 km-thick primitive mantle. The mass of mantle from which continental crust is segregated is called the depleted mantle (see Condie (1997) in Table 2.5 for chemistry). Thus, this estimation indicates that the present amount of this depleted mantle is enormous.

Next, let us estimate the amount of primitive mantle necessary for formation of upper continental crust for the Japanese Islands. For this purpose, we assume that the upper continental crust is 15 km thick. It is a little less than half of the 32–35 km-thick crust of the Japanese Islands. Then, an amount of the primitive mantle reaching to a depth of nearly 2,900 km beneath the Japan arcs is necessary to make this much upper crust. In general, a subducting oceanic plate separates the mantle prism from the lower thick mantle beneath an island arc. In the case of the Northeast Japan arc, for instance, the volume of such a prism beneath the arc is about 1/24 times the necessary amount, and thus it is too small. Even if some portion of the crust is assumed to have formed from sediments carried from the nearby Eurasian continent, an enormous amount of the primitive mantle must have been utilized to form the arc crust. To achieve this amount in the prism beneath the arc, convection could not be avoided in the prism. The incompatible-element enrichment ratios indicate that a large material exchange has taken place between the prism beneath the arc and the adjacent exterior large mantle via this convection. In other words, a great amount of the primitive mantle material must have flowed into the prism, and almost the same amount of depleted mantle material has flowed out from the prism.

References

Anderson DL (1983) Chemical composition of the mantle. J Geophys Res 88:B41–B52

Christensen NI, Mooney WD (1995) Seismic velocity structure and composition of the continental crust: a global view. J Geophys Res 100(B7):9761–9788

Cogley JG (1984) Continental margins and the extent and number of the continents. Rev Geophys Space Phys 22:101–122

Condie KC (1993) Chemical composition and evolution of the upper continental crust: contrasting results from surface samples and shales. Chem Geol 104:1–37

Condie KC (1997) Plate tectonics and crustal evolution. Butterworth-Heinemann, Boston, 282 p
Fahrig WF, Eade KE (1968) The chemical evolution of the Canadian shield. Can J Earth Sci 5:1247–1252
Gao S, Luo T-C, Zhang B-R, Zhang H-F, Han YW, Zhao Z-D, Hu Y-K (1998) Chemical composition of the continental crust as revealed by studies in East China. Geochim Cosmochim Acta 62:1959–1975
McDonough WF, Sun S-s (1995) The composition of the Earth. Chemical Geol 120:223–253
Poldervaart A (1955) Chemistry of the earth's crust. Geol Soc Am Spec Paper 62:119–144
Raitt RW (1963) The crustal rocks. In: Hill MN (ed) The sea, vol 3. Wiley-Interscience, New York, pp 85–102
Ringwood AE (1991) Phase transformations and their bearing on the constitution and dynamics of the mantle. Geochim Cosmochim Acta 55:2083–2110
Ronov AB, Yaroshevsky AA (1969) Chemical composition of the Earth's crust. In: Hart PJ (ed) The earth's crust and upper mantle, geophysical monograph, vol 13. American Geophysical Union, Washington, DC, pp 37–57
Rudnick RL, Fountain DM (1995) Nature and composition of the continental crust: a lower crustal perspective. Rev Geophys 33:267–309
Shaw DM, Cramer JJ, Higgins MD, Truscott MG (1986) Composition of the Canadian Precambrian shield and the continental crust of the earth. In: Dawson JB, Carswell DA, Hall J, Wedepohl KH (eds) The nature of the lower continental crust, vol 24, Geological Society Special Publication. Blackwell Scientific Publication, Oxford, pp 275–282
Taylor SR, McLennan SM (1981) The composition and evolution of the continental crust: rare earth element evidence from sedimentary rocks. Philos Trans R Soc Lond A 301:381–399
Taylor SR, McLennan SM (1985) The continental crust: its composition and evolution. Blackwell Scientific Publication, Carlton, 312 p
Wedepohl KH (1995) The composition of the continental crust. Geochim Cosmochim Acta 59:1217–1232

Chapter 3
Origin of Magmas of the Bowen's Series

3.1 Magmas of the Bowen's Series

Here, we examine history to identify how petrological problems related to the origin of continental crust have been studied up to the present day. Granitic plutons are abundant, and are representative rocks that characterize the continental crust. Their chemical compositions are quite different from those of basalts formed in the mantle. The problem of genesis of granitic plutons is the question of how to form a granitic magma from a basaltic magma produced in the mantle. N. L. Bowen of the Geophysical Laboratory at the Carnegie Institution of Washington was the first to engage in study to solve this problem, based on melting experiments. He eagerly and energetically conducted numerous melting experiments to derive rules of crystallization from the experimental data. Then, he selected and organized hypotheses that were discussed at that time, and finally built and proposed a unifying theory in 1928 to explain the genesis of various igneous rocks through crystallization differentiation from a parental basaltic magma (Bowen, 1928).

According to Bowen's theory of the evolution of igneous rocks, a basaltic magma finally becomes a residual magma rich in albite, potassium feldspar and quartz components through crystallization differentiation. These minerals together occupy more than 90% of the volume of granites. If granite is a product produced as a final step by crystallization differentiation, it must have the lowest melting point among various igneous rocks. He showed this with experiments in cooperation with O. F. Tuttle in 1958. Chemical compositions of granites were found to gather at the minimum melting point of the albite-potassium-feldspar-quartz-water system (Tuttle and Bowen 1958). He regarded this fact as important evidence in support of his theory.

However, Tuttle seems to have formed a different opinion (Young 1998). If a granitic magma had developed from a basaltic magma, gabbroic cumulate formed during the crystallization differentiation would have amounted to several tens of times the volume of that of the granite pluton. Nonetheless, such a large mass of gabbroic cumulate had not been found around granitic batholiths anywhere in the

T. Yanagi, *Arc Volcano of Japan*, Lecture Notes in Earth Sciences 136,
DOI 10.1007/978-4-431-53996-4_3,

world. In addition, it was generally assumed that a granitic batholith had pushed aside the country rocks during its emplacement. However, no such tectonic deformation had been found around batholiths. Furthermore, there were cases in which metamorphic rocks had been well heated and then partially melted to form granitic plutons during metamorphism. Therefore, the genesis of granitic plutons from basaltic magmas by crystallization differentiation did not seem to be supported by field surveys. The conflicts presented here caused a serious dispute between N. L. Bowen and H. H. Reed in the mid 1940s.

Bowen's theory had another serious problem, which was pointed out by C. N. Fenner (member of the Geophysical Laboratory of the Carnegie Institution of Washington) in the mid 1920s (Young 1998). One of his opinions is presented here.

Although Bowen claimed that a basaltic magma became enriched in the SiO_2 component during crystallization differentiation, Fenner argued that the basaltic magma became enriched in iron, because the interstitial glass in basalts was brown in color and contained abundant iron. Thus, he obtained a sample of volcanic rocks from the Antarctic Research Expedition, separated the groundmass from the sample and analyzed it to obtain its chemical composition. This sample was found to be poor in SiO_2 (43.2 wt%) and rich in iron, which confirmed the iron-enrichment. In addition, the SiO_2-enrichment presented another problem.

However, L. R. Wager of the University of Reading discovered the differentiated Skaergaard Layered Intrusion on the southeast coast of Greenland. In cooperation with W. A. Deer, he examined it in detail, and found that mineralogical and chemical variations in this intrusion coincided well with those expected from experiments by Bowen and his co-workers. Through detailed description of this intrusion (Wager and Deer 1939), he presented the decisive evidence for crystallization differentiation that was argued by Bowen to be the major mechanism of differentiation of a basaltic magma. It also became very clear that the basaltic magma differentiated not toward SiO_2-enrichment but toward iron-enrichment. After 95% crystallization of the parental basaltic magma of the Skaergaard Layered Intrusion, the magma started increasing in SiO_2 and finally became granophyre. The granophyre so formed was less than 1% in volume of the intrusion.

The whole picture of crystallization differentiation of a basaltic magma was confirmed by this work. However, it did not mean that the problem was solved, because different rock associations, namely gabbro-diorite-granodiorite-granite and basalt-andesite-dacite-rhyolite, were most common and overwhelmingly abundant in continents and mature island arcs. These rock associations evidently represented the SiO_2-enrichment series. Since Bowen was thinking about their origins, there was no other way for him to affirm his theory other than to exclude the Skaergaard Intrusion as an exceptional case.

To further explain the iron-enrichment according to Fenner's opinion, it represents the increase in ratio of total-iron content to MgO content (indicated as T.FeO/MgO herein) of a magma during crystallization differentiation. This evolutionary trend is not only shown by the Skaergaard Intrusion but also by volcanic rocks from volcanic fields, such as Iceland and the Hawaiian Islands. Although these volcanic rocks are now commonly referred to as the tholeiitic series, in this

book I term them the Fenner's series to commemorate their first recognition by Fenner, as noted by Miyashiro (1975). I also recognize a series of igneous rocks characterized by SiO_2-enrichment as the Bowen's series instead of using what is otherwise known as the calc-alkaline series. This terminology acknowledges how the problem was recognized historically. The aim of this book, naturally, is to elucidate the origin of the Bowen's series.

The above mentioned studies by Wager and Deer eventually aroused profound doubt in many researchers' minds regarding whether the origin of igneous rocks of the Bowen's series was truly due to crystallization differentiation. In the midst of this confusion, Osborn (1959) of Pennsylvania State University found that the T.FeO/MgO ratio of magma increased and the SiO_2 content remained almost unchanged during crystallization under a constant bulk composition of the system, and that the SiO_2 content of a magma rapidly increased during crystallization under constant oxygen pressure. The reason is as follows.

The key for understanding this process lies in the redox reactions of iron in magma. As exemplified by a reaction $Fe_2O_3 = 2FeO + 1/2O_2$, an abundance of Fe_2O_3 in magma depends on oxygen fugacity. In a usual case, iron stays mostly as FeO in magma. However, Fe_2O_3 content increases as the oxygen fugacity increases. A high Fe_2O_3 content promotes the crystallization of magnetite ($FeO{\cdot}Fe_2O_3$), and in turn, the crystallization of magnetite promotes enrichment of SiO_2 in the magma, because magnetite is free of SiO_2. In this case, oxygen should be continuously supplied from outside the system to compensate for the loss, and to maintain crystallization of magnetite, since oxygen is consumed during magnetite crystallization. If the oxygen supply continues, then SiO_2 content will continue to increase in the magma. If the supply of oxygen stops, a small amount of magnetite crystallization will rapidly decrease the Fe_2O_3 content of the magma. This suppresses the crystallization of magnetite until Fe_2O_3 is sufficiently concentrated again in the magma by crystallization of large amounts of silicate minerals. During crystallization of these minerals, the SiO_2 content of the magma remains almost unchanged, and the T.FeO/MgO ratio markedly increases. Thus, it is important to know which of the above trends appears dependent on the presence or absence of an oxygen buffer.

According to Osborn, the Fenner's series appears by crystallization differentiation of a basaltic magma in a closed system, and the oxygen fugacity decreases during crystallization differentiation. The Bowen's series, however, appears by crystallization differentiation of the basaltic magma at a constant oxygen fugacity. To confirm this relationship between magma evolution and oxygen fugacity, it became necessary to measure the oxygen fugacity of magmas. Thus, Fudari (1965) melted various volcanic rocks under controlled oxygen fugacities, and obtained the following results.

In the melting experiments of volcanic rocks of the Fenner's series, oxygen fugacity showed a tendency to rise with increase in T.FeO/MgO ratio of the volcanic rocks. This was opposite to what was expected. In the melting experiments of volcanic rocks of the Bowen's series, oxygen fugacity appeared both to rise and fall with increase in SiO_2 content, although a constant oxygen fugacity was

expected. It was certain that oxygen fugacity played some important role in this process. Nonetheless, Osborn's idea was not proven by these melting experiments.

Water appears to play an important role in magmatic differentiation. In melting experiments, Tilley et al. (1964) found that the T.FeO/(T.FeO + MgO) ratio of basaltic rocks of the Fenner's series linearly increased with falling liquidus temperature. This increase was found to be due to crystallization of olivine and clinopyroxene. Subsequently Brown and Schairer (1971) discovered that the liquidus of basalts, andesites, and dacites of the Bowen's series from the West Indies were always higher in temperature than the above liquidus line. This situation was found to be due to enrichment of plagioclase components in these volcanic rocks.

Yoder and Tilley (1962) noticed that the plagioclase enrichment is due to water vapor pressures. The reason is as follows. The melting point of silicate minerals generally falls with increase in water vapor pressure. To an extent, the temperature drop owing to water vapor pressure depends on degree of polymerization of SiO_2 in minerals. The drop is large for minerals having three-dimensional network structures of SiO_2, such as feldspar, and is small for minerals having crystal structures consisting of isolated SiO_2 tetrahedrons, such as olivine. On phase diagrams, the primary crystallization field of the former tends to shrink, and that of the latter tends to expand, with increase in water vapor pressure (Kushiro 1969, 1975). As a result, plagioclase crystallization is delayed and hence the plagioclase component is concentrated in the residual liquid under high water vapor pressures. This suggests an origin for the Bowen's series under high water vapor pressures. Lavas of this series explosively erupt from volcanoes with simultaneous discharge of large amounts of water vapor, and often contain hydrous minerals, such as hornblende. These observations are the evidence used to indicate that magmas of the Bowen's series contain water. However, this does not mean that high water pressure is directly connected to SiO_2-enrichment. This problem will be discussed further in Chap. 7.

While confusion remained unabated, near the end of the 1960s, A. E. Ringwood's group at the Australian National University discussed a mechanism of generation of magmas of the Bowen's series at island arcs by combining their results from melting experiments under high pressures with the newly developed idea of plate subduction. In their experiments, basalt was found to be transformed at pressures over 2.7 GPa into eclogite consisting of garnet and clinopyroxene. The partial melting of eclogite was found to result in formation of SiO_2-rich melts with low T.FeO/MgO ratios, such as basaltic andesites and andesites of the Bowen's series. This is because garnet is rich in iron and poor in SiO_2 (37–42%). Based on these experimental results, Green and Ringwood (1968) proposed that, when an oceanic plate with basaltic crust at its top subducted at a trench into the mantle beneath an island arc, the crust was transformed into an eclogite layer with increasing depth. Then, the eclogite heated and subsequently partially melted to form a melt of basaltic andesite to andesite in composition. This idea seemed to skillfully provide an explanation both for the origin of the volcanic activity and formation of volcanic rocks of the Bowen's series at island arcs. However, there were problems with this reasoning. One was in the idea that the melting occurred in

a seismic zone. It already was well known that if a rock was so hot as to melt, it would gradually flow under differential stresses and hence could not accumulate much strain. In such a case, no earthquake could occur in the subduction zone. Another problem was in the reaction between the SiO_2-rich melt and the mantle material. It was well expected that, since the mantle was rich in olivine, a SiO_2-rich liquid of basaltic andesite or andesite composition might react with the ambient mantle and then might be transformed into a basaltic liquid during ascent from the seismic zone to the surface. Therefore, it was expected that there was no chance for the SiO_2-rich liquid to directly erupt to the surface without chemical modification. Further problems also appeared, and eventually their idea came to be dismissed. Since then, the origin of the Bowen's series has remained unsolved to this day.

3.2 Partial Melting of Mantle Peridotite

Before beginning an examination of magma evolution, it is necessary to discuss experimental results concerning the question of whether magma formed in the mantle is actually basaltic. The answer depends on the SiO_2 content of magma. The magma is basaltic while its SiO_2 content is between 45 and 52 wt%, and andesitic while its SiO_2 content is between 52 and 63 wt%. Kushiro (1968, 1969) conducted high-pressure melting experiments on comparatively simple chemical systems relevant to mantle peridotite and found varied SiO_2 content of melts formed by partial melting depending on confining pressure and water vapor pressure. Then, he confirmed that a basaltic melt having SiO_2 contents between 45 and 52 wt% formed by partial melting of dry peridotite and that SiO_2 content decreased with increase in confining pressure (Hirose and Kushiro 1993).

Although Kushiro had already confirmed that water vapor pressure increased the SiO_2 content of melts, Nicholls and Ringwood (1973) reported that melts formed at depths greater than 30 km were all basaltic even under high water vapor pressures, because the upper limit of SiO_2 content of melts was constrained by olivine in mantle peridotite. Then Kushiro (1990) reconfirmed that the SiO_2 content could attain 56 wt% in melts formed by partial melting from hydrous peridotites at 1.2 GPa. This means that, when conditions are fulfilled, andesitic melts rich in MgO can be formed at shallow depths in the mantle. In general, seismic velocities are slightly slow in the surface layer of the mantle beneath island arcs. This may indicate that a very small amount of andesitic melt can be present in interstices between mineral grains in the surface layer of the mantle beneath arcs, if water is available. However, data so far reported from high-pressure melting experiments clearly indicate that melts formed by partial melting from the mantle at temperatures higher than 1,250°C are all basaltic in composition, independently of water vapor pressures. Such temperatures, for instance, are probably attained at depths greater than 40–50 km beneath the Japan arcs. Accordingly, almost all melts formed in such an arc mantle situation are considered to be basaltic.

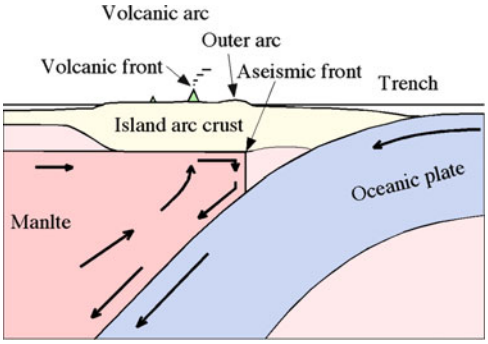

Fig. 3.1 Induced convection in the mantle prism beneath an island arc, caused by continuous subduction of an oceanic plate. *Arrows* show subduction directions of an oceanic plate (*blue color*), and flow directions in the mantle prism. Low-Q and low-V mantle behind the aseismic front is painted in red, and parts of the mantle with normal seismic velocities are painted in pink

It probably is not the case that partial melting occurs in the stationary mantle via heating from an unknown heat source. As already explained in Sect. 2.4 of Chapter 2, the mantle beneath an island arc is most likely convecting, owing to continuous subduction of an oceanic plate. The convection rises from depths of the mantle toward a volcanic front, then arrives at the mantle's surface, and changes its flow direction from vertical to horizontal. At this point, it flows horizontally toward the trench, extends behind the aseismic front, and changes its flow direction again from horizontal to vertical. Then, it descends, meets the subducting plate, goes down in parallel with this subducting plate and finally returns to depths of the mantle (Fig. 3.1).

A high-temperature, fertile mantle material adiabatically rises by being incorporated into this convection cell at depth within the mantle, and then begins to partially melt at a depth shallower than 150 km, which known as adiabatic decompression melting (McKenzie and Bickle 1988; Lee et al. 2009). The melt proportion increases with further ascent, until it reaches to a certain threshold value. After that, small melt grains so formed gather together, and eventually begin to separate from the host material as a mass of magma. Judging from results of high-pressure melting experiments, all such magmas are considered to be basaltic in composition.

Since magmas being formed in the mantle are found to be basaltic, the problem is again to know how andesite lavas, granitic plutons and, finally, continental crust are produced from these basaltic magmas at island arcs. The mechanism of this transformation is presented in Chaps. 4–7.

References

Bowen NL (1928) The evolution of the igneous rocks. Princeton University Press, Princeton, 332 p
Brown GM, Schairer JF (1971) Chemical and melting relations of some calc-alkaline volcanic rocks. Geol Soc Am Mem 130:139–157

Fudari RF (1965) Oxygen fugacities of basaltic and andesitic magma. Geochim Cosmochim Acta 29:1063–1075

Green TH, Ringwood AE (1968) Genesis of the calc-alkaline igneous rock suite. Contrib Miner Petrol 18:105–162

Hirose K, Kushiro I (1993) Partial melting of dry peridotites at high pressures: determination of compositions of melts segregated from peridotite using aggregates of diamond. Earth Planet Sci Lett 114:477–489

Kushiro I (1968) Compositions of magmas formed by partial zone melting of the Earth's upper mantle. J Geophys Res 73:619–634

Kushiro I (1969) The system forsterite-diopside-silica with and without water at high pressures. Am J Sci 267-A Schairer Volume, 269–294

Kushiro I (1975) On the nature of silicate melt and its significance in magma genesis: regularities in the shift of the liquidus boundaries involving olivine, pyroxene, and silica minerals. Am J Sci 275:411–431

Kushiro I (1990) Partial melting of mantle wedge and evolution of island arc crust. J Geophys Res 95:15929–15939

Lee C–T, Luffi P, Plank T, Dalton H, Leeman WP (2009) Constraints on the depths and temperatures of basaltic magma generation on Earth and other terrestrial planets using new thermobarometers for mafic magmas. Earth Planet Sci Lett 279:20–33

McKenzie D, Bickle MJ (1988) The volume and composition of melt generated by extension of the lithosphere. J Petrol 29:625–679

Miyashiro A (1975) Classification characteristics, and origin of ophiolites. J Geol 83:249–281

Nicholls IA, Ringwood AE (1973) Effect of water on olivine stability in tholeiites and the production of silica-saturated magmas in the island-arc environment. J Geol 81:285–300

Osborn EF (1959) Role of oxygen pressure in the crystallization and differentiation of basaltic magma. Am J Sci 257:609–647

Tilley CE, Yoder HS Jr, Schairer JF (1964) New relations on melting of basalts. Carnegie Inst Washington Yb 63:92–97

Tuttle OF, Bowen NL (1958) Origin of granite in the light of experimental studies in the system $NaAlSi_3O_8$-$KAlSi_3O_8$-SiO_2-H_2O. Geol Soc Am Mem 74:153

Wager LR, Deer WA (1939) Geological investigation in East Greenland: Part III, the petrology of the Skaergaard Intrusion, Kangerdluqssaq, East Greenland. Meddeleser om Gronland 105: 1–352

Yoder HS Jr, Tilley CE (1962) Origin of basalt magmas: an experimental study of natural and synthetic rock systems. J Petrol 3:342–532

Young DA (1998) N. L. Bowen and crystallization-differentiation-the evolution of a theory. Miner Soc Am, Monograph 4, 276

Chapter 4
Search for the Formation Mechanism of Continental Crust

4.1 Three Constraints

Once the first stage of separation of continental crust from the mantle was confirmed to be generation of basaltic magma in the mantle, the difficulty was to transform this magma into the granitic upper continental crust. To overcome this difficulty in a non-conventional manner, three new constraints needed to be established, as follows.

1. During both partial melting and crystallization, MgO is largely partitioned into solid silicate phases, and K_2O is mostly partitioned into the co-existing liquid phase. Chemical compositions of the primitive mantle, depleted mantle, primitive mid-ocean ridge basalts (MORBs) and upper continental crust are plotted in Fig. 4.1 to illuminate geochemical relationships among these major units of the silicate Earth in terms of the above two contrasting components.

   MgO contents of primitive MORBs lie within a narrow range of around 10 wt%, although K_2O contents are scattered widely (Fig. 4.1). This narrow distribution of MgO contents indicates the homogeneous nature of the mantle in terms of MgO content, because magmas are thought to be in chemical equilibrium with the ambient mantle during their formation. A compositional variation line of a melt formed by equilibrium partial melting from the primitive mantle also is shown in Fig. 4.1 as a reference, based on a numerical calculation (Ghiorso and Sack 1995). The slope of this reference line is almost constant within a compositional range where K_2O is less than 1 wt%. Observing the distribution of primitive MORBs while shifting this reference line horizontally, the mantle is found to be heterogeneous in terms of K_2O content. This is because primitive and depleted parts are present together in the mantle.

   The most effective mechanism to concentrate an incompatible element into a residual liquid is fractional crystallization. A linear arrangement of residual liquids successively formed by crystallization differentiation from the parental magma of the Skaergaard Intrusion (Fig. 4.1) is a clear example of the liquid line of descent of a primitive basaltic magma (Wager 1960; Wager and Brown 1967).

T. Yanagi, *Arc Volcano of Japan*, Lecture Notes in Earth Sciences 136,
DOI 10.1007/978-4-431-53996-4_4,

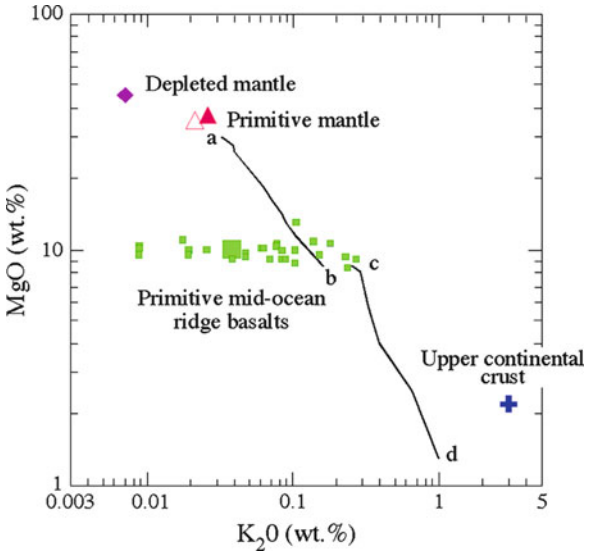

Fig. 4.1 Chemical compositions of the primitive mantle, depleted mantle, upper continental crust and primitive mid-ocean ridge basalts. *Red triangle*, primitive mantle (McDonough and Sun 1995); *red-edge triangle*, primitive mantle (Taylor and McLennan 1985); *violet lozenge*, depleted mantle (Condie 1997); *small yellowish-green square*, primitive mid-ocean ridge basalt (primitive MORB) (Hess 1992); *large yellowish-green square*, average composition of the primitive mid-ocean ridge basalts; *blue cross*, upper continental crust (Taylor and McLennan 1985); *line ab*, variation trend of a melt formed by partial melting of the primitive mantle, which is a result of the numerical calculation using Melts (Ghiorso and Sack 1995); *line cd*, variation trend of residual liquids of the Skaergaard Intrusion (Wager 1960; Wager and Brown 1967)

In other words, this line was traced by the residual liquid during fractional crystallization of the basaltic magma. The differentiation line starts from the K_2O-rich end of the MORB variation range. The upper continental crust is far more enriched in K_2O than this liquid line of descent, suggesting that the composition of the upper continental crust could not form by fractional crystallization even from such K_2O-rich primitive basaltic magma. Since the mantle ranges in composition from primitive to depleted, magma formed in the mantle mostly has a K_2O content less than the K_2O content of the parental magma of the Skaergaard Intrusion. Therefore, it is evident that the composition of the upper continental crust cannot be produced directly by fractional crystallization from primitive magma formed in the mantle. The mechanism to form the upper continental crust from primitive magma should have the power to concentrate K_2O by about 25 times the average K_2O content of the primitive magma, while the MgO content becomes 1/4 of the MgO contents of the primitive magma. More generally, the mechanism should be able to concentrate incompatible elements by more than 20 times the content of the primitive magma without serious depletion of compatible elements. This is the first constraint.

2. In addition, one more component is necessary in the search for the formation mechanism of continental crust. Although plagioclase occupies almost a half the total volume of minerals crystallizing from a basaltic magma, it contains neither MgO nor K_2O. Therefore, it is necessary to understand its crystallization with other elements. Strontium is the most suitable element to use for this purpose, because it is partitioned largely into plagioclase and to a much lesser degree into clinopyroxene. Strontium can enter neither olivine crystals nor orthopyroxene crystals. Plagioclase, clinopyroxene, olivine and orthopyroxene together occupy almost the entire volume of solids crystallizing from basaltic magma in early to middle stages of crystallization differentiation. Strontium is concentrated in a residual liquid during the crystallization of most of these mafic silicate minerals. However, the residual liquid becomes progressively depleted in strontium during the crystallization of plagioclase. When rubidium is used in place of K_2O, plagioclase crystallization results in a marked increase in Rb/Sr ratio of the residual liquid. Hence, plagioclase is the only mineral that can raise the Rb/Sr ratio of the primitive magma by its crystallization.

   Rubidium and strontium contents of the primitive mantle, oceanic crust, depleted mantle, lower continental crust, and upper continental crust are plotted in Fig. 4.2, along with the compositional domain of primitive magma, to reveal geochemical relationships among these major divisions of the solid Earth. Composition of a melt formed by partial melting from the primitive mantle

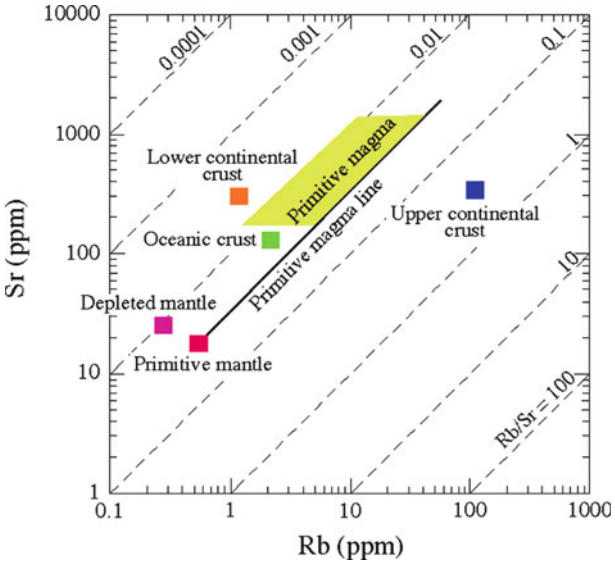

Fig. 4.2 Rb and Sr contents of primitive mantle, depleted mantle (Wänke et al. 1984), oceanic crust, upper continental crust (Taylor and McLennan 1985) and lower continental crust. *Primitive magma line* is a compositional trend of melts produced by partial melting of the primitive mantle under high pressures. *Yellowish-green* area indicates a compositional variation range of primitive magma

changes depending on melting degree along the primitive magma line, as shown in Fig. 4.2. Since both primitive and depleted parts are present together in the mantle, compositions of primitive magma formed in the mantle are distributed in the compositional domain on the left side of the primitive magma line (i.e. yellowish-green area of Fig. 4.2). The Rb/Sr ratio of the upper continental crust is much higher than the Rb/Sr ratio of the primitive magma line. To raise the Rb/Sr ratio from very low levels of the primitive magma to the level of the upper continental crust, plagioclase should crystallize from the primitive magma. Plagioclase crystallization occurs only at low confining pressures ($<$ ca.1.5 GPa). The upper limit of the confining pressure becomes much lower when the magma contains water. Accordingly, the crystallization site becomes shallower, and thus is almost limited to within the crust. This is the second constraint.

3. Reported chemical compositions of the post-Archean upper continental crust, which are listed in Tables 2.2 and 2.3 are almost the same regardless of which continents samples were collected for analyses. Chemical compositions of the upper continental crust neither depend on erosion depth nor on ages of present surface rocks. These facts indicate that the composition of the post-Archean upper continental crust is constant regardless of formation age or geography. This is the third constraint.

   If the major element composition of the upper continental crust matches the chemical composition of the minimum melting point on relevant phase diagrams, then the constancy of the upper continental crust's composition may be well understood. Such a composition has already been found by Tuttle and Bowen (1958), and contains $SiO_2 > 70$ wt%. The upper continental crust contains 66 wt% SiO_2, and differs from the composition of the minimum melting point. Basically, the uniformity not only in major element composition but also in minor element composition of the upper continental crust suggests that it is determined not only by phase relations of relevant minerals but also by the mechanism of crystallization differentiation.

4.2 Advantages of Using Minor Elements

In the following section, the reasons to assume that materials are being exchanged between continental crust and mantle are presented. In addition, it is shown that the chemical composition of continental crust is determined by this exchange. Finally, the rationale for adopting minor elements to disclose this exchange mechanism also is justified.

If there was no return of material from the crust to the mantle, then the crust would be basaltic in chemical composition. However, the reported compositions of continental crust listed in Table 2.4 are by no means basaltic. To form continental crust from basaltic magma, a substance with SiO_2 less than that of basaltic magma should return to the mantle. The same can be said for all major and minor elements. This indicates that some exchange mechanism lies between the mantle and

continental crust. This exchange determines the composition of continental crust. Therefore, to disclose the origin of continental crust is to clarify this exchange mechanism. Since it is already evident that the first stage of this exchange is the supply of basaltic magma to the crust, the problem that should be solved is the mechanism of material return from the crust to the mantle. This mechanism has two aspects. One is a physical aspect that continues the material exchange between crust and mantle, and the other is a chemical aspect that determines composition of the material returning to the mantle. The reasons why minor elements are adopted here to elucidate the mechanism will be presented in the following text.

Of course, it is necessary to prove that the major element composition of the upper continental crust forms from basaltic magma. However, it is very difficult to elucidate the mechanism based on major element compositions, because the major element composition of a liquid is not determined by the mechanism but is determined by liquidus phase relationships of relevant minerals. Therefore, the mechanism will be determined based on minor element compositions of relevant rocks, of primitive magmas and of magma sources such as the primitive and depleted mantles.

In addition, there is the very important fact that incompatible elements are concentrated in the upper continental crust by 120–190 times their contents in the primitive mantle. Therefore, if the major element composition of the upper continental crust is proved to form from basaltic magma through a certain differentiation mechanism, the same differentiation mechanism should simultaneously be shown to have the power to concentrate incompatible elements up to the above levels. If the same mechanism is not proven, any suggested mechanism may not be the actual process by which upper continental crust develops from basaltic magma.

The advantages of utilizing minor elements are the following. The first is that the geochemical behavior of typical incompatible elements during crystallization differentiation is not determined simply by liquidus phase relationships of major relevant minerals, but is by a mass ratio between the residual liquid and the solid that has crystallized. Similarly, in the case of partial melting of the mantle, the geochemical behavior of typical incompatible elements is basically determined by a mass ratio between the melt formed by partial melting and the remaining solid. One such element to illuminate this process is rubidium.

A second advantage is the presence of a minor element partitioned into a specific mineral. Mafic silicate minerals are always involved in magma evolution regardless of crystallization site in the mantle or the crust. Therefore, these minerals are not suitable to use for the search for a differentiation mechanism. The location of crystallization differentiation through which the upper continental crust develops from basaltic magma has already been found to lie at a place where plagioclase can crystallize. Strontium that is preferentially partitioned into plagioclase is therefore the most suitable element to use to focus the search. Therefore, an element pair of rubidium and strontium is utilized here in the search for a differentiation mechanism that transforms basaltic magma into magma with a composition of upper continental crust.

4.3 Partial Melting of the Mantle Beneath Island Arcs

In this section, the differentiation mechanism to produce upper continental crust from the mantle is analyzed by way of theoretical calculations of chemical compositions of relevant magmas. First, chemical compositions of magma being supplied to island arcs are estimated. Minerals remaining after partial melting of mantle peridotite are olivine, orthopyroxene, and clinopyroxene—the last of these being present in only small amounts. The compositional variation of a melt formed in chemical equilibrium with these minerals is shown in Fig. 4.3. Partition coefficients used in the calculation are listed in Table 4.1, and are cited from Yanagi (1975). To begin, I will present the conceptualization we used for estimating the chemical composition of the source mantle beneath island arcs.

Since it is commonly accepted that the upper mantle is a chemically depleted mantle, the upper mantle beneath island arcs must also be depleted mantle.

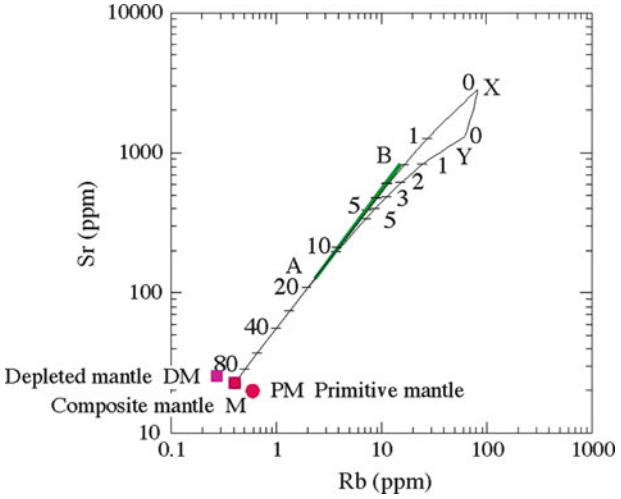

Fig. 4.3 Rb and Sr contents of melts formed by partial melting of the mantle beneath an island arc. *DM* depleted mantle (Wänke et al. 1984), *PM* primitive mantle (McDonough and Sun 1995), *M* harmonic mean of the primitive and depleted mantle; *numerals*, degrees of melting in percent; *green line AB*, range of initial melt compositions from which the following calculations begin (Modified from Yanagi (1975))

Table 4.1 Partition coefficients between phenocrysts and host groundmass

	Olivine	Orthopyroxene	Clinopyroxene	Garnet	Amphibole	Biotite	Plagioclase	Potassium feldspar
Potassium	0.0061	0.013	0.027	0.020	0.31	2.48	0.155	1.49
Rubidium	0.0049	0.0049	0.022	0.009	0.061	2.14	0.051	0.66
Strontium	0.0055	0.018	0.10	0.015	0.17	0.04	1.49	5.82

Cited from Yanagi (1975)

However, igneous activity at island arcs is not as steady as at oceanic ridges, rather it is episodic. Therefore, the igneous activity in these locations seems to be activated by partial melting of enriched mantle materials of high temperatures. Such mantle materials seem to occasionally come to be incorporated in the convection at depths of the mantle prism. The primitive mantle is chemically equivalent to that of an enriched mantle and represents one end member of the chemical variation of the mantle. The depleted mantle represents another end member on the opposite side of the chemical variation of the mantle. Basaltic magma appears to be generated by partial melting not only from the primitive mantle, but also from its surrounding depleted mantle. Point M in Fig. 4.3 represents such a composite composition. Thus, M is a harmonic mean of the primitive mantle (PM: Rb/Sr = 0.0302: McDonough and Sun 1995) and the depleted mantle (DM: Rb/Sr = 0.0106: Wänke et al. 1984). This composite composition of the mantle explains well the abundant occurrence of primitive basalts at island arcs having Rb/Sr ratios of about 0.02.

The curve MX (Fig. 4.3) is a compositional variation line traced by a melt during partial melting of the above source mantle M, where olivine and orthopyroxene remain in chemical equilibrium with the melt. The curve MY is a compositional variation line traced by a melt during partial melting, when clinopyroxene remains as 10% in addition to the above mineral assemblage. Numbers attached to these curves represent melting degrees as percentages.

The strontium content of arc basalts ranges from 150 to 1,500 ppm (Fig. 5.5). This range corresponds to 15–1% melting (Fig. 4.3). However, melting degrees of this range may be somewhat lower than actual, because strontium tends to be concentrated by fractional crystallization of mafic minerals. Such fractionation is expected to occur while magmas stay in chambers beneath the crust. This inference comes from the fact that the strontium content of basalts tends to increase with thickness of the crust. Where the crust is about 20 km thick, strontium content of basalts is about 150–200 ppm. However, where the thickness of the crust reaches about 70 km, it becomes 2,000–3,000 ppm. A thick crust probably increases the difficulty for magma to pass through from the chamber to the surface. This process results in an increase in residence time of the magma beneath the crust. Therefore, the actual melting degree seems to be larger. The strontium content of basalts extruded upon the thin oceanic arc crust is 150–200 ppm. This variation range of strontium contents corresponds to 15–10% melting (Fig. 4.3). This range seems likely to be much closer to the actual situation. In this range of melting degree, the curves MX and MY (Fig. 4.3) overlap one another, and the Rb/Sr ratio of the melt is almost identical with that of point M. Fractional crystallization of mafic silicate minerals, which occurs following melt generation, has insignificant effects on the Rb/Sr ratio of the melt (Fig. 4.4). Based on the above reasoning, straight line AB of Fig. 4.3 is defined as marking the range of initial melt compositions from which the following calculations begin.

4.4 Fractional Crystallization of Magma

The chemical variation of a liquid caused by fractional crystallization is examined here. Melts that have risen through the mantle accumulate first at the base of the crust and then begin to crystallize. There are two types of mineral assemblages of fractionating solids. One is formed by crystallization at rather high pressures, and consists of olivine, clinopyroxene and orthopyroxene. The other is formed by crystallization at low pressures, such as those realized within the crust, and always contains plagioclase together with the above minerals.

Compositional variations of liquids formed by fractional crystallization at high pressures are shown in Fig. 4.4. Line AB shows the range of initial liquid compositions. As an example, liquid compositions formed from an initial liquid O on line AB will be considered. Liquid compositions produced by fractional crystallization of single mineral phases are as follows. Line OC is a compositional variation line traced by the liquid during fractionation of olivine or orthopyroxene. Two variation lines overlap and are indistinguishable. One is traced by a liquid during olivine fractionation and the other is traced by a liquid during orthopyroxene fractionation. Line OD is shown for the case of fractionation of clinopyroxene.

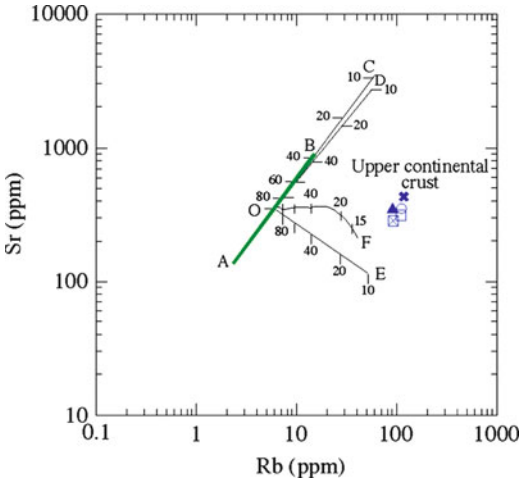

Fig. 4.4 Rb and Sr contents of liquids formed by fractional crystallization from parental liquid O. *Line AB* represents the range in composition of the primitive basaltic liquid. Reported chemical compositions of upper continental crust are indicated by ×, Hurley et al. (1962); *triangle*, Taylor (1965); *circle*, Taylor and McLennan (1985); *square*, Shaw et al. (1986) and *square with* ×, Condie (1993). *Lines OC, OD* and *OE* are compositional variation lines traced by liquids during fractionation of a single mineral of olivine (or orthopyroxene), clinopyroxene, and plagioclase, respectively. *Curve OF* is a compositional variation line traced by a liquid during multi-mineral fractionation and is estimated by tracing the change in partition coefficients caused by both mineralogical variation of a fractionating solid and compositional variation of fractionating plagioclase. *Numerals* represent fractions of residual liquid in percent (Modified from Yanagi (1975))

Since minerals crystallized from a basaltic liquid at high pressures are olivine, orthopyroxene and clinopyroxene, the chemical composition of liquids formed by fractionation of these minerals from the initial liquid O lies within a narrow area between lines OC and OD. Such liquids have Rb/Sr ratios between 0.018 and 0.03. These are much lower than the Rb/Sr ratio of the upper continental crust.

Compositional variations of liquids formed at low pressures are examined next. For cases of single-phase fractionation of olivine, orthopyroxene, and clinopyroxene, the above fractionation lines are again employed. Line OE is a compositional variation line traced by a liquid during plagioclase fractionation. In this case, both partition coefficients for rubidium and strontium between plagioclase and the co-existing liquid are assumed to be constant. The Rb/Sr ratio of the liquid increases rapidly with the advance of fractional crystallization. Since minerals crystallized from the basaltic liquid generally comprise plagioclase together with olivine, clinopyroxene and orthopyroxene, the chemical composition of a liquid formed from the initial liquid O by fractional crystallization under low-pressure conditions must lie in an area between lines OC and OE. The upper continental crust lies in this area. However, we cannot easily judge whether the upper continental crust is indeed formed by low-pressure fractional crystallization, because the above estimated compositional area is too wide. In this case, it is necessary to trace the variation of the liquid composition in detail.

Curve OF (Fig. 4.4) is a compositional variation line traced by a liquid during fractional crystallization of basaltic liquid O. This compositional variation line is estimated by tracing the change in partition coefficients caused by both mineralogical variation of a fractionating solid and compositional variation of fractionating plagioclase. Examination of curve OF reveals that strontium content stays almost constant until the residual liquid proportion becomes 25%. After that, strontium content abruptly drops, well before attainment of the concentration level of rubidium in the upper continental crust. This drop is due to both an increase of plagioclase abundance in the fractionating solid and an increase of the albite component in the fractionating plagioclase. Thus, it is evident that the composition of the upper continental crust can hardly be formed by fractional crystallization at low pressures.

4.5 Partial Melting of Basaltic Crust

Partial melting of the lower part of a thick sequence of basaltic crust is examined here. The melt formed at low pressures is compared in chemical composition with upper continental crust in Fig. 4.5. In this case, plagioclase and clinopyroxene together occupy almost all the partial melting residue. Strontium is partitioned largely into plagioclase, and to a lesser degree into clinopyroxene. Rubidium is partitioned slightly into plagioclase and clinopyroxene. Other minerals such as olivine, orthopyroxene and magnetite are represented in small amounts, but contain neither rubidium nor strontium. Accordingly both melting degree and proportion of plagioclase and clinopyroxene in the residue determine the Rb/Sr ratio of the melt.

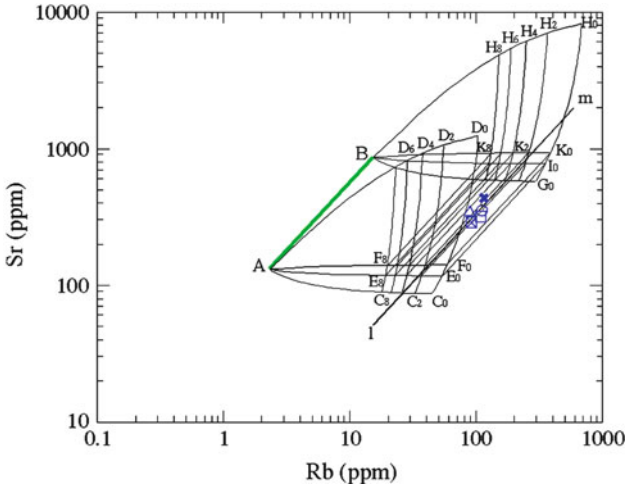

Fig. 4.5 Rb and Sr contents of melts formed by equilibrium partial melting from thick basaltic crust. *Line AB* represents the range in composition of basaltic crust. *Curves* AC_0 (or BG_0) and AD_0 (or BH_0) are compositional variation lines traces by melts during melting of basaltic crust A (or B) when one of plagioclase and clinopyroxene is assumed to remain in the residue, respectively. For *curves* AE_0 (or BI_0) and AF_0 (or BK_0), see text. *Subscript numerals* represent degrees of partial melting in percent. *Curve* C_iD_i (or G_iH_i) represents a compositional variation of the melt at *i*% melting. This variation is caused by variation in plagioclase and clinopyroxene proportions in the melting residue. *Line lm* represents the average Rb/Sr ratio of the upper continental crust. For sources of reported compositions of the upper continental crust (indicated by *blue marks*), see Fig. 4.4 (Modified from Yanagi (1975))

Because what we want to know is whether the process under consideration can produce magma with a Rb/Sr ratio identical to that of the upper continental crust, the other minerals can be ignored.

Line AB (Fig. 4.5) shows the range of compositions of basaltic crust. At first, partial melting of the crust at point A is considered. Curve AC_0 is a compositional variation line traced by a melt during melting when only plagioclase is assumed to remain in the residue. Curve AD_0 is a compositional variation line traced by a melt during melting when only clinopyroxene is assumed to remain in the residue. Points C_n and D_n represent the melt compositions at *n*% melting, and the 0% signifies an infinitely small melting degree. Curve C_0D_0 represents a compositional variation of the melt at 0% melting. This compositional variation is caused by variation in plagioclase and clinopyroxene proportions in the melting residue. Therefore, to obtain a more realistic range of the melt composition, it is necessary to know a probable variation range of the mineral proportion. In estimating this range, the salient point is that the residue and the melting basalt are almost the same in major element composition, while the melting degree is small. Therefore, to estimate proportions of plagioclase and clinopyroxene, the basalt reported by Kuno (1976) from Izu, Japan was adopted as representing primitive basalt composition, and the basalt reported by Yanagi et al. (1991) from Mount Sakurajima was adopted as

representing evolved basalt composition. For the conversion from chemical to mineralogical compositions, the CIPW normative calculation technique was employed. Since rubidium and strontium contents of the melt largely depend on abundance of plagioclase, the adoption of other basalts yields insignificant effects on the following conclusions. Curve AF_0 (Fig. 4.5) is a compositional variation line traced by the melt when mineralogical composition estimated from the Izu basalt is applied to the residue. Curve AE_0 is a compositional variation line traced by the melt when mineralogical composition estimated from the Sakurajima basalt is applied to the residue.

When the composition of basaltic crust changes from point A to B, all the melt compositions realized from point A move in parallel with line AB, keeping their Rb/Sr ratios constant (Fig. 4.5). The change in major element compositions in association with this source change from point A to B may affect the new melt composition by means of changes in ratio between plagioclase and clinopyroxene in the residue. However, since the new melt composition largely depends on the abundance of plagioclase, and in addition, the plagioclase and clinopyroxene ratio do not change so much in association with this source shift from point A to B, the total effects are almost negligible. Subscript numerals in Fig. 4.5 represent melting degrees as a percentage. Parallel lines associated with these letters indicate the melt compositions at equal values of melting degree. The compositions of upper continental crust thus far reported also are shown for comparison. It appears that the mean Rb/Sr ratio of the upper continental crust (Line lm) coincides with Rb/Sr ratio of the melt formed by only a few percent partial melting from basaltic crust. Therefore, as far as rubidium and strontium are concerned, it is evident that the partial melting of basaltic crust can form a melt identical in composition to upper continental crust. However, the melting degree is so small that the melt would not be able to be separated from the host basaltic crust. Equilibrium crystallization of primitive basaltic magma also can produce the same liquid. In this case, the problem remains as to how to separate a very small amount of liquid from the associated cumulate.

4.6 Crystallization Differentiation in a Chamber That Is Continuously Supplied with Primitive Magma

Magmatic differentiation caused by crystallization in a chamber that is continuously but very slowly supplied with primitive magma is examined next. Yanagi (1975) first examined this type of differentiation. The chamber in which crystallization continues is assumed to lie at the base of the crust. It also is assumed that upwelling flow in the mantle continuously carries the parental magma of primitive composition into the chamber on the one hand, and on the other, removes cumulate away from the chamber (Fig. 3.1).

What happens with respect to rubidium content in the magma chamber is discussed first. Since rubidium is carried into the chamber along with a supply of parental magma and is concentrated in the magma by crystallization in the chamber, it is progressively concentrated in the magma as long as the supply of parental magma continues. Contrastingly, rubidium is partitioned into the cumulate formed in the chamber as much as the amount determined by its partition coefficient and its concentration in the magma. Accordingly rubidium partitioned into the cumulate proportionally increases with increase in its concentration in the magma. Finally, the amount of rubidium brought into the chamber by supply of parental magma becomes equal to the amount carried away from the chamber by removal of the cumulate, at which point steady state of rubidium concentration is achieved in the chamber. Rubidium concentration in the magma under steady state conditions is determined by its concentration in the parental magma and its partition coefficient between magma and cumulate. The amount of parental magma necessary to achieve steady-state concentration depends on magnitude of the partition coefficient. The smaller the partition coefficient, the greater the necessary amount of parental magma. Therefore, an increase in concentration of an incompatible element in the magma in the chamber continues even after the steady-state concentration of a compatible element is attained, and until the steady-state concentration of the incompatible element is reached. In other words, the incompatible element concentration increases without a decrease in compatible element concentration after attainment of its steady state concentration, since the compatible element concentration remains constant after this point.

Results of the calculation are shown in Fig. 4.6. Line AB indicates the range in parental magma compositions. Magma compositions formed from the parental magma at point A are discussed first.

Minerals crystallized under dry conditions are olivine, orthopyroxene, clinopyroxene, plagioclase, and magnetite. They are composed of amphibole when the parental magma contains water, even though the water content is very small, because water becomes concentrated in the magma in the chamber. Therefore, the effects of amphibole crystallization also are examined. Our interest lies in the increase of Rb/Sr ratio of the magma in the chamber. Minerals that yield effects on the Rb/Sr ratio are plagioclase and clinopyroxene under dry conditions. However, in water-saturated conditions the important minerals are plagioclase and amphibole. Other minerals are minor in amount and have insignificantly small partition coefficients of rubidium and strontium. Therefore, crystallization of these minerals may be neglected.

Curve AC^1 (Fig. 4.6) is a compositional variation line traced by magma in the chamber while the parental magma at point A is continuously supplied to the chamber where, simultaneously, only plagioclase continues to crystallize. Curve AD^1 is for a case in which only clinopyroxene continues to crystallize, and curve AE^1 is for a case in which only amphibole continues to crystallize in the chamber. Points C^1, D^1, and E^1 represent magma compositions at steady-state concentrations of rubidium and strontium.

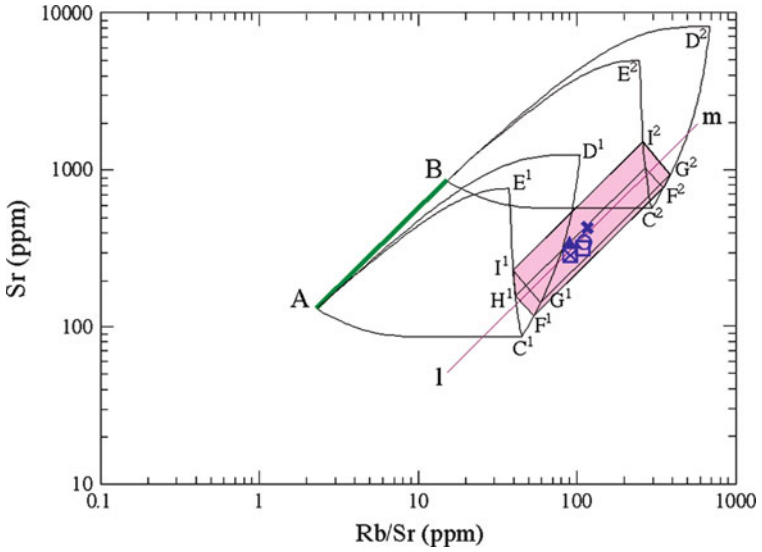

Fig. 4.6 Rb and Sr contents in magma in a chamber which is slowly and continuously supplied with parental magma, and from which cumulate is continuously removed. *Line AB* represents the range in composition of the parental magma. *Curves* AC^1 (or BC^2), AD^1 (or BD^2) and AE^1 (or BE^2) are compositional variation lines traces by magma in the chamber while the parental magma at point A (or B) is continuously supplied to the chamber where, simultaneously, only one phase of plagioclase, clinopyroxene and hornblende continues to crystallize, respectively. *Points* C^1 (C^2), D^1 (D^2) and E^1 (E^2) represent magma compositions at steady state. *Curve* C^1D^1, for instance, represents variation in composition of magma in the chamber at steady state. This variation is caused by variation in plagioclase and clinopyroxene proportions in the fractionating solid. For other points such as F^1, G^1, H^1 and I^1, see text. *Pink area* $F^1H^1I^1I^2G^2F^2F^1$ represents a range of the magma composition formed at steady state from the parental magma on line AB. *Line lm* represents the average Rb/Sr ratio of the upper continental crust. For sources of reported compositions of the upper continental crust (indicated by *blue marks*), see Fig. 4.4 (Modified from Yanagi (1975))

Henceforth, we examine magma compositions at steady-state concentrations. Curves C^1D^1 and C^1E^1 are compositional variation lines traced by the magma while the mineralogical composition of the cumulate varies along the plagioclase-clinopyroxene pair, and plagioclase-amphibole pair, respectively. Points G^1 and I^1 indicate steady-state magma compositions for cases in which mineralogical compositions of the cumulate are identical to those estimated from the Izu basalt, and points F^1 and H^1 indicate steady-state magma compositions for cases in which mineralogical compositions of the cumulate are identical to those estimated from the Sakurajima basalt. When estimating mineralogical compositions of cumulates, it should be remembered that major element compositions of parental magma and cumulates are the same under steady-state conditions. The amount of amphibole is estimated from amounts of actinolite and pargasite calculated from normative olivine, wollastonite, orthopyroxene and plagioclase, until olivine and pyroxenes are used up. Since, in general, crystallization condition is expected to range from

dry to water-oversaturated, the magma composition formed from the parental magma at point A lies within the area $F^1H^1I^1G^1F^1$.

When parental magma composition changes from point A to point B, the magma compositions formed from the parental magma at point B are given by the parallel displacement of the compositions reached from the parental magma at point A along line AB, as shown in Fig. 4.6. During displacement in parallel with line AB, all Rb/Sr ratios are kept constant. Superscript 2 attached to the letters in Fig. 4.6 indicates the parental magma composition at point B. Effects that derive from the difference in major element composition between the parental magmas at points A and B are examined later in this section.

In conclusion, the magma composition formed from the parental magma on line AB lies within the area $F^1H^1I^1I^2G^2F^2F^1$. Upper continental crust compositions so far reported are found to lie at the center of this area. The line lm of the average Rb/Sr ratio of the upper continental crust passes through the center of this area. This fact signifies that a magma of the composition of upper continental crust forms by crystallization differentiation in the chamber that is continuously supplied with parental magma of primitive composition.

Figure 4.7 illustrates an example for rubidium and potassium compositions. Line AB indicates the compositional range of the parental magma. When the chamber is continuously supplied with parental magma of point A, and only plagioclase continues to crystallize, the magma composition in the chamber changes from point A to point Pl^1 along line APl^1. Point Pl^1 represents the composition at steady-state concentrations of rubidium and potassium. Points Px^1 and Hb^1 represent steady-state compositions attained when only one phase of clinopyroxene and hornblende continues to crystallize, respectively. Points C^1 and E^1 also represent steady-state compositions for cases where mineralogical compositions of the cumulate crystallizing in the chamber are given by those estimated from the Izu basalt. Conversely points D^1 and F^1 represent steady-state compositions for cases where mineralogical compositions of the cumulate are given by those estimated from the Sakurajima basalt. Superscript 2 attached to the letters in Fig. 4.7 indicates the parental magma at point B. Therefore, steady-state composition achieved from the range of parental magmas on line AB is shown within the area $C^1D^1F^1E^1E^2C^2C^1$. All compositions of the upper continental crust thus far reported concentrate at the center of this area.

Rubidium is one of the typical incompatible elements characterized by its very small partition coefficients. Accordingly, a great amount of the parental magma is necessary to attain its steady-state concentration. Since its partition coefficients for plagioclase, clinopyroxene, and hornblende lie around 0.05, the amount necessary to attain steady-state concentration is more than 30 times the mass of the chamber.

Although they are both basaltic, the parental magmas at points A and B differ slightly in major element composition. Accordingly, we next examine its effects on steady-state magma compositions.

It has been postulated that the Rb/Sr ratio is constant over the whole range of the parental magma. However, as it is evident from lines OX and OY in Fig. 4.3 that the Rb/Sr ratio slightly increases with increase in strontium content, when the magma

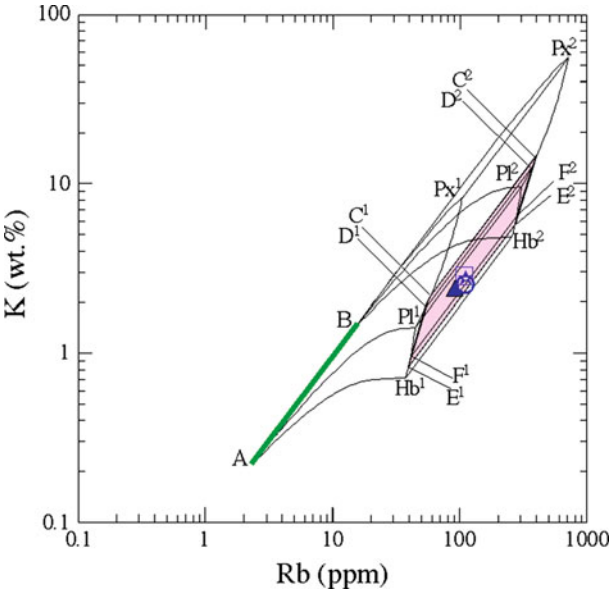

Fig. 4.7 K and Rb contents in magma in a chamber which is slowly and continuously supplied with parental magma, and from which cumulate is continuously removed. *Line AB* represents the range in composition of the parental magma. *Curves* APl^1 (or BPl^2), APx^1 (or BPx^2) and AHb^1 (or BHb^2) are compositional variation lines traces by magma in the chamber while the parental magma at point A (or B) is continuously supplied to the chamber where, simultaneously, only one phase of plagioclase, clinopyroxene and hornblende continues to crystallize, respectively. *Points* Pl^1 (Pl^2), Px^1 (Px^2) and Hb^1 (Hb^2) represent magma compositions at steady state. *Curve* Pl^1Px^1, for instance, represents variation in composition of magma in the chamber at steady state. This variation is caused by variation in plagioclase and clinopyroxene proportions in the fractionating solid. For points C^1 (C^2), D^1 (D^2), E^1 (E^2), and F^1 (F^2), see text. *Pink area* $C^1D^1F^1E^1E^2C^2C^1$ represents a range in composition of magma formed at steady state from the parental magma on line AB. Reported chemical compositions of upper continental crust are indicated by *circle*, Shaw et al. (1986); *star*, Taylor and McLennan (1985); *triangle*, Condie (1993); and *square*, Wedepohl (1995) (Modified from Yanagi (1975))

forms in the mantle. This trend also is found in primitive basalts from Japan (Fig. 5.5). The primitive basalts with higher strontium contents tend to have slightly higher Rb/Sr ratios.

The parental magma at point A has low strontium content and is classified as low-alkali tholeiitic basalt based on its major element composition. The parental magma at point B has a high strontium content and is classified as olivine basalt based on its major element composition. The latter is slightly richer in potassium. Accordingly when the parental magma at point B is continuously supplied to the chamber, the magma therein may reach a value of about 10% potassium (as in cases at points C^2 and D^2 in Fig. 4.7) during its crystallization differentiation. In reality, however, biotite and/or alkali feldspar start crystallizing before attainment of this level of potassium concentration. As a result, the Rb/Sr ratio of the magma at steady

state concentration of rubidium falls, because rubidium is highly partitioned into these potassium-rich minerals.

The potassium content of the parental magma is low at point A and increases, together with strontium content, because potassium behaves similarly to rubidium during magma generation in the mantle. Therefore, magma in the chamber starts crystallization of potassium-rich minerals earlier as the parental magma composition becomes closer to point B, because the magma closer to point B is richer in potassium. At the same time, the amount of potassium-rich minerals crystallized from the magma becomes greater. As a result, the Rb/Sr ratio at steady-state concentration of rubidium is lowered, since crystallization of potassium-rich minerals reduces the rubidium content of the magma in the chamber. However, since the parental magma closer to point B originally had a slightly higher Rb/Sr ratio, these two effects offset one another. Thus, no significant variation occurs in Rb/Sr ratio at steady-state concentration of rubidium. The Rb/Sr ratio at the steady state condition is kept almost constant independently of the strontium content of the parental magma.

4.7 Removal of Cumulate into the Mantle

Crystallization differentiation in a chamber that is continuously supplied with parental magma has emerged as the most likely mechanism to produce the known chemical composition of the upper continental crust. The problem is the disposal of a great amount of cumulate, at least, more than 30 times the chamber mass, which should be removed from the chamber into the mantle. A problem that arises from this process will be presented by examining a case from the Japan arcs.

The upper half of the present crust of the Japan arcs, which is about 15 km thick, almost represents the upper crust. If this upper crust is formed by crystallization differentiation in magma chambers that are continuously supplied with parental magma, the amount of cumulate formed during development of this upper crust may be at least 30 times the mass of the upper crust. This is about 4.3 times the mass of the mantle prism beneath the crust.

Concerning this issue of how to remove cumulate from the chamber, convection is an inescapable mechanism, and occurs in the mantle prism beneath the arc crust. The problem is what kind of convection it should be. Volcanic activity, topography and geology of the Japanese Islands, and the distributions of terrestrial heat flow rates and seismic hypocenters in and around the Japanese Islands are all well-understood by assuming convection in the mantle prism as shown in Fig. 3.1. If convection continues to be simply mixing within the mantle prism, the prism would soon be filled up with cumulate. As stated in the previous section, if convection was limited within the mantle prism, the crust of the Japanese Islands at their present size could never be formed. The mantle prism should be connected by convection with the outside mantle. This convection carries high-temperature, fertile mantle material from the outside mantle into the mantle prism on the one

hand, and conversely carries cumulate away from the mantle prism to the outside mantle. Removal of cumulate not only means transport of cumulate from the chamber to the mantle prism, but also includes the subsequent transport of the cumulate from the prism to the vast outside mantle. From the viewpoint of the origin of continental crust, the existence of this type of convection is critical and occurs in the mantle prism beneath the crust of the island arc.

References

Condie KC (1993) Chemical composition and evolution of the upper continental crust: contrasting results from surface samples and shales. Chem Geol 104:1–37

Condie KC (1997) Plate tectonics and crustal evolution. Butterworth-Heinemann, Boston, 282 p

Ghiorso MS, Sack RO (1995) Chemical mass transfer in magmatic process IV. A revised and internally consistent thermodynamic model for the interpolation of liquid-solid equilibria in magmatic systems at elevated temperatures and pressures. Contrib Miner Petrol 119:197–212

Hess PC (1992) Phase equilibria constraints on the origin of ocean floor basalts. In: Morgan JP, Blackman DK, Sinton JM (eds) Mantle flow and melt generation at mid-ocean ridges, vol 71, Geophysical monograph. American Geophysical Union, Washington, DC, pp 67–102

Hurley PM, Hughes H, Faure G, Fairbairn HW, Pinson WH (1962) Radiogenic strontium-87 model of continental formation. J Geophys Res 67:5315–5334

Kuno K (1976) Volcanoes and volcanic rocks. Iwanami, Tokyo, 283 p, (In Japanese)

McDonough WF, Sun S-s (1995) The composition of the earth. Chem Geol 120:223–253

Shaw DM, Cramer JJ, Higgins MD, Truscott MG (1986) Composition of the Canadian Precambrian shield and the continental crust of the earth. In: Dawson JB, Carswell DA, Hall J, Wedepohl KH (eds) The nature of the lower continental crust, vol 24, Geological Society Special Publication. Blackwell Scientific Publication, Oxford, pp 275–282

Taylor SR (1965) The application of trace element data to problems in petrology. In: Ahrens LH, Press F, Runcorn SK, Urey HC (eds) Physics and chemistry of the earth, vol 6. Pergamon, London, pp 133–214

Taylor SR, McLennan SM (1985) The continental crust: its composition and evolution. Blackwell Scientific Publication, Carlton, 312 p

Tuttle OF, Bowen NL (1958) Origin of granite in the light of experimental studies in the system $NaAlSi_3O_8$-$KAlSi_3O_8$-SiO_2-H_2O. Geol Soc Am Mem 74:153

Wager LR (1960) The major element variation of the Layered Series of the Skaergaard Intrusion and a re-estimation of the average composition of the hidden layered series and of the successive residual magmas. J Petrol 1:364–399

Wager LR, Brown GM (1967) Layered igneous rocks. W. H. Freeman, San Francisco, 588 p

Wänke H, Dreibus G, Jagoutz E (1984) Mantle chemistry and accretion history. In: Kröner A, Hanson GN, Goodwin AM (eds) Archean geochemistry. Springer, Berlin, pp 1–24

Wedepohl KH (1995) The composition of the continental crust. Geochim Cosmochim Acta 59:1217–1232

Yanagi T (1975) Rubidium-strontium model of formation of the continental crust and the granite at the island arc. Mem Fac Sci, Kyushu Univ Ser D 22:37–98

Yanagi T, Ichimaru Y, Hirahara S (1991) Petrochemical evidence for coupled magma chambers beneath the Sakurajima volcano, Kyushu, Japan. Geochem J 25:17–30

Chapter 5
Differentiation Mechanism of Magma at Arc Volcanoes

5.1 Open-System Magma Chamber Repeatedly Supplied with Primitive Magma

Crystallization differentiation in open-system magma chambers appears to be the most suitable differentiation mechanism that can transform primitive basaltic magma into magma of upper continental crust composition. However, the evidence to support existence of such a differentiation mechanism is necessary. If this differentiation mechanism is working, the potassium content, for example, of magma in the chamber will increase first rapidly with time, and then gradually increase, and finally it will become constant at steady-state concentration. The steady-state concentration of this element is about 20 times the initial concentration. This time-dependant variation is simple and hence would likely be captured in the geologic record. To find this pattern, it is necessary to survey volcanoes where evolving magma often erupts at the surface. Such a survey enables us to trace a time-dependent variation of potassium contents in the lavas. It takes some effort to determine which volcanoes yield the expected variation. Volcanoes that appear in the following discussion are shown on a map of the Japanese Islands in Fig. 5.1.

To capture the time-dependant variation, it is extremely helpful to know the exact extrusion sequence of lavas. To know this, however, is very difficult. It is usually achieved based on the law of superposition of strata. There is, however, no such place where all the lavas accumulated in a single succession. Therefore, radiometric dating is necessary. Its accuracy, however, is not sufficient to show the exact sequence of lava extrusions, because, for instance, a single Quaternary volcano may extrude lava at intervals of a few decades or a few centuries, over millions of years. These time intervals are too short to be resolved by ordinary radiometric dating. In field surveys, the overall succession of stratigraphic units of a volcano usually has been determined based on summarizing the accumulated, fragmental stratigraphic data obtained through geological surveying over a wide area in and around the volcano. The lava extrusion sequence so gained, however, naturally has its own limits in accuracy and reliability, because, for instance, these

T. Yanagi, *Arc Volcano of Japan*, Lecture Notes in Earth Sciences 136,
DOI 10.1007/978-4-431-53996-4_5,

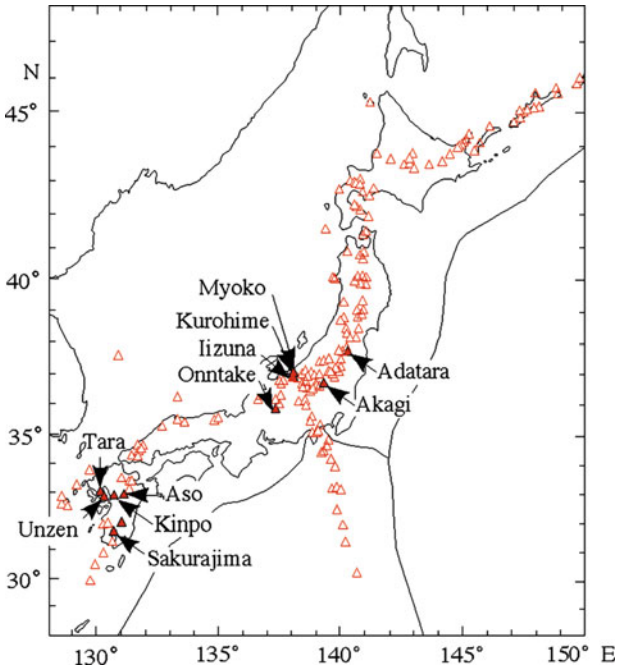

Fig. 5.1 Distribution of Quaternary volcanoes in Japan. *Red-edge triangles* are Quaternary volcanoes. *Red triangles* are volcanoes that are referred to in the text

stratigraphic units of mappaple sizes sometimes constitute a single lava flow, but often comprise many lava flows.

The extrusion sequences of lavas of Mounts Iizuna, Kurohime and Myoko, which are adopted in this book, are results of geological surveys conducted by Dr. Hayatsu (Hayatsu 1976). These volcanoes lie on an NS-trending line on the Japan Sea side of central Honshu. They started their activities almost simultaneously about 300,000 years ago. The Iizuna and Kurohime volcanoes continued their activity until 150,000 and 90,000 years ago, respectively (Hayatsu et al. 1994). Mount Myoko is still active today.

5.1.1 Time-Dependent Variation in a Serrated Pattern

Below, I first present the thought process by which we noticed crystallization differentiation in an open-system magma chamber (Yanagi and Ishizaka 1978). It originated from the fact that potassium content changed in a saw-toothed pattern with increase of stratigraphic height of lava samples at Mount Myoko. When we examined lava compositions from the bottom to the top of the sequence (Table 5.1), potassium content was found to repeat five times the pattern of increase and abrupt

Table 5.1 Chemical compositions of lava samples from Myoko volcano

Rock type	K (wt.%)	Rb (ppm)	Sr (ppm)	K/Rb	Rb/Sr	Chemical step
Andesite	1.825	67.9	297	269	0.229	MK 5
Andesite	1.36	55.0	371	247	0.148	MK 5
Andesite	1.32	48.1	361	276	0.133	MK 5
Andesite	1.201	38.7	365	310	0.106	MK 5
Basalt	0.9553	31.8	393	300	0.081	MK 5
Andesite	1.717	65.8	284	261	0.232	MK 4
Andesite	1.178	40.8	349	289	0.117	MK 4
Basalt	1.185	40.4	350	293	0.115	MK 4
Basalt	1.141	40.1	343	285	0.117	MK 4
Basalt	0.7822	24.1	318	325	0.076	MK 4
Andesite	1.737	60.5	250	287	0.242	MK 3
Andesite	1.263	38.3	308	330	0.124	MK 3
Andesite	1.139	37.5	260	304	0.144	MK 3
Andesite	1.102	36.1	258	305	0.140	MK 3
Basalt	1.000	27.6	308	362	0.090	MK 3
Basalt	0.9223	24.4	307	378	0.079	MK 3
Andesite	1.553	56.5	238	275	0.237	MK 2
Andesite	1.415	47.7	360	297	0.133	MK 2
Andesite	1.201	44.9	275	267	0.163	MK 2
Andesite	1.009	33.1	279	305	0.119	MK 2
Basalt	1.168	37.0	328	316	0.113	MK 1
Basalt	0.7856	23.9	326	329	0.073	MK 1

Cited from Yanagi and Ishizaka (1978)

drop. Hence, the most important finding is that at Mount Myoko, potassium content repeats a large drop several times as the stratigraphic height of the lava sampling increases. If the lava was occasionally and repeatedly extruded from a chamber where crystallization differentiation continued, its potassium content ought to increase in the sequence of lava extrusion, because potassium would be progressively concentrated in the magma during crystallization differentiation. As a probable mechanism causing the large potassium drop, there is probably no other process besides mixing between injected primitive magma and residual magma in the chamber. Because such mixing causes a large drop of potassium concentration in the bulk magma in the chamber, and subsequent crystallization causes a progressive increase of the potassium concentration, the repetitive inflow of primitive magma into the chamber where crystallization differentiation continues will drive potassium content of the magma to zig-zag in a sawtooth pattern with time, as long as the magma inflow recurs over a reasonably long time interval.

For this type of crystallization differentiation to continue, both the recurring inflow of primitive magma into the chamber and the successive removal of cumulate from the chamber should occur spontaneously. Figure 5.2 shows a model for an open-system magma chamber working near the boundary between mantle and crust. Mantle upwelling flow is assumed to rise beneath the chamber. In this hypothetical configuration, the upwelling flow carries primitive magma into the

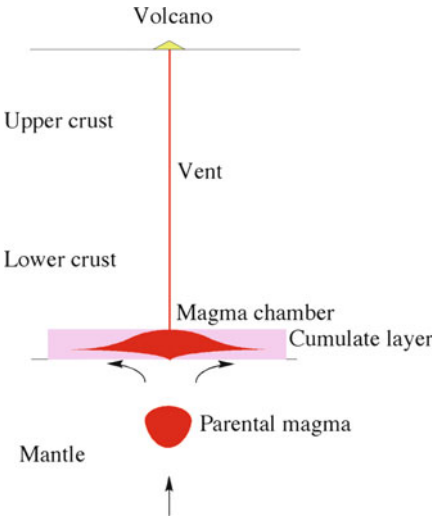

Fig. 5.2 A magma chamber that is repeatedly supplied with parental magma. *Arrows* indicate mantle upwelling flow that carries parental magma into the chamber and removes cumulate from the chamber (Modified from Yanagi and Ishizaka (1978))

chamber on the one hand, and on the other hand it removes cumulate away from the chamber. In this case, primitive magma is assumed to form by decompression melting from a high-temperature source material entrained in the mantle upwelling flow. The time-dependant sawtooth type variation of potassium concentration may therefore, in principle, be explained by this configuration of the differentiation system.

5.1.2 *Crystallization Differentiation in a Chamber Periodically Supplied with Parental Magma*

Let us consider a time-dependant change in chemical composition of magma caused by crystallization differentiation in a chamber that is periodically supplied with parental magma. Time is the number of repetitions of magma supply. Let us define a partition coefficient of a minor element to be a ratio D of concentration C_x in the cumulate to concentration C in the magma ($D = C_x/C$). Partition coefficient D is assumed to be constant. Let us define one chemical step to be a period from one supply of parental magma to the next supply. The amount of parental magma supplied at any step is assumed to be constant, and this amount is assumed to be a unit mass. Furthermore, F represents the fraction of magma that remains at the end of a chemical step, and F is assumed to be constant. In addition, let us assume that the mass of the minor element is conserved during magma mixing and crystallization, and that chemical equilibrium is maintained between the magma and the coexisting cumulate at any chemical step. Then the concentration C_n of a minor element in the residual magma at the n-th step is expressed in the following

equation with D, F, and C_0. C_0 stands for concentration of the element in the parental magma.

$$C_n = C_0/D \times \{1 - (F/A)^n\}/(1 - F^n),$$

where, $A = F + D(1 - F)$.

When n becomes infinitely large, C_n converges to C_0/D, because F < 1

$$C_\infty = C_0/D.$$

In the case that perfect fractional crystallization repeats at every chemical step, the concentration C_n in the residual magma at the nth step is expressed by the following equation.

$$C_n = C_0\left(F^D - F^{(n+1)D}\right)(1 - F)/\left\{F(1 - F^n)\left(1 - F^D\right)\right\}.$$

In this case, the partition coefficient is defined between the magma and the cumulate surface. When the chemical step n increases infinitely, concentration C_n becomes,

$$C_\infty = C_0 F^D(1 - F)/\left\{F\left(1 - F^D\right)\right\}.$$

It converges to a specific concentration defined by C_0, D, and F.

As stated above, in both cases of equilibrium and perfect fractional crystallization, concentration in the residual magma always converges when the chemical step infinitely increases. Therefore, when it is confirmed that the chemical composition of volcanic rocks converges to a steady-state composition with an increase in time, it is likely that the differentiation mechanism working beneath the volcano is of the type stated above.

5.1.3 Steady-State

Potassium contents of primitive lava samples from island arcs concentrate at about 0.2 wt%. There is a basaltic rock sample of 0.24 wt% potassium from Mount Iizuna. Its Rb/Sr and K/Rb ratios are 0.011 and 664, respectively. Both of these are values of primitive magmas. Therefore, magmatic evolution seems to have started from these values. When we look at variation ranges of potassium contents for individual steps of volcanic rocks of Mounts Iizuna, Kurohime and Myoko, we see the following sawtooth-type variations of the potassium content with increase in stratigraphic height of lava samples. At Mount Iizuna, potassium content increases from 0.24 to 0.81 wt% at the second step, and from 0.69 to 0.97 wt% at the third step, and from 0.65 to 1.10 wt% at the fourth step. At Mount Kurohime, it increases

from 0.46 to 1.60 wt% at the first step, and from 0.86 to 0.87 wt% at the second step. At Mount Myoko, it increases from 0.79 to 1.17 wt% at the first step, from 1.01 to 1.55 wt% at the second step, from 0.92 to 1.74 wt% at the third step, from 0.78 to 1.72 wt% at the fourth step and from 0.96 to 1.83 wt% at the fifth step. Peak values of potassium content at each step are 1.2, 1.6, 1.7, 1.7, and 1.8 wt% for Mount Myoko. The last three values are almost identical. Therefore, it seems clear that a steady state has been attained at these steps.

Figure 5.3 shows how the variation range of Rb/Sr ratio within a step changes with increase of the chemical step. A vertical length of a rectangle in Fig. 5.3 shows the variation range of the Rb/Sr ratio within one chemical step. In the case that plagioclase crystallizes from magma in a repeatedly refilled magma chamber, the behavior of Rb/Sr ratio is similar to the behavior of potassium. It increases during crystallization differentiation, and drops during mixing between the injected primitive magma and the residual magma in the chamber. Therefore, this pattern of evolution of the variation ranges (Fig. 5.3) is a reflection of the time-dependent change of Rb/Sr ratio in the sawtooth pattern. Figure 5.3 clearly shows that the variation range of Rb/Sr ratios moves upwards with increase of chemical step, and finally comes to a standstill, indicating attainment of steady state.

The Rb/Sr ratio increases from 0.011 at the beginning of the second step to 0.116 at the end of the fourth step at Mount Iizuna. During this growth time period, the

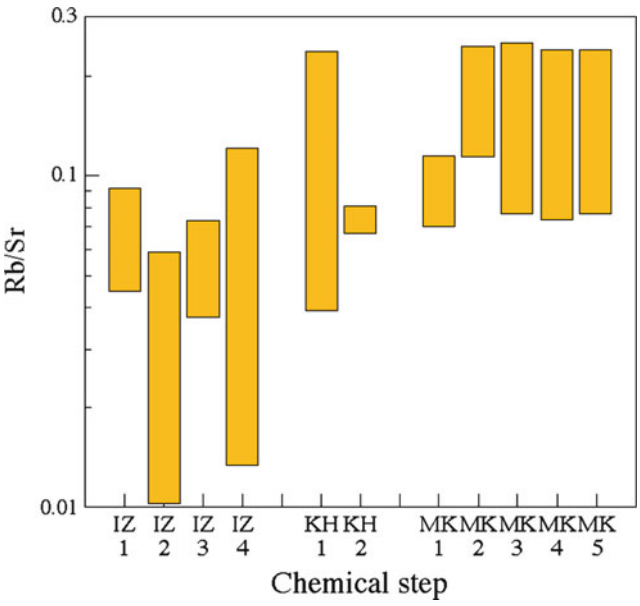

Fig. 5.3 Variation ranges in Rb/Sr ratio of lavas at individual chemical steps, and the mode of their progressive migration towards the higher Rb/Sr ratio side, in order of chemical step. A vertical length of a *yellow rectangle* shows a variation range in Rb/Sr ratio of lavas within one chemical step. *IZ*, *KH* and *MK* stand for Izuna, Kurohime and Myoko volcanoes, respectively (Modified from Yanagi and Ishizaka (1978))

Table 5.2 K, Rb and Sr contents of upper continental crust

No	K (ppm)	Rb (ppm)	Sr (ppm)	K/Rb	Rb/Sr	References
1	20,700	90	357	230	0.25	Taylor (1965)
2	28,200	112	350	252	0.32	Taylor and McLennan (1985)
3	26,500	110	316	241	0.35	Shaw et al. (1986)
4	27,100	99	280	274	0.35	Condie (1993)[a]
5	22,200	85	276	261	0.31	Gao et al. (1998)[b]

[a]Restored 2.5–1.8 Ga upper continental crust
[b]Upper continental crust of Central East China (H_2O and CO_2 were eliminated)

variation in the sawtooth pattern recurs three times. It increases from 0.041 to 0.23 at Mount Kurohime. At Mount Myoko, the time-dependant variation in the sawtooth pattern repeats four times. However, the variation range of Rb/Sr ratios is limited to between 0.07 and 0.24. The peak Rb/Sr ratios are almost identical at 0.24, 0.24, 0.23, and 0.23 at the last four steps. It is evident that steady state has been reached for these last four steps. This is the inescapable fact that arises from the model of crystallization differentiation in the repeatedly refilled magma chamber.

Although there is a difference in the form of magma supply, the chamber that is periodically supplied with parental magma and the chamber that is continuously supplied with parental magma are both the same open-system refilled magma chamber. Therefore, the facts observed in the Myoko volcano group contribute important evidence indicating presence of a magmatic differentiation mechanism that produces magma with a chemical composition of continental crust derived from the primitive magma. In the case of a continuous magma supply, the chemical composition of upper continental crust is realized in the chamber when it reaches steady state. At Mount Myoko, the steady state has nearly been achieved at the point when the Rb/Sr and K/Rb ratios attained values of 0.23–0.24, and 260–290, respectively. Although the Rb/Sr ratios are little lower, and the K/Rb ratios are little higher, both of these ratios lie within their reported ranges of upper continental crust (Table 5.2). Hence, as far as Rb/Sr and K/Rb ratios are concerned, magma composition appears to have evolved beneath these volcanoes towards the chemical composition of upper continental crust and to finally have reached it.

5.1.4 Remaining Two Problems

Although the above explanation has proceeded so far by assuming that a set of lavas of changing chemical steps was extruded from a magma undergoing crystallization differentiation, Sakuyama (1981) examined lavas from Mounts Myoko and Kurohime and found reverse zoning of orthopyroxene phenocrysts, bimodal distributions of plagioclase phenocryst compositions, and non-equilibrium coexistence of olivine and orthopyroxene phenocrysts, and thus concluded that many lavas had been extruded during mixing between injected basaltic magmas and residual magmas. After that, similar findings have been reported from Mounts

Sakurajima and Unzen, and other volcanoes, and indicate lava extrusion during magma mixing. Based on subsequent studies of magma mixing to date, the notion of repetitive magma supply into magma chambers where crystallization differentiation continues has been well established. Results of these more recent studies have clearly confirmed the existence of the repeatedly refilled magma chamber. Nonetheless, the reported stratigraphic variation of lava compositions within one chemical step at Mount Myoko corresponds to a chemical change of a magma that continues to crystallize. Therefore, there remains a question as to whether a stratigraphic succession of lava flows in one volcanic step actually formed during crystallization differentiation of magma, or during mixing of magmas of different compositions.

Another problem remains: mineralogical compositions of lavas from the Myoko volcano group seem to limit the maximum possible depth of the chambers. The basaltic lavas contain both phenocrysts of plagioclase and olivine. These two minerals can coexist at pressures less than about 0.8 GPa under dry conditions. These pressures become much lower under wet conditions. Therefore, the chamber cannot be positioned at the boundary between the mantle and the thick crust (a little more than 30 km) beneath Mount Myoko. The reason for setting the chamber at the boundary in the previous discussion was to impose both a magma supply and cumulate removal on the mantle upwelling flow. Because both the repetitive magma supply and the successive removal of cumulate are necessary to keep a refilled magma chamber working, a mechanism that can spontaneously and continuously maintain these two functions should be devised to situate the chamber within the crust. This is a serious problem directly related to the existence of the open-system magma chamber. This problem was solved by study of Mount Sakurajima and is presented in detail in Chap. 6.

5.2 Evolution Limit of Volcanic Rocks, and Its Relation to Chemical Composition of the Upper Continental Crust

Volcanic rocks from Mount Myoko were found to have evolved until the composition of the upper continental crust was attained in terms of Rb/Sr and K/Rb ratios. Next it is necessary to examine arc volcanic rocks to determine whether this is a general consequence. Since Mount Myoko is a typical arc volcano, it is expected that the same process occurs at other arc volcanoes. However, care must be taken when examining other regions. It is not always certain that the serrated time-dependent variation of lava compositions reaches a steady state. When the repetitive magma supply is arrested during the growth of a volcano, development of the serrated Rb/Sr ratio pattern immediately stops. Mounts Iizuna and Kurohime appear to represent such cases. Although the Rb/Sr ratio of 0.23–0.24 represents the evolutionary limit at Mount Myoko, Rb/Sr ratios of volcanic rocks from Mounts Iizuna and Kurohime are all lower. Naturally, volumes of these volcanoes would be

expected to be smaller. When compared, it was found that the volume of Mount Myoko is 50 km^3, that of Mount Iizuna is 25 km^3 and that of Mount Kurohime is 15 km^3 (Fourth Stage Volcano Catalog Committee for Quaternary Volcanoes 2002). Thus the volumes of Mounts Iizuna and Kurohime are certainly smaller. The magma supply seems to have stopped at these volcanoes before the attainment of the steady-state value of the Rb/Sr ratio.

5.2.1 *Variation Ranges of Rb/Sr Ratios at Individual Volcanoes*

Before we examine the convergent value of the Rb/Sr ratio, we should confirm that lava compositions show a time-dependant variation in the serrated pattern. For this purpose, it is necessary to understand the detailed stratigraphic succession of all volcanic rocks. In addition, it is also necessary to measure rubidium and strontium contents of all lavas. Even so, there is almost no example meeting such requirements. However, there are some volcanoes from which many lava samples have been collected and measurements of both the rubidium and strontium contents of the samples have already been made. In such cases, the variation range of the Rb/Sr ratios at each of these volcanoes is easily calculated. Such examples are shown in Fig. 5.4a.

The lower and upper limits of the variation ranges at Mounts Tara (Ogata 1993), Unzen (Sugimoto 1999), Ontake (Kimura and Yoshida 1999), Akagi (Notsu et al. 1985) and Adatara (Fujiwara 1988) commonly lie at 0.01 and 0.3, respectively. The consistency of the lower limits suggests that the parental magma is the same at these

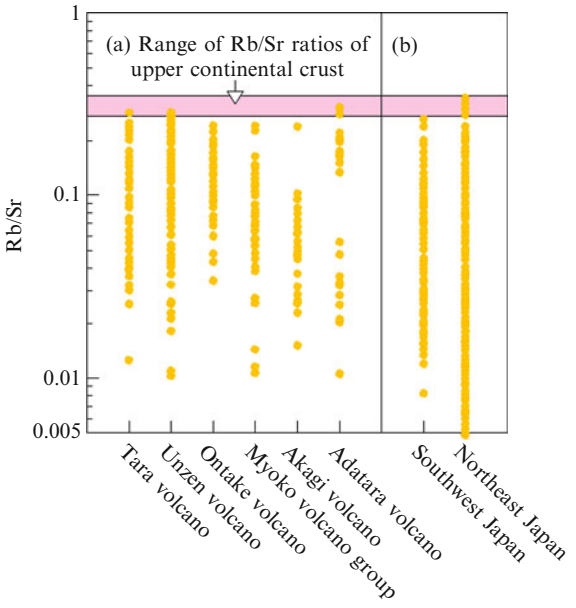

Fig. 5.4 Variation ranges of Rb/Sr ratios at individual volcanoes (**a**), and in individual regions (**b**). Mount Unzen represents volcanic activity on Shimabara peninsula. Each *dot* represents a reported value of Rb/Sr ratio (Data are from Yanagi and Ishizaka (1978), Notsu (1985), Fujiwara (1988), Ogata (1993), Kimura and Yoshida (1999), Sugimoto (1999) and others)

volcanoes. The more important facts are that an upper limit is common to all these well-grown arc volcanoes, and that this upper limit coincides with the Rb/Sr ratio of the upper continental crust. These findings suggest that the same differentiation mechanism is working beneath all these arc volcanoes.

Although the number of measurements is very few for individual volcanoes, when such measurements are collected in a region where a considerable number of volcanoes are present, the total number of measurements becomes sufficiently enough to define the variation range of Rb/Sr ratios in the region. Results for Northeast and Southwest Japan were shown in Fig. 5.4b. The variation range in Southwest Japan coincides well with those of the above volcanoes (Fig. 5.4a). The variation range in Northeast Japan, however, is a little different. The lower limit lies at 0.005, reflecting the occurrence of low alkali tholeiitic basalts in this region. The upper limit, however, lies at about 0.3. It is identical with those of the other volcanoes (Fig. 5.4a). Thus, while the lower limits are different, the upper limits are identical, which seems strange. The explanation of this phenomenon is described in Chap. 7.

In conclusion, the Rb/Sr ratio of lavas starts increasing from values of primitive basalts and finally converges on values of 0.23–0.35 at well-grown stratovolcanoes in Japan. The range of convergent Rb/Sr ratios is identical with the reported range of Rb/Sr ratios of upper continental crust. These facts strongly suggest that a differentiation mechanism is common to all these stratovolcanoes in Japan, and that it is that of crystallization differentiation in magma chambers repeatedly supplied with primitive magma.

5.2.2 *Rb and Sr Contents of Volcanic Rocks and Composition of the Upper Continental Crust*

To understand geochemical behaviors of rubidium and strontium during crystallization differentiation of magma, it is necessary to analyze variations of not only their ratios but also their concentrations. Therefore, rubidium and strontium contents of Quaternary volcanic rocks from Japan are shown in Fig. 5.5.

As far as rubidium and strontium contents are concerned, there are two contrasting evolutionary trends in crystallization differentiation. One is that concentrations of both elements increase simultaneously in magma during crystallization differentiation, and hence Rb/Sr ratio remains almost constant at low values. The other is that rubidium concentration increases while variation of the strontium concentration is largely suppressed during crystallization differentiation, and hence the Rb/Sr ratio grows quickly. Therefore, volcanic rocks plotted closer to the lower left-hand end of Fig. 5.5 are more primitive.

In regard to the former evolutionary trend, the strontium content ranges from 150 to 1,500 ppm in the basaltic rocks. This trend is represented by basaltic rocks lying along the left-hand side boundary of the distribution of the Quaternary volcanic

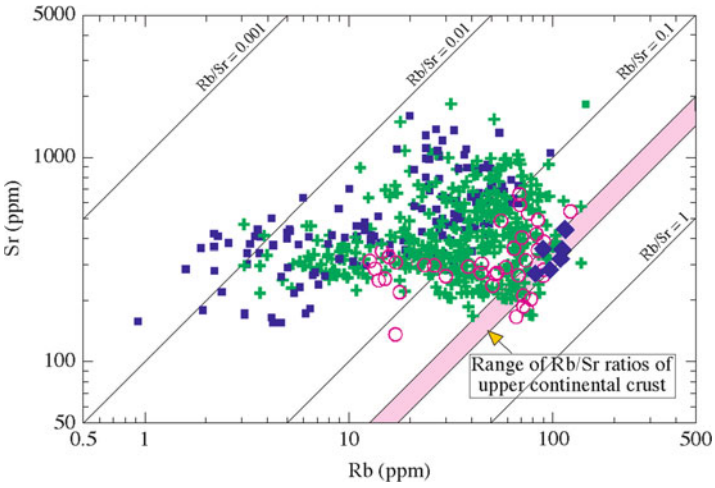

Fig. 5.5 Rb and Sr contents of Quaternary volcanic rocks from Japan. *Deep blue square*, basalt; *green cross*, andesite; *pink circle*, dacite; *deep blue lozenge*, chemical compositions of upper continental crust, reported by Hurley et al. (1962), Taylor (1965), Taylor and McLennan (1985), Shaw et al. (1986), Condie (1993), Wedepohl (1995) and Gao et al. (1998); *pink band*, range of estimated Rb/Sr ratios of the upper continental crust (Modified from Yanagi and Yamashita (1994))

rocks in Fig. 5.5. This increase in strontium content is caused by both a decrease in partial melting degree in the mantle and by progress of the subsequent crystallization of mafic minerals at high pressures (Figs. 4.3 and 4.4). In this range of strontium contents, major element composition changes with increase in strontium content, from tholeiitic basalt through high-alumina basalt to alkali olivine basalt.

In regard to the latter evolutionary trend, the Rb/Sr ratio increases from about 0.01 in primitive basalts and basaltic andesites to 0.2–0.3 in dacites and dacitic andesites. This increase is due to low-pressure crystallization differentiation that involves plagioclase fractionation (Fig. 4.4). This low-pressure crystallization differentiation is well represented by volcanic rocks that are arranged in a belt along the lower boundary of the distribution of Quaternary volcanic rocks, shown in Fig. 5.5. This differentiation trend is different from line OF in Fig. 4.4, which indicates the trend traced by the liquid formed simply by a single fractional crystallization. In volcanic rocks arranged along the lower boundary of the distribution in Fig. 5.5, rubidium is more concentrated with progress of differentiation. However, the concomitant decrease of strontium is not so large, as indicated by line OF in Fig. 4.4.

Another characteristic of this phenomenon is that the distribution of volcanic rocks is sharply demarcated at about 0.3 of the Rb/Sr ratio, as illustrated in Fig. 5.5. Therefore, the characteristics of the low-pressure differentiation shown in Fig. 5.5 are of two types. One is the abrupt increase in Rb/Sr ratio, and the other is the presence of the evolution limit of Rb/Sr ratio at about 0.3. These two aspects are well accounted for by assuming low-pressure crystallization differentiation in the repeatedly refilled magma chamber.

Reported chemical compositions of the upper continental crust lie on the right-hand-side boundary of the distribution of Quaternary volcanic rocks (Fig. 5.5). This distribution starts from the lower left-hand end of Fig. 5.5, then extends towards the right-hand side, and finally is sharply demarcated by a boundary upon which the compositions of the upper continental crust lie. In other words, the Quaternary volcanic rocks distribute within a compositional space limited between primitive basalts and upper continental crust (Fig. 5.5). To obtain sufficient evidence for the presence of varied types of crystallization differentiation in the repeatedly refilled magma chamber, it is important to investigate many individual arc volcanoes. The distribution of volcanic rocks plotted in Fig. 5.5 is especially important in indicating the presence of many differentiation routes under varied physical conditions beneath island arcs. For instance, there is a differentiation route that travels along the lower boundary of distribution of volcanic rocks in Fig. 5.5, from primitive basalts to the reported compositions of upper continental crust. This route is realized at island arcs with rather thin crust. The strontium content is always kept low during differentiation. On the contrary, there is a route passing through the high-strontium area of the plot. Such a route is achieved under thick arc crust.

At this point, it is necessary to describe some exceptions. Pumice blocks and essential lenses contained in large-scale pyroclastic flows often have Rb/Sr ratios larger than 0.35, along with much evolved chemical compositions. Such chemical characteristics indicate their evolution beyond steady state compositions. This finding probably is due to chambers positioned at quite shallow levels in the crust. This subject, however, is one that should be clarified in future research. For the purposes of this discussion, such samples were excluded from Fig. 5.5.

5.2.3 *Crustal Assimilation and Its Effects on Magma Compositions*

Since magma exists at high temperatures, it seems to more or less melt and assimilate the surrounding rocks. Therefore, it is necessary to investigate whether the arguments presented above are affected by this crustal assimilation.

The Rb/Sr ratios of the upper continental crust are higher than those of the mantle by about 17 times, and hence $^{87}Sr/^{86}Sr$ ratios of the upper continental crust are, in most cases, higher than $^{87}Sr/^{86}Sr$ ratios of the mantle. Therefore, the $^{87}Sr/^{86}Sr$ ratio of magma increases with increase in amount of assimilated crust. This suggests that the assimilation can be detected by measurement of $^{87}Sr/^{86}Sr$ ratios of volcanic rocks.

The lower continental crust has more chances to encounter higher-temperature magmas. Accordingly the effect of lower crust assimilation should also be investigated. Fragments of lower crust have erupted to the surface with alkali basalts in Southwest Japan. They have very low Rb/Sr ratios of less than 0.02, and mildly high $^{87}Sr/^{86}Sr$ ratios from 0.704 to 0.707. These $^{87}Sr/^{86}Sr$ ratios are

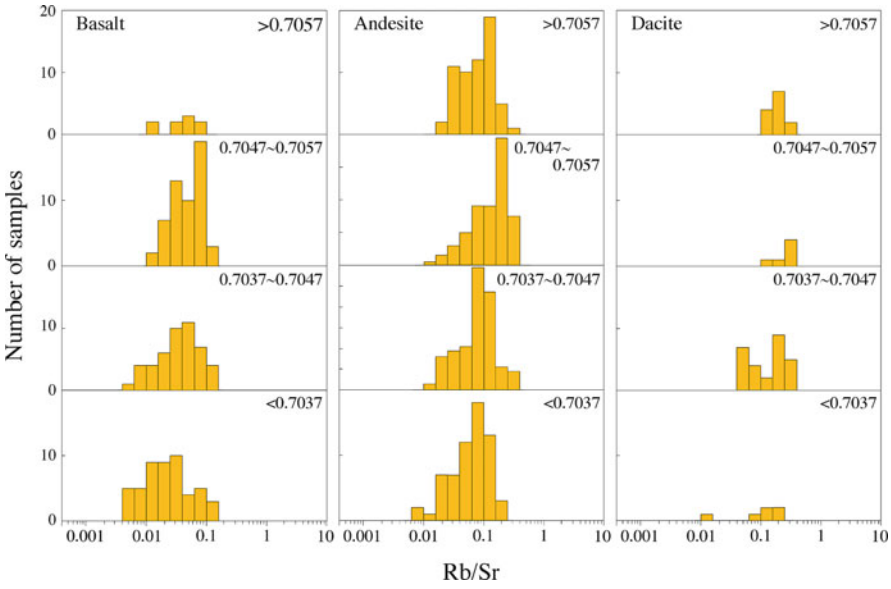

Fig. 5.6 Histograms of Rb/Sr ratios of Quaternary volcanic rocks with different $^{87}Sr/^{86}Sr$ ratios. Volcanic rocks from Japan were classified into four groups depending on heights of their $^{87}Sr/^{86}Sr$ ratios to see effects of crustal assimilation. Increase in Rb/Sr ratio associated with increase in $^{87}Sr/^{86}Sr$ ratio is insignificantly small within any rock-type group

distinctly higher than those of primitive basalts formed in the mantle. This suggests that assimilation of either of lower crust or upper crust can similarly raise the $^{87}Sr/^{86}Sr$ ratio of the magma, at least in Southwest Japan.

Assimilation of upper continental crust results in a marked increase in Rb/Sr ratio of the magma. On the contrary, assimilation of lower continental crust yields an almost insignificant effect on the Rb/Sr ratio of magma, because Rb/Sr ratios of the lower crust are equal to or lower than those of primitive magmas. Therefore, investigation of whether the Rb/Sr ratio has increased, together with increase in $^{87}Sr/^{86}Sr$ ratio, seems to indicate which crust type was assimilated.

Depending on their $^{87}Sr/^{86}Sr$ ratios, Quaternary volcanic rocks from Japan have been classified into four groups, with $^{87}Sr/^{86}Sr$ ratios < 0.7037, 0.7037 to 0.7047, 0.7047 to 0.7057, and > 0.7057 (Fig. 5.6). In this case, we can evaluate whether their Rb/Sr ratios increase in accordance with increase of their $^{87}Sr/^{86}Sr$ ratios. Figure 5.6 clearly shows that there are no systematic increases of Rb/Sr ratio with increase in $^{87}Sr/^{86}Sr$ ratio. It is clear that assimilation occurred during formation of these volcanic rocks, since many of them have high $^{87}Sr/^{86}Sr$ ratios. Nonetheless, any coordinated increase of Rb/Sr ratio with the $^{87}Sr/^{86}Sr$ ratio is found to be insignificantly small. This means that the assimilation occurred mostly in the lower crust. Therefore, it is evident that assimilation does not cause serious problems for the arguments presented above.

References

Condie KC (1993) Chemical composition and evolution of the upper continental crust: contrasting results from surface samples and shales. Chem Geol 104:1–37

Fourth Stage Volcano Catalog Committee for Quaternary Volcanoes (2002) Volcano data base web version. http://www.geo.chs.nihon-u.ac.jp/tchiba/volcano/kaz-table.htm

Fujiwara A (1988) Tholeiitic and calc-alkaline magma series at Adatara volcano, northeast Japan: geochemical constraints on their origin. Lithos 22:135–158

Gao S, Luo T-C, Zhang B-R, Zhang H-F, Han YW, Zhao Z-D, Hu Y-K (1998) Chemical composition of the continental crust as revealed by studies in East China. Geochim Comsochim Acta 62:1959–1975

Hayatsu K (1976) Geological study of the Myoko volcanoes. Part 1, Stratigraphy. Mem Coll Sci, Kyoto Univ, Ser B 42: 131 p

Hayatsu K, Shimizu S, Itaya T (1994) Volcanic history of Myoko volcano group, Central Japan, Poly-generation volcano. J Geogr Tokyo Geogr Soc 103:207–220 (In Japanese with English abstract)

Hurley PM, Hughes H, Faure G, Fairbairn HW, Pinson WH (1962) Radiogenic strontium-87 model of continental formation. J Geophys Res 67:5315–5334

Kimura JI, Yoshida T (1999) Magma plumbing system beneath Ontake volcano, central Japan. Island Arc 8:1–29

Notsu K, Kita I, Yamaguchi T (1985) Mantle contamination under Akagi volcano, Japan, as inferred from combined Sr-O isotope relationships. Geophys Res Lett 12:365–368

Ogata M (1993) Magmatic differentiation and growth history of Taradake volcano, Northwestern Kyushu, Japan. Ph.D. Thesis, Kyushu University, 140 p

Sakuyama M (1981) Petrological study of the Myoko and Kurohime volcanoes, Japan; crystallization sequence and evidence for magma mixing. J Petrol 22:553–583

Shaw DM, Cramer JJ, Higgins MD, Truscott MG (1986) Composition of the Canadian Precambrian shield and the continental crust of the earth. In: Dawson JB, Carswell DA, Hall J, Wedepohl KH (eds) The nature of the lower continental crust, vol 24, Geological Society Special publication. Blackwell Scientific Publication, Oxford, pp 275–282

Sugimoto T (1999) Magmatic differentiation and evolution of a chamber system beneath the Unzen Volcano. Ph.D. Thesis, Kyushu University, 141 p

Taylor SR (1965) The application of trace element data to problems in petrology. In: Ahrens LH, Press F, Runcorn SK, Urey HC (eds) Physics and chemistry of the earth, vol 6. Pergamon, London, pp 133–214

Taylor SR, McLennan SM (1985) The continental crust: its composition and evolution. Blackwell Scientific Publication, Carlton, 312 p

Wedepohl KH (1995) The composition of the continental crust. Geochim Cosmochim Acta 59:1217–1232

Yanagi T, Ishizaka K (1978) Batch fractionation model for the evolution of volcanic rocks in an island arc: an example from central Japan. Earth Planet Sci Lett 40:252–262

Yanagi T, Yamashita K (1994) Genesis of continental crust under island arc conditions. Lithos 33:209–223

Chapter 6
Configuration and Dynamics of Magma Chambers Beneath Arc Volcanoes

6.1 Open-System Magma Chamber in the Crust

Instead of a chamber at the crust-mantle boundary, as shown in Fig. 5.2, a repeatedly refilled magma chamber situated in the crust is analyzed in this chapter.

It is well known that the surface of an active volcano and its surrounding area are gently elevated during a quiet period, they quickly subside immediately after a great eruption, and then become gently elevated again. This type of inflation and deflation is repeated in active volcanoes, resulting in a serrated type of ground deformation over time. It also is well known that the rapid subsidence is due to a pressure drop in the chamber caused by an eruption, and that the gentle uplifting is due to increasing pressure resulting from magma injection into the chamber.

Based on the idea that rapid subsidence immediately after the massive Taisho eruption was due to a pressure drop, Mogi (1958) estimated location of the magma chamber at a depth of 10 km beneath the center of the Bay of Kinko, north of Mount Sakurajima. After subsiding, the ground started rising again. Magma inflow into the chamber has been confirmed to be ongoing today (Kamo and Ishihara 1980). Mount Sakurajima is a typical arc volcano, and therefore, its chamber appears to be an open-system magma chamber. The present magma inflow probably represents the current aspect of such a chamber. A few dacite lava flows containing about 2 wt% K_2O have been extruded from Mount Sakurajima. To concentrate K_2O to that amount from the level found in primitive basalts (about 0.2 wt%), crystallization differentiation and magma supply must have alternated many times. During this period, a large amount of the total parental magma must have been supplied, and almost the same amount of cumulate must have been removed from the chamber. If this is true, it seems likely that investigation of Mount Sakurajima should provide basic information on an open-system magma chamber. Results of such an investigation (Yanagi et al. 1991) are presented below.

T. Yanagi, *Arc Volcano of Japan*, Lecture Notes in Earth Sciences 136,
DOI 10.1007/978-4-431-53996-4_6,

6.1.1 *Regularity of Change in the Chemical Composition of Lava Flows*

At first, a brief outline of the geology of Mount Sakurajima is presented here based on works reported by Fukuyama and Ono (1981) and Kobayashi (2002). Mount Sakurajima started its growth about 23,000 years ago on the southern rim of the Aira caldera, which formed after a large-scale eruption about 25,000 years ago. Four historic massive eruptions are reported in the literature. They are the Bunmei eruption of 1475–1476, the An-ei eruption of 1779, the Taisho eruption of 1914, and the Showa eruption of 1946. The amounts of lava extruded during these eruptions were estimated by Ishihara et al. (1981). In the Bunmei eruption, 0.49 km^3 of lava was extruded from craters opened on the northeast and southwest flanks. In the An-ei eruption, 1.7 km^3 of lava was extruded from craters opened on the north and south flanks. In the Taisho eruption, 1.34 km^3 of lava flowed from craters opened on the east and west flanks. In the Showa eruption, 0.18 km^3 of lava was extruded from craters opened on the east flank. Subsequently, eruptions of volcanic ash have continued intermittently from 1955 until the 2000s. The total amount of ash is thought to exceed the amount of Showa lava flow.

The dynamics inside the chamber seem to be reasonably described by examining lava flows. However, materials that were extruded from the top of the chamber at the early stage of the massive eruptions will be omitted from this examination because it is reasonable to expect that such materials represent an extremely fractionated part of the magma in the chamber.

In general, magma becomes lower in MgO and more enriched with K_2O over time during crystallization differentiation. However, MgO is lowest in the oldest historic lava flow and increases in the subsequent lava flows of the massive eruptions. In addition, K_2O is highest in the oldest historic lava flow and becomes lower in the subsequent lava flows of the massive eruptions at Mount Sakurajima. These time-dependent changes in composition are opposite to what is expected to occur during crystallization differentiation of the magma in the chamber. Thus, we need to examine petrological information recorded in the lava flows to better understand how the eruptions occurred.

In the serrated type of time-dependent variation in lava compositions at Mount Myoko, the rapid drop in K_2O was found to be due to the inflow of primitive magma into the chamber. Accordingly, it is expected that, if the progressive K_2O drop observed at Mount Sakurajima is due to the same process of magma injection, then the lava flows extruded to the surface must contain two types of plagioclase phenocrysts. One type would represent those components originally included in the injected magma, and the other would delineate those components of the residual magma in the chamber. Figure 6.1 shows compositional distributions of plagioclase phenocrysts contained in the Bunmei, An-ei, Taisho and Showa lava flows. Although these distributions are somewhat complicated, they are all bimodal distributions, commonly having two peaks at An_{83} and An_{57}. The position of each peak is fixed, and its height changes in sequence with the massive eruptions.

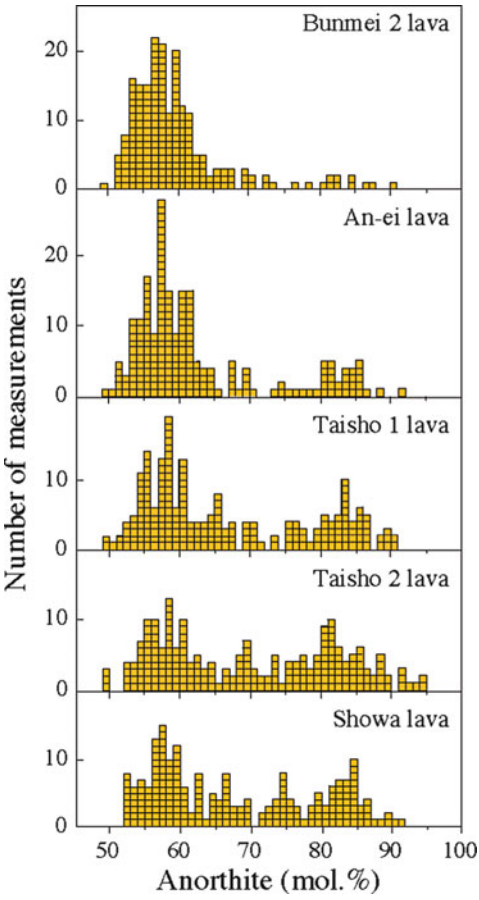

Fig. 6.1 Frequency distributions of chemical compositions of plagioclase phenocrysts in historic lava flows at Mount Sakurajima. Since several extrusions of lava flows occurred in Bunmei and Taisho eruptions, lava flows are numbered in the sequence of extrusions in each of these eruptions (Modified from Yanagi et al. (1991))

The An_{83} peak is the lowest in the Bunmei lava flow and grows in the subsequent lava flows of the massive eruptions. The An_{57} peak is highest in the Bunmei lava flow, and its height declines in subsequent lava flows of the massive eruptions. These time-dependent variations are explained well by assuming injection of basaltic magma into residual magma in the chamber.

In addition, there are linear relationships between height of these peaks and K_2O content of the host lava flow. The higher the An_{83} peak, the lower the K_2O content, and the higher the An_{57} peak, the higher the K_2O content. There also is a linear relationship between K_2O content and each of $T.Fe_2O_3$ (total iron), CaO, and SiO_2 contents of the host lava flows (Fig. 6.2). Based on these three relationships, it is possible to estimate the compositions of the two mixing-end-members. Since the residual magma in the chamber must originally have lacked An_{83} phenocrysts, its K_2O content is estimated at 2.61 wt% by extrapolating the linear relationship between K_2O content and An_{83} peak height until the latter becomes zero. Based on both this and the linear relationships shown in Fig. 6.2, the major element composition of the residual magma is estimated as listed in Table 6.1. Since the

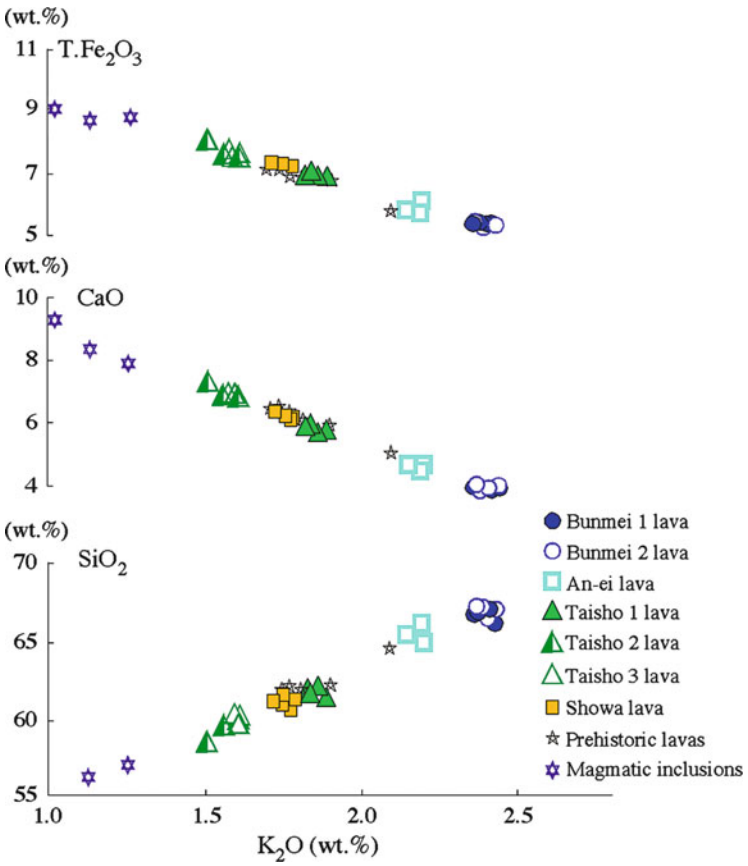

Fig. 6.2 Linear relationships between K_2O and other oxide components in prehistoric and historic lava flows at Mount Sakurajima. Since several extrusions of lava flows occurred in Bunmei and Taisho eruptions, lava flows are numbered in the sequence of extrusions in each of these eruptions. Magmatic inclusions are seen in any lava flow (Modified from Yanagi et al. (1991))

Table 6.1 Chemical compositions of mixing endmembers

	Dacite magma (wt.%)	Basalt magma (wt.%)
SiO_2	68.88	51.94
TiO_2	0.76	0.85
Al_2O_3	14.62	18.77
$T.Fe_2O_3$	4.8	9.97
MnO	0.14	0.19
MgO	0.47	5.35
CaO	3.04	10.12
Na_2O	4.21	2.36
K_2O	2.61	0.71
P_2O_5	0.22	0.12
Total	99.75	100.38

Cited from Yanagi et al. (1991)
$T.FeO_3$ total iron as Fe_2O_3

magma injected into the chamber must originally have lacked An_{57} phenocrysts, its K_2O content is estimated at 0.71 wt% by extrapolating the linear relationship between K_2O content and An_{57} peak height until the latter becomes zero. Based on both this and the linear relationships shown in Fig. 6.2, the major element composition of the injected magma is estimated as listed in Table 6.1. The residual magma in the chamber was found to be dacitic in composition, and the magma injected into the chamber was found to be basaltic in composition.

6.1.2 *Another Regular Change in Chemical Composition of Lava Flows of the Massive Eruptions*

Another regular compositional change of lava flows of the massive eruptions is presented here. Let us set ordinal numbers on the Bunmei, An-ei, Taisho, and Showa eruptions as the 1st, 2nd, 3rd, and 4th eruptions, and then plot K_2O contents of lava flows in this order, as shown in Fig. 6.3. K_2O content of the residual magma in the chamber before the start of these historical eruptions is plotted on the y-axis. K_2O content is found to decrease in the massive eruptions at a constant rate, except for K_2O content of the Taisho lava flows. A vertical data array in Fig. 6.3 indicates a variation range in K_2O content of lava flows extruded during a single massive eruption. The explanation for the behavior of K_2O contents of the Taisho lava flows

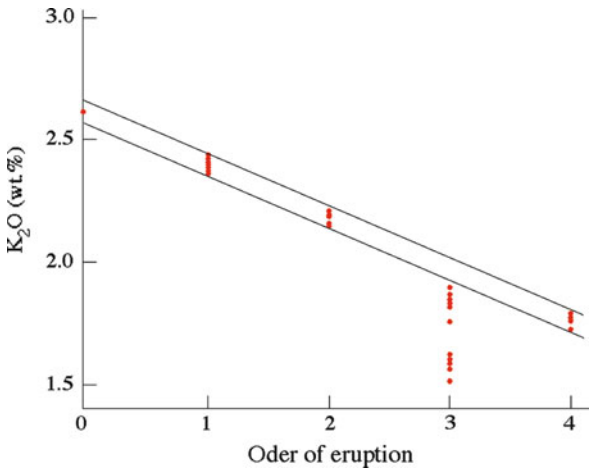

Fig. 6.3 Progressive drops at a constant rate of K_2O in historic lava flows, in order of the gigantic eruptions. Bunmei, An-ei, Taisho, and Showa eruptions are indicated as 1st, 2nd, 3rd, and 4th eruptions. Each dot represents an analytical value of K_2O content. The point on the Y-axis indicates K_2O content of magma in the chamber before start of basaltic magma injection. *Two parallel lines* indicate the range of compositional variation in lava flows (Modified from Yanagi et al. (1991))

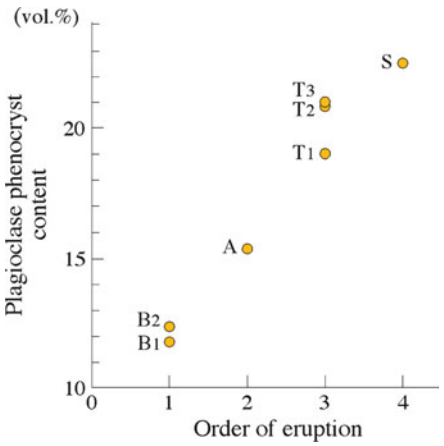

Fig. 6.4 Plagioclase phenocryst contents of historic lava flows versus order of gigantic eruptions. B_1 Bunmei first lava flow, B_2 Bunmei second lava flow, A An-ei lava flow, T_1 Taisho first lava flow, T_2 Taisho second lava flow, T_3 Taisho third lava flow, S Showa lava flow (Modified from Yanagi et al. (1991))

will be given subsequent to presentation of a similar diagram for plagioclase phenocryst contents.

Plagioclase phenocryst contents of the lava flows are plotted in Fig. 6.4 for the massive eruptions. Since the extrusion of lava flows occurred several times during the Bunmei and Taisho eruptions, they are expressed in Fig. 6.4 by subscripts of 1, 2 and 3 in order of extrusion. It is evident that the plagioclase phenocryst content of the lava flow first extruded for each massive eruption increases regularly in sequence of the massive eruptions (Fig. 6.4). This increase indicates that plagioclase phenocrysts are more abundant in the basaltic magma injected into the chamber. The plagioclase phenocryst content also increases in lava flows in order of extrusion in the case of the Taisho and Bunmei eruptions. This increase suggests that the second and third extrusions occurred before sufficient mixing took place after the injection of the basaltic magma.

Similarly, K_2O contents of the Taisho lava flows show the following time-dependent change. K_2O content was relatively high in the lava extruded at the beginning of the extrusion. Then, it gradually decreased with time and reached its minimum, and finally it again increased to its original level in the last phase of the extrusion, about 1 year later. Therefore, it is possible to conclude that this time-dependent variation in K_2O content indicates extrusion of Taisho lava flows before homogeneous mixing of the mixed magma had occurred.

Since it is evident that compositional variation of lava flows was caused by mixing between basaltic magma injected into the chamber and magma in the chamber, it is possible to estimate how much the mass of magma in the chamber increased before the start of a massive eruption. In other words, it is possible to determine the chamber mass increase that triggered the massive volcanic eruption. This estimation can be obtained based on the chemical composition of the lava flows and the two end-member magmas.

Let us set the magma chamber mass and its K_2O content at the time of the nth eruption as M_n and $(K_2O)_n$, respectively. Then let us set K_2O content of the basaltic magma injected into the chamber as $(K_2O)_p$. Let us also suppose that K_2O is

conserved during magma mixing. Then the mass ratio M_n/M_{n-1} is given by the following equation, because $(M_n - M_{n-1})$ is the mass of basaltic magma injected into the chamber.

$$M_n/M_{n-1} = \left\{(K_2O)_{n-1} - (K_2O)_p\right\} / \left\{(K_2O)_n - (K_2O)_p\right\}.$$

If magma composition in the chamber at the time of a massive eruption is represented by composition of the lava flow extruded from the chamber on that occasion, and its K_2O content for the Taisho eruption is estimated by interpolation of the linear relationship shown in Fig. 6.3, then the mass ratio M_n/M_{n-1} is almost constant at 1.16 ± 0.03 through all massive eruptions. To accept this result, however, it is necessary to understand the reason for the constant mass ratio. The important point is that water is conserved during magma mixing. Hence, the mass ratio is expressed with the water content $(H_2O)_p$ of the injected basaltic magma, the maximum water content $(H_2O)_{max}$ of magma in the chamber immediately before an eruption, and the minimum water content $(H_2O)_{min}$ immediately after the eruption, as shown by the following equation.

$$M_n/M_{n-1} = \left\{(H_2O)_p - (H_2O)_{min}\right\} / \left\{(H_2O)_p - (H_2O)_{max}\right\}.$$

Now it is evident that the mass ratio is determined by the water contents before and after the massive eruption. Therefore, the mass ratio is constant as long as these water contents are constant.

6.1.3 *Configuration of the System of Magma Supply and Cumulate Removal*

The constancy of the mass ratio (1.16 ± 0.03) indicates that the chamber is growing at a constant rate of expansion for every massive eruption. The expansion is, in order of historic eruptions, 1.2, 1.3, 1.6, and 1.8 times the initial mass, i.e. the mass of the chamber before the start of magma inflow. The chamber mass at the time of the successive eruptions that continued intermittently from 1955 to the 2000s can be estimated from the composition of ejecta (Aramaki 1980) to be about 2.1 times the initial mass. At a depth of about 10 km, the chamber lies at a depth of about one-third of the thickness of the crust. The distance from there to the mantle is a little more than 20 km. However, the chamber has expanded up to 2.1 times the initial mass.

Another important observation is that prehistoric lava flows lie exactly on the variation line defined by the historic lava flows, as shown in Fig. 6.2. This suggests that the same process took place in prehistoric times. This means that the magma chamber has passed through the following history.

Basaltic magma of the same composition as the basalt listed in Table 6.1 was injected in prehistoric times into a chamber that was occupied by dacite magma of the same composition as the dacite listed in Table 6.1. During this magma injection, prehistoric lava flows were extruded several times. Their compositions, as far as have been analyzed, are almost identical to those of the An-ei, Taisho, and Showa lava flows. After termination of this magma injection, crystallization differentiation continued in the chamber, and finally dacite magma formed again in the chamber. The chemical composition of this residual dacite magma is listed in Table 6.1. Then, injection of basaltic magma of the composition listed in Table 6.1 started again, and during this injection, the extrusion of historic lava flows, namely the Bunmei, An-ei, Taisho, and Showa lava flows, has repeated until the present.

This history signifies that the chamber is surely a refilled magma chamber that is repeatedly supplied with basaltic magma. However, the process can only be imagined within an allowable range of conditions, from which we can adopt a reasonable model. The conditions of this model are as follows. The chamber in the crust is repeatedly supplied with basaltic magma. In addition, when magma is supplied, the chamber volume expands according to the amount of inflow of basaltic magma, finally doubling in mass.

It may be that there is no other possible model besides the one shown in Fig. 6.5. It consists of upper and lower chambers, and a set of a cylinder and a plug between the two chambers. The upper chamber lies in the crust, and the lower chamber lies near the crust-mantle boundary. Basaltic magma supplied from the mantle accumulates first in the lower chamber. Then the plug starts falling after sufficient accumulation. Simultaneously, magma in the lower chamber starts moving upward toward the upper chamber through a narrow opening between the plug and the cylinder. The space necessary for the magma to move within is formed, without any excess or shortage, both in the upper chamber and between the plug and the cylinder. The magma space lost by plug subsidence in the lower chamber is exactly the same as the magma space formed by plug subsidence both in the upper chamber and between the plug and the cylinder. In this configuration of the chamber system,

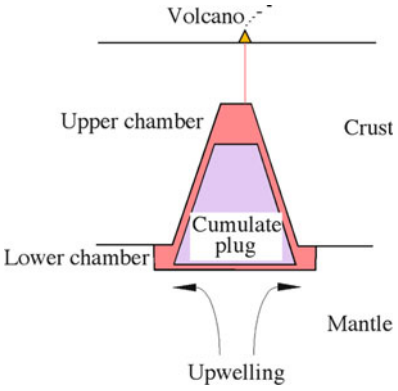

Fig. 6.5 Cross section of the coupled upper and lower chambers. *Red area* represents magma, and *purple area* represents cumulate formed in the upper chamber. *Arrows* indicate flow directions in the mantle beneath the lower chamber (Modified from Yanagi et al. (1991))

it is possible for the magma to move into the upper chamber as stated above, and as a result, it also is possible for the upper chamber to double in volume.

However, this configuration cannot allow the upper chamber to repeatedly accept magma from the mantle. Some mechanical scheme is necessary for this to occur. In the case of the upwelling flow touching the floor of the lower chamber, as shown in Fig. 6.5, it carries basaltic magma into the lower chamber. At the same time, it erodes the lower end of the plug that touches the floor and removes it away from the lower chamber, enabling the plug to subside again. Therefore, in this new configuration, the magma formed from the mantle is carried by the upwelling flow into the lower chamber, and then it moves from the lower chamber to the upper chamber. Thus, cumulate formed in the upper chamber successively subsides into the lower chamber, and then is removed from the lower chamber to the mantle by mantle convection flow. This process continues as long as magma genesis continues in the mantle beneath the chamber. The chamber system, in contact with the upwelling convection flow in the mantle, is the basic model of the repeatedly-refilled magma chamber working in the crust.

Next, plug shape will be examined based on regularity of quiet time intervals between historic massive eruptions. The intervals have become progressively shorter with time, with 303 years between the Bunmei and An-ei eruptions, 135 years between the An-ei and Taisho eruptions, and 32 years between the Taisho and Showa eruptions. Since the difference in K_2O content is constant between lava flows that were extruded first during each of the successive massive eruptions (Fig. 6.3), the magma supply rate must have progressively increased. The mechanism that causes the rate to increase in this way lies in a frustum form of the plug. In the case that the plug is a frustum, the opening between the plug and the cylinder progressively expands with plug subsidence. Then, the magma can move more and more easily with progressive plug subsidence, resulting in an accelerated increase of the subsidence rate. This means that the magma flow rate from the lower to upper chamber accelerates with progressive plug subsidence.

Next, the mechanism of action of this chamber system is presented. Since the density of basaltic magma is high when it accumulates in the lower chamber, the plug may not subside. It starts subsiding after the density sufficiently drops as a result of crystallization differentiation in the chamber. Simultaneously with this start of subsidence, magma starts moving from the lower chamber to the upper chamber. The opening between the plug and the cylinder is very narrow at that time. The magma moves very slowly, taking much time. Water content in the magma in the upper chamber increases because of inflow of the wet basaltic magma. Water pressure increases in the upper chamber and finally reaches the threshold of explosion, resulting in a volcanic eruption. As a result, the water pressure drops quickly, the volcano stops erupting, and the vent is finally closed because of both collapse of walls and solidification of magma in the vent. Subsidence of the plug continues independently of this eruption termination, and the movement of magma from the lower chamber to the upper chamber also continues. Then, water pressure finally reaches the threshold value again, resulting in a second volcanic eruption. Therefore, as long as plug subsidence continues, the volcano erupts again. During

this time, the opening between plug and cylinder expands because of plug subsidence, and the movement of the magma becomes progressively easier with time, resulting in more frequent episodes of eruptions and, sometimes, finally resulting in an eruption that continues over an extended period (i.e., several decades).

Next, the duration of a single basaltic magma injection is estimated. The quiet time interval between massive eruptions has progressively shortened with time, such that there were 303 years between the Bunmei and An-ei eruptions, 135 years between the An-ei and Taisho eruptions, 32 years between the Taisho and Showa eruptions, and 9 years between the Showa eruption and the long-term eruption that has continued intermittently for more than 45 of the years since 1955. If this trend is extrapolated into the past, the origin is estimated to be at 550 years before the Bunmei eruption. This estimate may represent the time when basaltic magma injection began. Since the SiO_2 content of lava flows progressively decreases in order of the massive eruptions and, in addition, the SiO_2 content of bombs ejected during the recent long-term eruption is very close to the minimum found at Mount Sakurajima, a series of historic massive eruptions seems to have come close to its end. If so, injection of the basaltic magma appears to have continued for about 1,000 years.

Even if basaltic magma is injected into the chamber, it may not easily and spontaneously mix with residual dacite magma in the chamber. However, each lava flow extruded during the massive eruptions has been homogeneous. The magmas in the chamber must have been stirred together to become a single homogeneous magma, as discussed further below.

The density of magnetite is 5.2 g/cm^3, and the densities of clinopyroxene and orthopyroxene are 3.2–3.4 g/cm^3. The density of plagioclase is 2.7–2.75 g/cm^3, and the density of the magma is 2.4–2.6 g/cm^3. Since the densities of these phenocrysts are higher than the density of the magma, the former seem to be quickly deposited and lost from the magma. However, the lava flows at Mount Sakurajima contain these phenocrysts in abundance. Figure 6.6 shows a linear relationship between density and the inverse square of the maximum grain size of these phenocrysts.

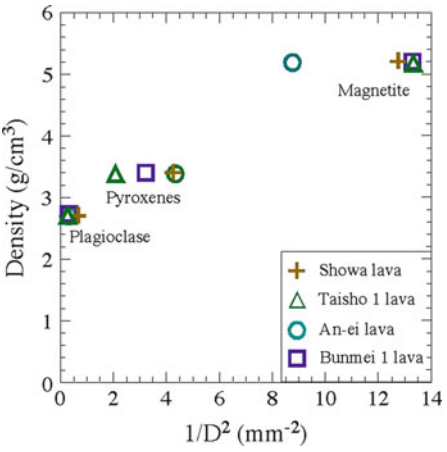

Fig. 6.6 Relationship between sizes and densities of phenocrysts in historic lava flows at Mount Sakurajima. *D* stands for maximum grain sizes of plagioclase, pyroxene and magnetite phenocrysts in each of historic lava flows

The grain size of a phenocryst was expressed by a harmonic mean of lengths of its long side and short side. The maximum size of phenocrysts of a mineral was expressed by the size at 0.5% of the cumulative curve of relative number-frequencies of phenocrysts of sizes greater than 20 μm. In this case, accumulation started from the larger size toward the smaller size. Since the largest phenocrysts are very few, the maximum sizes plotted in Fig. 6.6 are subject to large errors (ca. ±40%). It is, however, evident that the density is nearly proportional to the inverse square of the maximum size. The origin of this linear relationship lies at 2.6 g/cm^3. This linear relationship is a reflection of the fact that the phenocryst with a lower density is larger, and the phenocryst with a higher density is smaller. This means that the magma was stirred, as described below.

Suppose that a spherical phenocryst has continued to sink in magma and finally has attained its terminal velocity. In this situation, gravity acting on the phenocryst is balanced by the resultant force of both buoyancy of the phenocryst and viscous resistance acting on the phenocryst. Therefore, the relationship between the density ρ_x and diameter d of the phenocryst is expressed by the following equation with the density ρ and viscosity η of the magma and the terminal velocity v of the phenocryst and the gravitational acceleration g.

$$\rho_x = 18\eta v/\left(g\,d^2\right) + \rho.$$

This equation signifies that the difference in density between the phenocryst and magma is proportional to the inverse square of diameter of the phenocryst. This is what was observed between the grain sizes and densities of the phenocrysts as shown in Fig. 6.6. Although, in general, phenocrysts in a quiet magma tend to settle on the chamber floor, the lava flows at Mount Sakurajima contain abundant phenocrysts. This means that the magma in the chamber was in motion at the time of lava extrusion and that its upward velocity component was equal to the falling velocity of the phenocrysts. In other words, the magma was stirred and phenocrysts were dynamically suspended in the magma. It is possible that subsidence of the massive plug might have caused the magma in the upper chamber to move, which created this state of magma motion.

6.1.4 Histogram of Orthopyroxene Phenocryst Compositions

As large phenocrysts, plagioclase crystals of low densities are expected to preserve a long-term historical record of the magma, while magnetite phenocrysts of high densities are expected to record only magma characteristics immediately before a lava eruption. This is because the latter are deposited rapidly. Herein, I show that orthopyroxene phenocrysts carry different information than plagioclase phenocrysts.

In Fig. 6.7, an Mg-value (100 × MgO/(MgO + FeO)) of an orthopyroxene phenocryst in a lava flow is plotted on the horizontal x-axis, a T.FeO/MgO ratio

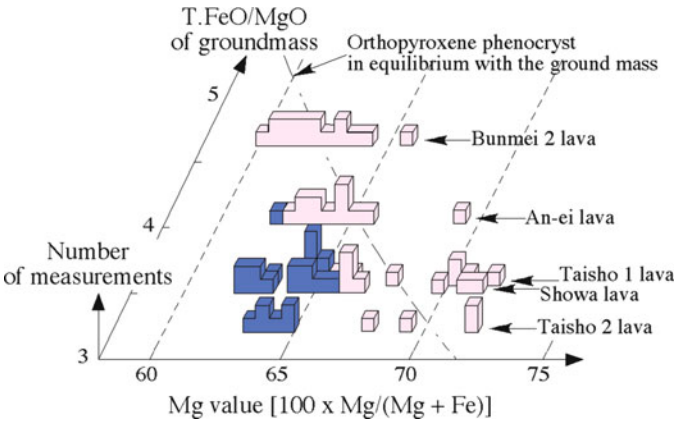

Fig. 6.7 Frequency distributions of orthopyroxene phenocryst compositions in historic lava flows at Mount Sakurajima. *Blue box*, reversely zoned orthopyroxene phenocryst; *pink box*, normally zoned orthopyroxene phenocryst. Mg value is expressed as molar fraction, and T.FeO/MgO is expressed as weight ratio (Modified from Yanagi et al.(1991))

of the host groundmass in the lava flow is plotted on the horizontal y-axis, and the number of measurements of the Mg-value at the center of the orthopyroxene phenocrysts is plotted on the vertical z-axis. Since phenocrysts lie in the common groundmass of the lava flow, Mg-value data for orthopyroxene phenocrysts in the lava flow are arranged in a horizontal row, parallel to the x-axis. From the back row toward the front row in Fig. 6.7, the values are of orthopyroxene phenocrysts from Bunmei's second lava flow, An-ei lava flow, Taisho's first lava flow, Showa lava flow and Taisho's second lava flow. Pink boxes represent normally zoned orthopyroxene phenocrysts and blue boxes represent reversely zoned orthopyroxene phenocrysts. The broken line on the horizontal x-y plane represents orthopyroxene composition in chemical equilibrium with the host groundmass.

From the observations depicted in Fig. 6.7, the Mg-values (62–67) of orthopyroxene phenocrysts from the An-ei, Taisho, and Showa lava flows appear to be slightly larger than the Mg-values (60–64) of the phenocrysts from the Bunmei lava flow. In addition, most of the phenocrysts from the Bunmei and An-ei lava flows appear to have compositions in chemical equilibrium with the host groundmass, while the Taisho and Showa lava flows lack such phenocrysts. These data indicate that crystallization continued even during magma injection and mixing. Furthermore, it is clear that degree of crystallization of orthopyroxene phenocrysts depends on the length of the quiet time interval between massive eruptions. Orthopyroxene phenocrysts in chemical equilibrium with their host groundmass become abundant when the quiet interval is longer than 303 years, which is the time period that elapsed before eruption of the host An-ei lava flows. In this case, crystallization was inevitable because the chamber was at the depth of one-third of the thickness of the Earth's crust and, magma injection continued for about 1,000 years.

6.2 Inevitability of Formation of Coupled Chambers

So far in this book, we have built up a picture of a repeatedly refilled magma chamber for arc volcanoes, in a system of coupled upper and lower chambers, in combination with upwelling convection flow in the mantle that provides material exchange between mantle and crust. In this section is a discussion as to why such a system is formed.

Masses of magma that have successively risen through the mantle accumulate at the base of the crust to form a magma chamber. Since the chamber is repeatedly supplied with magma from the mantle, its ceiling is repeatedly heated and hence continuously melted. Simultaneously, the crystals formed from the magma and melt residue of the ceiling continue to fall through the chamber and accumulate on the chamber floor. As a result, the chamber starts to move upward. When magma from the mantle accumulates beneath the cumulate layer, this layer may break and fall into the magma as long as it is thin. However, with time, the cumulate layer grows in thickness. When it reaches sufficient thickness, magma from the mantle comes to rest beneath it and forms a magma chamber. This is the birth of the coupled chamber system. Since the upper chamber is repeatedly supplied with magma from the mantle *via* the lower chamber, the upper chamber continues to rise. However, the lower chamber always forms between the cumulate layer and the mantle. Accordingly, the cumulate layer becomes progressively thicker with time and acquires a frustum shape, which is the cumulate plug.

Furthermore, there are more important physical implications with regard to crystallization differentiation. In order for crystallization to continue while the chamber is repeatedly supplied with magma from the mantle, the chamber should discharge more heat than the amount of heat repeatedly supplied by the magma from the mantle. To achieve this condition, the upper chamber must continue to rise into progressively lower temperature layers in the crust. This enables the magma in the upper chamber to continuously cool and to continue crystallization differentiation. The reason why this takes place is because the solidus temperature of the crust is almost the same as that of the magma. Because of this, as it is repeatedly supplied with primitive magma, the upper chamber continues to rise by assimilating crust around it. As a result, crystallization differentiation continues in the upper chamber and finally forms magma evolved at low temperatures. Thus, assimilation of the crust is an inescapable magmatic process.

6.3 Lower Crust Assimilation and Its Effect on the Differentiation Path of Magma

As lower crust assimilation has been found to be inevitable, both the chemical composition of a melt formed by partial melting of the lower crust and its effect on magma evolution are examined here.

Fragments of the lower crust often have erupted to the surface together with basaltic magmas. These fragments give us an opportunity to identify the average chemical composition of the lower crust. Basaltic lava flows on the Japan Sea side of southwest Japan contain such lower crustal fragments. They consist mostly of gabbros, norites, and pyroxenites. The average chemical composition is 48.8 wt% SiO_2, 1.3 wt% TiO_2, 17.7 wt% Al_2O_3, 9.9 wt% T.FeO, 0.2 wt% MnO, 8.0 wt% MgO, 11.4 wt% CaO, 2.4 wt% Na_2O, 0.3 wt% K_2O, and 0.1 wt% P_2O_5. Since the liquidus mineral phases at pressures of about 1 GPa are clinopyroxene (50–53 wt% SiO_2), orthopyroxene (53–55 wt% SiO_2) and plagioclase (48–53 wt% SiO_2), the SiO_2 content of the residue formed by partial melting from this lower crust is greater than the SiO_2 content of the lower crust. Therefore, the melt produced by partial melting from this lower crust is basaltic in composition. When water is present, amphibole (ca. 40 wt% SiO_2) and plagioclase are liquidus phases. Accordingly, the residue formed by partial melting from the amphibolite lower crust is lower in SiO_2 content than the lower crust. Thus, dacitic to andesitic magma forms initially at low temperatures. With increase in the degree of melting, the residue separates from the chamber ceiling. It then falls through the magma and finally accumulates on the chamber floor. During this period, it continues to be heated. Heating continues even after accumulation on the floor until it attains the temperature of the magma in the chamber. Therefore, the composition of the total melt formed all through this process is basaltic, when the magma in the chamber is basaltic.

In addition, because the lower crust is made of basaltic cumulates, the melt produced by partial melting from the lower crust traces the same path as that of a basaltic magma in major element composition, although the direction of compositional change of the melt during melting is opposite to the direction of compositional change of basaltic magma during crystallization differentiation. Therefore, assimilation of the lower crust has an insignificant effect on the path of magmatic differentiation.

As long as the degree of melting is small, the concentration of an incompatible element in the melt is almost the same as that in the magma in the chamber. However, it falls when the melting degree increases. On the other hand, assimilation promotes crystallization of the basaltic magma and hence raises the concentration of the incompatible element. Since these effects offset each other, it is not easy to recognize assimilation from an analysis of incompatible element concentrations in the magma. However, magma evolution is related to assimilation. The input of the open-system magma chamber is the supply of parental magma, and the output is removal of the cumulate from the chamber. Insomuch as the assimilation is associated with magma evolution, the assimilation works as a part of the input. Therefore, it is necessary to examine its effect on the convergent composition.

Since, as stated above, the open-system magma chamber continues to rise in the crust toward the surface, the temperature of the magma continues to fall, and crystallization differentiation in the chamber continues to advance. Even in the case that the temperature finally becomes low enough not to melt the surrounding crust, the chamber continues to be repeatedly supplied with parental magma. Under

these conditions, the convergent composition of the magma in the chamber is simply determined by the composition of the parental magma. The crustal assimilation that continued until then has an almost insignificant effect on the convergent composition. Aspects relevant to this process will be presented in the next section.

6.4 Lower Crust Assimilation as Observed in Volcanic Rocks

Clearly, for the refilled magma chamber to rise by assimilating the crust is an inevitable result of the repetitive supplying of parental magma. The following example supports this assertion.

Since the upper and lower crustal components of southwest Japan are both higher in $^{87}Sr/^{86}Sr$ ratio than the mantle, crustal assimilation is elucidated by measuring $^{87}Sr/^{86}Sr$ ratios of volcanic rocks. Results of such studies on Mount Kinpo (Yanagi et al. 1988) are as follows.

Mount Kinpo, west of the city of Kumamoto in Kyushu, Japan, is a composite stratovolcano that was active about 1 million years ago. It consists mostly of andesite lava flows and related pyroclastic rocks. These volcanic rocks are stratigraphically classified into four groups. They are, in chronological order, the Matsuo, the Older Kinpo, the San-notake, and the Ninotake Group. The results of $^{87}Sr/^{86}Sr$ ratio measurements of these volcanic rocks are shown in Fig. 6.8.

In the diagram, mixtures of two end-member magmas having different $^{87}Sr/^{86}Sr$ ratios lie on a straight line that connects these end-members. This diagram is used

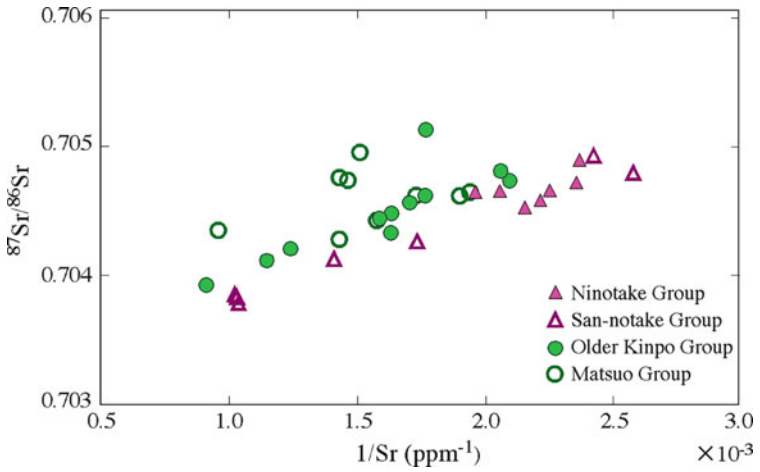

Fig. 6.8 Relationship between 1/Sr and $^{87}Sr/^{86}Sr$ ratio of volcanic rocks from Mount Kinpo. Matsuo Group is the oldest, and Ninotake Group is the youngest. Volcanic rocks are arranged in stratigraphic order (Modified from Yanagi et al. (1988))

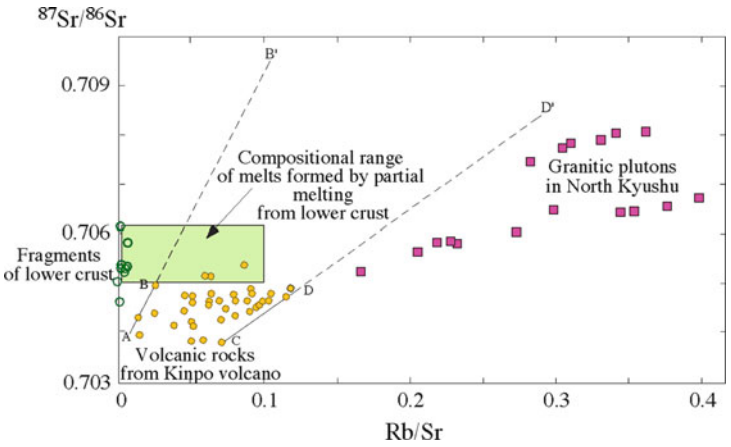

Fig. 6.9 Relationship between Rb/Sr and $^{87}Sr/^{86}Sr$ ratios of volcanic rocks from Mount Kimpo. Granitic plutons in North Kyushu are shown as representative rocks of upper crust. Volcanic rocks lie between lines AB and CD (Modified from Yanagi et al. (1988))

because such linear arrangement makes the data easy to analyze. Although there are a few exceptions, volcanic rocks from a single volcanic group tend to show a linear array, and volcanic rocks from different groups lie on different lines, as shown in Fig. 6.8. The array line for older rocks tends to lie at a position higher in $^{87}Sr/^{86}Sr$ ratios, and the array line for younger rocks tends to lie at a position lower in $^{87}Sr/^{86}Sr$ ratios.

Since the linear array seems to reflect mixing of two end-member magmas having different $^{87}Sr/^{86}Sr$ ratios, these end-members should be examined first. By extrapolating the array lines in Fig. 6.8 toward the left hand side, they appear to converge at 1,200 ppm of Sr and 0.7037–0.7040 of $^{87}Sr/^{86}Sr$ ratio. The $^{87}Sr/^{86}Sr$ ratio of this point is low and corresponds to those found in the mantle. Therefore, one end-member seems to be common to volcanic rocks of all groups, and appears to be a magma derived from the mantle.

Figure 6.9 shows the other end-member with a high $^{87}Sr/^{86}Sr$ ratio. The x-axis shows the Rb/Sr ratio of various rocks. In general, Rb/Sr ratio varies greatly depending on rock types. Hence, this diagram makes the identification of rock type of the end-member easier, where mixtures between two end-members also are arranged on a line that connects them.

Small yellow circles on the lower left-hand side of the diagram represent volcanic rocks. Lines AB' and CD' limit the distribution of volcanic rocks to the left-hand and right-hand sides, respectively. Therefore, the mixing end-members should lie between these two lines. Since one end-member has now been found to be magma of mantle origin, the problem is to confirm the other end-member with a high $^{87}Sr/^{86}Sr$ ratio. Granitic plutonic rocks from northern Kyushu, which represent rocks of the upper crust, lie on the right-hand side of line CD'. Hence, they are unlikely candidates. The white circles arranged along the y-axis represent

fragments derived from the lower crust of southwest Japan. These fragments lie on the left-hand side of line AB'. However, partial melting of these fragments produces melts of compositions that lie in between lines AB' and CD'. They have high $^{87}Sr/^{86}Sr$ ratios. The compositional range of such melts is shown by the green rectangle in Fig. 6.9. Thus, it is evident that such melts fulfill the conditions of an end-member having a high $^{87}Sr/^{86}Sr$ ratio. In other words, a series of primitive magmas supplied to the chamber partially melted the lower crust and formed crust-derived melts. Such melts were successively incorporated into the magma in the chamber. On the other hand, the various magmas formed during mixing between such chamber magma and repeatedly supplied primitive magmas built up Mount Kinpo through repetitive extrusions.

We have already discussed the fact that the array line for rocks of the younger group tends to lie at a position of lower $^{87}Sr/^{86}Sr$ ratios (Fig. 6.8). The implication of this trend is examined next.

While the chamber was positioned at the base of the crust, the temperature of the magma in the chamber was kept high due to repetitive supplies of parental magma from the mantle. Accordingly, the magma in the chamber assimilated the ambient lower crust with high $^{87}Sr/^{86}Sr$ ratios, and the chamber kept rising in the crust. During this period, the $^{87}Sr/^{86}Sr$ ratio of the magma was maintained at a high value. However, the more the chamber moved up, the more the ambient temperature fell. Thus, heat lost from the chamber in unit time progressively increased. As a result, the temperature of the magma in the chamber progressively fell, and thus its assimilation ability progressively dropped. This resulted in progressive drop of the $^{87}Sr/^{86}Sr$ ratio of the magma in the chamber, because the supply of primitive magma with low $^{87}Sr/^{86}Sr$ ratios from the mantle continued. Therefore, the fact that the array line for younger rocks tends to lie at a position of lower $^{87}Sr/^{86}Sr$ ratio (Fig. 6.8) is the most important evidence for progressive rise of the chamber in the crust during growth of the volcano.

Lower crust assimilation has already been reported at Mounts Unzen, Tara, Myoko, and other volcanoes in Japan. Volcanic rocks whose Rb/Sr ratios are low, as those of primitive magmas and whose $^{87}Sr/^{86}Sr$ ratios are higher than those of primitive magmas, are abundant in Japan (Fig. 5.6). They are all volcanic rocks that have assimilated the lower crust. The fact that the $^{87}Sr/^{86}Sr$ ratio is high in volcanic rocks of early stages and low in volcanic rocks of late stages is also commonly observed in many other volcanoes, such as Mounts Unzen, Tara, and Myoko. This suggests that rise of the chamber by assimilating crust is common to arc volcanoes.

References

Aramaki S (1980) Chemical compositions of recent ejecta from the south crater at Sakurajima volcano. The 3rd Joint Observations of Sakurajima Volcano, Kyoto University Disaster Prevention Research Institute, Sakurajima Volcano Research Centre, pp 105–109 (In Japanese)

Fukuyama H, Ono K (1981) Geological map of Sakurajima volcano, 1:25,000. Geological map of volcanoes. Geol Surv Japan 1:1–8 (In Japanese with English abstract)

Ishihara K, Takayama T, Tanaka Y, Hirabayashi J (1981) Lava flows at Sakurajima volcano (1), Volume of the historical lava flows. Annu Disas Prev Res. Inst Kyoto Univ 24B:1–10 (In Japanese with English abstract)

Kamo K, Ishihara K (1980) Volcanic activity of Sakurajima as inferred from the ground deformation. Sakurajima regional science investigation conference's research report, 19–28 (In Japanese with English abstract)

Kobayashi T (2002) Eruption history of Sakurajima volcano, 8th open lecture, Volcanol. Society Japan. (http://hakone.eri.u-tokyo.ae.jp/kazan/jishome/koukai01/kobayashi.html)

Mogi K (1958) Relations between the eruptions of various volcanoes and the deformations of the ground surface around them. Bull Earthq Res Inst 36:99–134

Yanagi T, Arikawa H, Hamamoto R, Hirano I (1988) Petrological implications of strontium isotope compositions of the Kinpo volcanic rocks in Southwest Japan: ascent of the magma chamber by assimilating the lower crust. Geochem J 22:237–248

Yanagi T, Ichimaru Y, Hirahara S (1991) Petrochemical evidence for coupled magma chambers beneath the Sakurajima volcano, Kyushu, Japan. Geochem J 25:17–30

Chapter 7
Island Arc Volcanic Rocks and the Upper Continental Crust

7.1 Magma Evolution in Incompatible Element Compositions

It has been found that primitive basaltic magma evolves by crystallization differentiation in the repeatedly refilled magma chamber to magma of chemical composition of the upper continental crust, and that arc volcanic rocks are lavas extruded from the chamber in the act of undergoing this transformation. To confirm these observations further, it is necessary to examine major element and other minor element compositions of arc volcanic rocks. First minor element compositions and then major element compositions are presented.

7.1.1 Incompatible Element Ratios, and Concentration Limits of Incompatible Elements

To understand the characteristics of behavior of an incompatible element composition during crystallization differentiation of magma, let us assume potassium and rubidium concentrations of the parental magma to be 2,000 and 4 ppm, respectively. In addition, let us assume their partition coefficients to be 0.1 and 0.05, respectively. These concentrations and partition coefficients are all approximate values. Figure 7.1 shows a comparison between compositional variations caused by fractional crystallization in closed-system and open-system magma chambers. Line PL shows the compositional change of magma in a closed-system chamber. Letters M and R, respectively, represent mixed-magma and residual magma compositions in an open-system chamber that is periodically supplied with parental magma. Curves PM_∞ and PR_∞ represent traces of mixed and residual magmas in an open-system chamber, respectively. Line $M_\infty R_\infty$ indicates the compositional

T. Yanagi, *Arc Volcano of Japan*, Lecture Notes in Earth Sciences 136,
DOI 10.1007/978-4-431-53996-4_7,

change caused by fractional crystallization in the open-system chamber at steady state.

During fractional crystallization in the closed-system chamber, concentrations of these two elements proportionally increase in logarithmic coordinates (Fig. 7.1a). In principle, the concentration of both elements increases infinitely as long as crystallization differentiation continues. There are no upper concentration limits. On the other hand in the open-system chamber, rubidium concentration increases more than potassium concentration, and there are concentration limits of these two incompatible elements at point R_∞ (Fig. 7.1a).

Figure 7.1b shows variations in the Rb/K ratio of the magma caused by fractional crystallization in the closed-system and open-system chambers. Although the increase in Rb/K ratio is rather small in the closed-system chamber, it increases

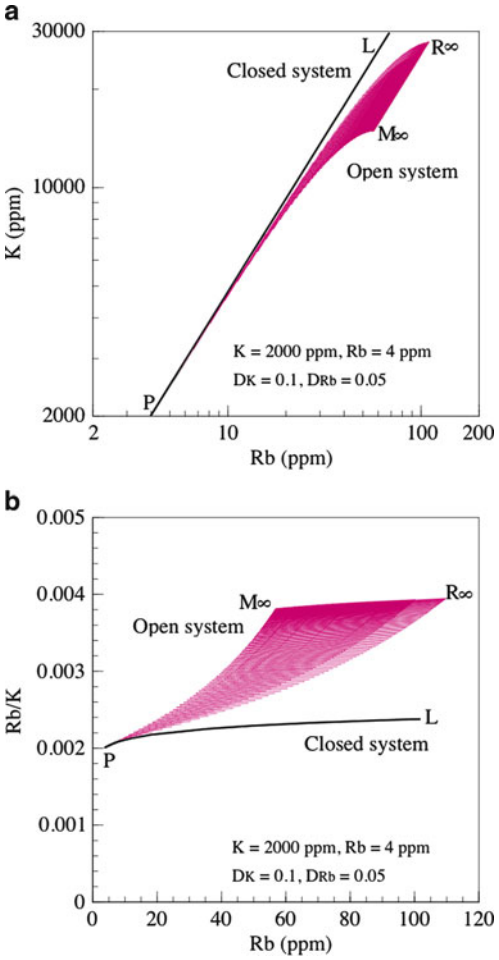

Fig. 7.1 Variations in Rb, K contents and Rb/K ratio of magma during fractional crystallization in closed and open system magma chambers. *P* stands for parental magma. D_K and D_{Rb} stand for partition coefficients of potassium and rubidium, respectively. *Line PL* in (**a**) and (**b**) shows a compositional change of magma during fractional crystallization in a closed-system chamber. *M* stands for mixed magma, and *R* stands for residual magma in an open-system chamber. *Points* M_∞ and R_∞ represent compositions of mixed and residual magma at steady state, respectively. *Curve* $M_\infty R_\infty$ in (**a**) and (**b**) shows compositional change of magma during fractional crystallization at steady state. *Fractionation line* M_nR_n at *n*th chemical step is nearly parallel to Curve $M_\infty R_\infty$ in (**a**) and (**b**). *Curves* PM_∞ and PR_∞ in (**a**) and (**b**) represent traces of mixed and residual magma compositions, respectively

markedly in the open-system chamber, and finally becomes twice the Rb/K ratio of the parental magma, due to accumulation of small increments by fractional crystallization that repeats at every chemical step. This large growth in Rb/K ratio is caused by the small difference in magnitude between their partition coefficients.

7.1.2 *Incompatible Element Compositions and Ratios of Volcanic Rocks*

Figure 7.2 shows Rb/K ratios of Quaternary volcanic rocks from Japan. Although the distribution of volcanic rocks in Fig. 7.2 is akin to what is expected from fractional crystallization in the open-system chamber (Fig. 7.1b), the distribution of volcanic rocks over a range less than 30 ppm of rubidium is much wider and hence different from the result of the model calculation. Thus this should be accounted for first in the analysis.

In the calculation, the open-system chamber is repeatedly supplied with parental magma of the same composition. Both potassium and rubidium concentrations, however, fluctuate over half an order of magnitude in primary magmas because of the chemical heterogeneity of the mantle. Therefore, the above stated wider distribution of volcanic rocks in the diagram (Fig. 7.2) is thought to be a reflection of this heterogeneity. Nonetheless, the vertical width of the distribution on the diagram, which represents the variation range of the Rb/K ratios becomes narrower with

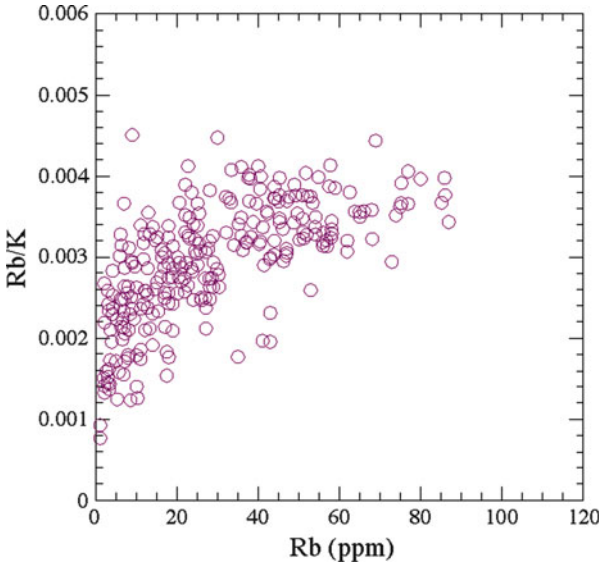

Fig. 7.2 Rb contents and Rb/K ratios of Quaternary volcanic rocks from Japan. Data for volcanic rocks are from a lot of literature

increase of rubidium concentration. This observation will be accounted for in the following example.

With respect to rubidium, a parental magma of 2 ppm and another parental magma of 10 ppm come to have 4 and 20 ppm after 50% crystallization in closed-system chambers, respectively. The concentration ratio of the latter to the former is five. This ratio is maintained all through fractional crystallization in closed-system chambers. In the case that the chamber is repeatedly supplied randomly with these parental magmas, the rubidium concentration in magma in the chamber fluctuates in the early stage of magma evolution, caused by continuous fractional crystallization in the chamber. When the concentration reaches 80 ppm, for instance, the fluctuation is reduced to within a range of ±6% of the concentration. This occurs because the fluctuation becomes relatively narrower owing to increase in rubidium concentration driven by continuous crystallization in the chamber. Namely, this is an enrichment effect. The same phenomenon will also happen with potassium. This is the reason why the Rb/K ratio does not fluctuate once the rubidium concentration exceeds a certain level.

The Rb/K ratio of volcanic rocks increases from 0.0008 to 0.0028 to 0.004 with increase in rubidium concentration, i.e., the Rb/K ratio almost doubles. This magnitude of increase could not occur in a closed-system chamber (Fig. 7.1). It is, however, possible in the open-system chamber (Fig. 7.1). In addition, the increase is stopped at 0.004. This value corresponds to the Rb/K ratio realized at steady state in the open-system chamber (Fig. 7.1). With only a few exceptions, there are no volcanic rocks with Rb/K ratios greater than 0.004.

Figure 7.3 shows incompatible element compositions of Quaternary volcanic rocks from Japan. It reveals that there are concentration limits unique to respective incompatible elements.

Scatterings of volcanic rocks are generally large at low concentrations of incompatible elements. These scatterings commonly become narrower with an increase in the incompatible element concentrations. And simultaneously the distribution densities of rocks commonly become higher. Then, the distributions of volcanic rocks are suddenly interrupted at points of both the highest concentrations and highest distribution densities. These characteristics of the distributions suggest that these points represent the concentration limits. These common behaviors of incompatible elements could not be expected from magma evolution caused by fractional crystallization in a closed-system chamber. To the contrary, they coincide well with those expected from magma evolution caused by fractional crystallization in an open-system chamber. The large scatterings in the ranges of low concentrations reflect mantle heterogeneity. By contrast, the narrowing of the scattering ranges with an increase in their concentrations reflects the enrichment effect stated above. Finally, these concentration limits are reasonably expected to represent the concentrations in the residual magma formed by fractional crystallization at steady state in an open-system chamber. These concentration limits are identical with reported compositions of upper continental crust (Fig. 7.3).

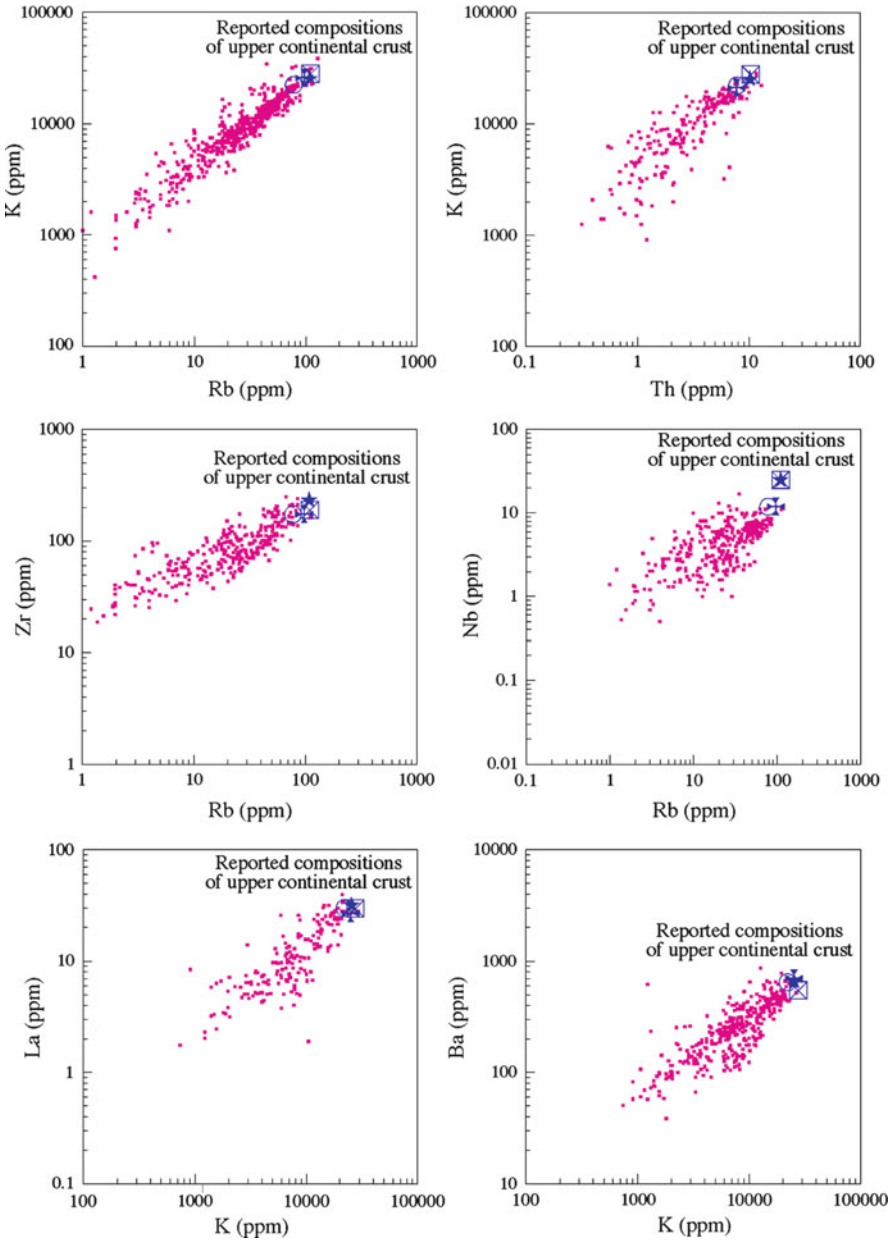

Fig. 7.3 Incompatible element contents of upper continental crust and Quaternary volcanic rocks from Japan. Reported compositions of upper continental crust are from Taylor and McLennan (1985), *box with* x; Condie (1993), *cross*; Wedepohl (1995), *star*; Gao et al. (1998), *circle*. Data for volcanic rocks are from a lot of literature

7.2 Evolution of Volcanic Rocks in Major Element Compositions

Petrological characteristics of volcanic rocks and the upper continental crust are determined by their major element compositions. Whether the same conclusion can be made for major element compositions is examined in the following section.

7.2.1 Volcanic Rocks from Shimabara Peninsula

In this book, examination of major element compositions of volcanic rocks starts with analysis of the time-dependant variation in chemical compositions of volcanic rocks from the Shimabara Peninsula, western Kyushu, based on a study conducted by Sugimoto (1999). The Shimabara Peninsula is semicircular in shape and about 18 km across. Mount Unzen lies at the center of the peninsula, and volcanic rocks extruded during the growth of this volcano cover the entire peninsula.

Volcanic activity started with extrusion of basaltic lava flows about 4.60 million years ago. Mostly basalts were formed in the early stages, while pyroxene andesites and related rocks formed during the middle stages, and hornblende andesites, dacites and related rocks formed in late stages of the growth history of this volcano. Although Sugimoto recognized 11 stages in its growth history, 4 of these 11 stages are periods of deposition of clastic sediments. The remaining seven stages are numbered from 1 to 7 in order of their formation, and the term ‘stage’ used here signifies a mappable stratigraphic unit usually containing few chemical steps. Variation ranges of K_2O contents and Rb/Sr ratios of volcanic rocks of individual stages are shown in Fig. 7.4 in order of these stages. The sequence patterns of these ranges shown in Fig. 7.4 indicates sawtooth time-dependant variations in both K_2O content and Rb/Sr ratio, suggesting magma evolution due to crystallization differentiation in a chamber repeatedly supplied with parental magma. Characteristics of the sawtooth time-dependant variation are as follows. The first is that the chemical variation range in a stage strongly overlaps that of the next stage. The second is that the top of the chemical variation range progressively moves upward (toward more evolved magma compositions) together with an increase in stages. The third is that a movement rate of the top from one stage to the next gets smaller with time, and almost vanishes in the last four stages. These characteristics suggest that chemical variations in the last four stages have almost reached steady state. The volcanic rocks at the top of the variation range of these last four stages are the most evolved, having both the highest potassium contents and highest Rb/Sr ratios. Conversely, volcanic rocks at the lower end of the first stage are the most primitive, having both the lowest potassium contents and the lowest Rb/Sr ratios. Although our interest lies in the major element compositions of the most-evolved volcanic rocks from the last four stages, petrological variations of volcanic rocks are presented first.

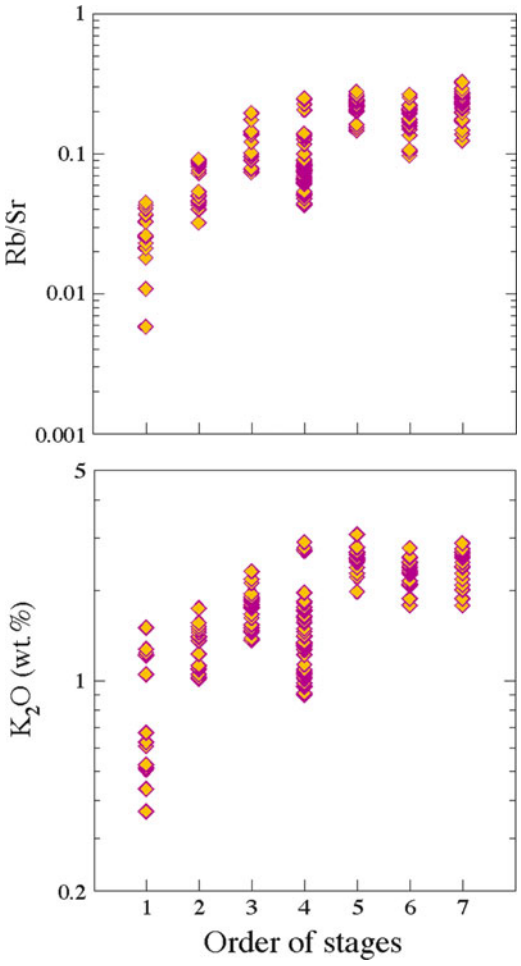

Fig. 7.4 Variation ranges in K_2O content and in Rb/Sr ratio of lavas from individual volcanic stages at Shimabara peninsula (Modified from Sugimoto (1999))

At Mount Sakurajima, the extrusion of magma to the surface was found to have repeated during a period of magma injection into the chamber. Disintegration and melting of phenocrysts, caused by heating of a low-temperature magma by an injected basaltic high-temperature magma, also are observed in almost all volcanic rocks from the Shimabara Peninsula. The most frequently observed pieces of evidence are: (1) opacite produced by dehydration from hornblende and biotite phenocrysts; (2) clear glass produced by melting from a quartz phenocryst; and (3) dusty melt inclusions produced by partial melting of a plagioclase phenocryst. These features are scarce in dacites and abundant in andesites. Opacites derived from both hornblende and biotite phenocrysts are very few in dacites. If present, they formed as very thin films around hornblende and biotite phenocrysts. In basaltic andesites, however, almost all hydrous-mineral phenocrysts have completely changed to opacites by dehydration reactions. These facts suggest that

the proportion of injected high-temperature magma was small in the dacites, whereas it was very large in the basaltic andesites. It is often observed that a single rock sample from a lava flow contains phenocrysts of all rock-forming minerals that appear in subalkaline volcanic rocks such as olivine, clinopyroxene, orthopyroxene, hornblende, biotite, plagioclase, quartz, and magnetite. Originally, however, orthopyroxene, hornblende, biotite, quartz and magnetite crystallize from low-temperature magmas. Conversely, olivine crystallizes from high-temperature basaltic magmas, and clinopyroxene commonly crystallizes from high-temperature basaltic magmas.

Collectively these data suggest that lavas were extruded from the chamber during injection of high-temperature basaltic magmas into low-temperature dacitic magmas. Any lava extrusion seems to have occurred before evidence for magma mixing was erased by high-temperature reactions. Therefore, it stands to reason that any chemical variation range of volcanic rocks in any stage in Fig. 7.4 represents a range of compositional changes that occurred in the period of injection of the basaltic magma. The proportion of injected basaltic magma in stages under steady state conditions can be roughly estimated from the magnitude of K_2O-content drop that occurred within a single stage, because the drop is considered to be due to magma injection.

The primitive parental magma is assumed to contain about 0.4 wt% of K_2O. K_2O contents at the top and the bottom of the variation ranges of the sixth and seventh stages (Fig. 7.4) are almost identical at 2.8, and 1.7 wt%, respectively. Most likely, volcanic rocks at the top and bottom of these K_2O variation ranges represent magma compositions at the start and end of basaltic magma injection, respectively. If this was the case, then the volume of magma in the chamber might have nearly doubled because of the injection of basaltic magma. This magnitude nearly corresponds to the magnitude of volume expansion estimated for the chamber beneath Mount Sakurajima.

Next, we examine the outline of the differentiation course followed by the magma in the chamber beneath the Shimabara Peninsula. The most primitive lava flows were extruded in the first stage. Their K_2O and Rb contents and Rb/Sr ratio are 0.4 wt%, 4 ppm and 0.006, respectively. All these are values commonly found in primitive magmas derived from the mantle. Magmatic evolution started from these values. Then the peak Rb content reached 30 ppm in the first stage, 45 ppm in the second stage, 70 ppm in the third stage, and became constant at 91 ppm in the following four stages. Peak K_2O content followed a similar variation trend and finally became constant at 2.8 wt% in the last four stages. Peak Rb/Sr ratio also increased with increase in stage and then became constant at 0.3 over the last four stages. Likewise, it is confirmed that the chemical variations were almost at steady state in the last four stages. Peak values of K_2O, Rb and Rb/Sr ratios of dacites extruded in the last four stages were 2.8 wt%, 91 ppm and 0.3, respectively. All these values are identical to reported chemical compositions of the upper continental crust listed in Tables 2.2 and 5.2. The average major element composition of dacites extruded in the last three stages also matches reported major element compositions of the upper continental crust (Table 7.1), which are the same as

Table 7.1 Average compositions of dacites

	Dacite Unzen (wt.%)	Dacite Tara (wt.%)
SiO_2	64.97	65.55
TiO_2	0.68	0.65
Al_2O_3	15.88	16.21
$T.Fe_2O_3$	5.01	4.56
MnO	0.09	0.10
MgO	2.46	2.00
CaO	4.58	4.18
Na_2O	3.61	3.84
K_2O	2.56	2.73
P_2O_5	0.16	0.18
Total	100.00	100.00

$T.Fe_2O_3$, total iron as Fe_2O_3

the average chemical composition at the surface of the continental crust in Canada (Table 2.2).

7.2.2 Volcanic Rocks from Mount Tara

Mount Tara is located about 35 km northwest of Mount Unzen, and is an isolated stratovolcano with a radius of about 25 km. The compositional evolution of its volcanic rocks is presented in the following section, based on a study conducted by Ogata (1993).

The volcano started its activity 1 million years ago with extrusion of basaltic lava flows and ended its activity 640,000 years ago with extrusion of dacite lavas. Its growth history has been divided into five stages (Ogata 1993). Figure 7.5 shows frequency distributions in SiO_2 content of volcanic rocks from the first, second, third and fifth stages. The first stage was a period of extrusion of an enormous volume of basaltic lava flows that formed the lava plateau upon which the stratovolcano grew. These basaltic lava flows range in composition from tholeiitic to olivine basalts. Rubidium, barium, potassium, niobium, strontium, phosphorus, zirconium, titanium, and yttrium abundances in primitive members of the basalts have the same characteristics as those in hot-spot-type oceanic island basalts, suggesting that the Tara basalts originated from the same source as the source mantle for oceanic island basalts. The second stage constituted a period of extrusion of volcanic rocks of the Fenner's series, which range from basalts to andesites, and the third stage was a period of extrusion of volcanic rocks of the Bowen's series, which range from pyroxene andesites to hornblende dacites. Thermal disintegration of hornblende and biotite phenocrysts, partial melting of plagioclase phenocrysts, and corrosion of quartz phenocrysts characterize volcanic rocks of the third and fifth stages. The fourth stage consisted of a period of extrusion of basaltic lava flows around the periphery of the volcano, in an interval between the third and fifth stages.

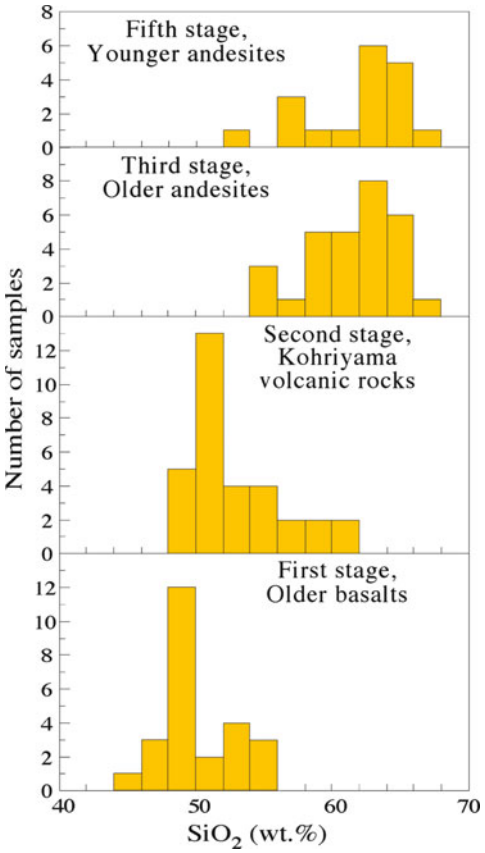

Fig. 7.5 Progressive migration toward the higher SiO_2 side of the frequency distributions of SiO_2 contents of lavas from individual volcanic stages at Mount Tara (Modified from Ogata (1993))

The basalts are the same composition as those extruded in the first stage, suggesting a continued supply of the same primitive magma. The andesitic and dacitic lavas and pyroclastic rocks of Bowen's series in the fifth stage cover the entire volcano. These volcanic rocks are the same composition as those of the third stage (Fig. 7.5).

Since the stratigraphic division is coarse, the time-dependent chemical variation in these volcanic rocks could not be traced in detail. However, Fig. 7.5 shows a sawtooth-type time-dependent compositional variation. This supports crystallization differentiation in the open-system magma chamber. Peak values of SiO_2 contents in the third and fifth stages are identical to each other at 66 wt%. Peak values of Rb/Sr ratios in these stages are also similar to each other at 0.3. These data suggest that volcanic rocks having these peak values formed under steady state conditions. Their average chemical composition listed in Table 7.1 is the same as reported compositions of the upper continental crust (Table 2.2). Hence, it is again confirmed that magma with a chemical composition identical to upper continental crust formed at Mount Tara.

7.2.3 Closed-System Versus Open-System Magma Chambers

So far, we have studied how magma identical in major element composition to the upper continental crust was formed beneath a few arc volcanoes. Examples cited up to this point, however, are very few. It is necessary now to examine whether island-arc volcanic rocks were all produced by the same mechanism.

Volcanic rocks from the Nasu volcanic zone in northeast Japan, which were collected and analyzed by Masuda and Aoki (1979), are plotted in Fig. 7.6. Since they found that volcanic rocks of the Fenner's series were commonly lower in K_2O content, and that those of the Bowen's series were commonly higher in K_2O content, they concluded that the former had been produced by fractional crystallization from a low-K_2O parental magma, and that the latter had been produced by fractional crystallization from a high-K_2O parental magma. However, there is a problem with this interpretation. Because the crystallization temperature of an MgO-rich member is generally higher than that of an Fe-rich member in a solid solution series of mafic silicate mineral crystallization, the MgO-rich member crystallizes earlier than the Fe-rich member during crystallization differentiation of basaltic magma. This results in an increase in T.FeO/MgO ratio of the residual magma. This relationship between crystallization temperature and composition of the solid solution series is not affected by K_2O contents of magmas. The T.FeO/MgO ratio always increases in K_2O-rich magmas by crystallization of such mafic silicate minerals. This conflicts with data used for recognition of the Bowen's series, where T.FeO/MgO ratio does not increase with evolution of Bowen's series volcanic rocks.

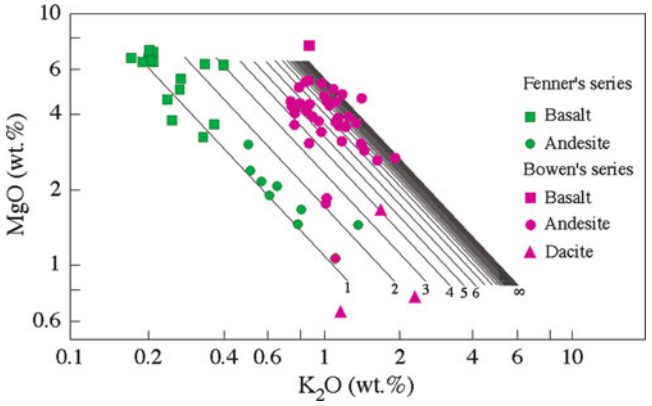

Fig. 7.6 Chemical compositions of volcanic rocks from the Nasu volcanic zone, and magma evolution by fractional crystallization in the repeatedly refilled chamber. Compositional data for volcanic rocks are from Masuda and Aoki (1979). A set of *diagonal lines* shows the entire process of magma evolution caused by fractional crystallization in a chamber that is repeatedly supplied with parental magma. *Numerals* attached to some of these lines show chemical steps. The *rightmost line* with a mark of ∞ shows magma evolution caused by fractional crystallization at steady state. The *leftmost line* is a linear approximation of the compositional variation in residual liquids of the Skaergaard Intrusion (Modified from Yanagi and Yamashita (1994))

The reason Masuda and Aoki (1979) assumed a high-K_2O parental magma for volcanic rocks of the Bowen's series is explained here by referring to the fractionation trend shown in Fig. 7.7. The linear arrangement of the residual liquid compositions of the Skaergaard Layered Intrusion (Wager 1960; Wager and Brown 1967) represents a natural compositional change that the magma traced during fractional crystallization. This and two other linear arrays (Fig. 7.7) are almost identical to each other. One is of respective average compositions of basalts, basaltic andesites, andesites, and dacites of the Fenner's series from the Nasu volcanic zone in northeast Japan (Yagi et al. 1963). The other is of respective average compositions for basalts, basaltic andesites, andesites, and dacites of the Fenner's series from the Izu-Hakone volcanic region in Central Japan (Kuno 1959). If the variation in residual liquids of the Skaergaard Intrusion is assumed to actually represent magma evolution during fractional crystallization, the linear distribution of volcanic rocks of the Fenner's series from Nasu volcanic zone in Fig. 7.6 should be well accounted for by fractional crystallization of low-K_2O parental magma. But volcanic rocks of the Bowen's series cannot be produced simply by fractional crystallization from such low-K_2O parental magma. As far as fractional crystallization is simply assumed, it is necessary that a high-K_2O parental magma evolves to produce volcanic rocks of the Bowen's series. Hence, this is the reason two parental magmas were assumed for volcanic rocks from the Nasu volcanic zone.

The classification of volcanic rocks into two series seems to indicate presence of two types of volcanoes, but this is not the case. In fact, volcanic rocks of these two series occur together, and may be discriminated through petrological examination. Furthermore, rocks of the Fenner's series tend to be predominant during early stages, and rocks of the Bowen's series tend to become overwhelmingly abundant in later stages of growth histories of individual volcanoes.

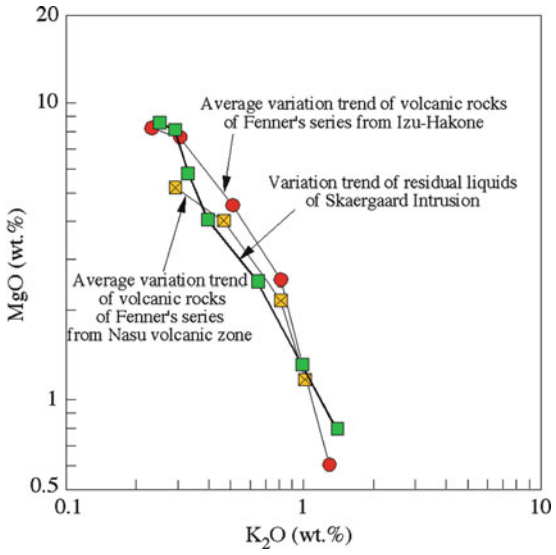

Fig. 7.7 Evolution trends of Fenner's series volcanic rocks and of residual liquids of the Skaergaard Layered Intrusion. Points for volcanic rocks represent respective average compositions of basalts, basaltic andesites, andesites, and dacites (Data are from Kuno (1959) and Yagi et al.(1963). Compositional data for residual liquids of Skaergaard Intrusion are from Wager (1960) and Wager and Brown (1967))

Based on the variation trend of residual liquid compositions of the Skaergaard Intrusion, magma evolution caused by fractional crystallization in the open-system magma chamber is examined next. Calculation results shown in Fig. 7.6 indicate an overlap with data for volcanic rocks from the Nasu volcanic zone. A set of straight lines shows the entire process of magma evolution caused by fractional crystallization in a chamber that is repeatedly supplied with primitive parental magma. And an individual line of this set shows compositional change caused by fractional crystallization at one chemical step. The leftmost line is a linear approximation of the compositional variation in residual liquids of the Skaergaard Intrusion. This fractionation line moves step by step toward the right hand side because the magma is enriched in K_2O step by step. This enrichment continues until steady state is reached. The rightmost line represents compositional change by fractional crystallization at steady state.

Additional explanation for the diagram also can be provided from another viewpoint. By fixing the leftmost line, the main points of magma evolution are determined as follows. The MgO-rich end of this line gives the composition of the parental magma, and its slope determines relative partition coefficients of MgO and K_2O between the magma and the surface of the cumulate. If the residual magma proportion at the MgO-poor end of the line is given based on the partition coefficient of potassium (Table 4.1), then all fractionation lines that follow the first will be successively and automatically determined. Mixing lines are eliminated here for simplicity. Mixing and fractionation lines almost overlap with each other.

Examining Fig. 7.6, a set of fractionation lines is found to almost completely cover the distribution of the volcanic rocks. Fractionation lines at early steps encompass volcanic rocks of the Fenner's series, and fractionation lines at later stages cover the volcanic rocks of the Bowen's series. This matches well the fact that extrusion of volcanic rocks of the Fenner's series occurs in early stages, and extrusion of volcanic rocks of the Bowen's series occurs in later stages in the growth histories of arc volcanoes. These data indicate that the entire variation range of volcanic rocks from the Nasu volcanic zone is fully explained by supposing fractional crystallization in an open-system magma chamber that is repeatedly supplied with parental magma. In other words, it is reasonably concluded that the full range of volcanic rocks was derived from parental magma of a single primitive composition through fractional crystallization in the repeatedly refilled magma chamber. The reason why volcanic rocks of the Bowen's series are produced in later stages is presented in the next section.

7.2.4 Open-System Magma Chamber, and Magmatic Evolution of Major-Element Compositions

A marked variation in differentiation path with regard to major-element composition is caused by crystallization differentiation in an open-system magma chamber. The basic aspects of this phenomenon are presented below.

The differentiation path of a magma composition generally depends on the liquidus phase relations of relevant minerals, and this is determined by physical conditions when the system is chemically defined. Therefore, the path is the same in both the closed- and open-system chamber. There is no need for the path to be considered by introducing an open-system magma chamber. The characteristic of fractional crystallization in an open-system magma chamber, however, is the marked incompatible-element enrichment. Incompatible elements are generally concentrated from originally negligibly low levels to high concentrations that are defined by their partition coefficients. H_2O and K_2O are both representative incompatible components. When concentrated, they yield profound effects on the phase relation and hence change the differentiation path of magmatic evolution.

The direction of change in a magma's composition depends on a crystallizing mineral or minerals, and the differentiation path of the magma's composition is determined by the crystallization sequence of minerals. In the case of crystallization differentiation of an anhydrous subalkaline primitive magma at low pressures, crystallization proceeds in the following order: olivine → olivine + plagioclase → olivine + plagioclase + Ca-rich clinopyroxene → plagioclase + Ca-rich clinopyroxene + Ca-poor clinopyroxene → plagioclase + Ca-rich clinopyroxene + Ca-poor clinopyroxene + magnetite. In the case of crystallization differentiation of a hydrous primitive magma, the crystallization sequence of minerals is as follows: olivine → olivine + Ca-rich clinopyroxene → Ca-rich clinopyroxene + Ca-poor clinopyroxene + plagioclase + magnetite. If water content increases in the magma, the initiation of plagioclase crystallization will be delayed and will even become concurrent with the start of magnetite crystallization. Water in the magma drives earlier magnetite crystallization and later plagioclase crystallization. Here it should be remembered that plagioclase occupies almost half of the total mineral volume crystallized from primitive basaltic magmas. When magnetite begins to crystallize, the magma progressively becomes poorer in iron and richer in SiO_2, and hence begins to trace the differentiation path of the Bowen's series.

Since, in general, the parental magma is very low in water content and hence nearly dry, magnetite starts crystallizing after solidification by crystallization of 90% or more of the amount of the parental magma. During crystallization differentiation before the start of magnetite crystallization, variation in SiO_2 content of the magma is suppressed, and its T.FeO/MgO ratio continues to increase. Accordingly, the magma follows Fenner's trend. In crystallization differentiation in an open-system magma chamber, the differentiation trends are as follows. While the chamber is repeatedly supplied with parental magma after crystallization of, for example, half a mass of mixed magma, Fenner's differentiation trend is repeated at any early step. During this period, water and potassium are both concentrated step by step. This hydrous enrichment drives earlier magnetite crystallization. As a result, magnetite begins to crystallize before crystallization of half a mass of the mixed magma. Then enrichment in T.FeO/MgO ratio comes to be suppressed and SiO_2 starts being concentrated just a little. While the repetition continues, crystallization of magnetite continues to start much earlier and the step-by-step increment of SiO_2 accumulates. Finally, the magma in the chamber comes to trace the Bowen's trend

during crystallization differentiation. Therefore, in crystallization differentiation in an open-system magma chamber, the magma is low in K_2O and traces Fenner's differentiation path in early stages of magmatic evolution, and in the later stages, the magma in the chamber is high in K_2O and traces Bowen's differentiation path.

7.2.5 *Major Element Compositions of Island Arc Volcanic Rocks and the Upper Continental Crust*

In Japan, because there are volcanic rocks extruded in various stages of the growth histories of volcanoes, their compositional data plotted on a single diagram provide an outline of the entire compositional variation in the growth history of volcanoes. Because the problem is whether the model can explain all these data, the following argument is presented by assuming that all the major element compositions are achieved in a single magma chamber. Compositional data for 634 samples from mostly Quaternary volcanic rocks in Japan are plotted in Fig. 7.8.

When volcanic rocks from a volcano are plotted on Fig. 7.8 after identification of their differentiation series based on their mineralogical and chemical compositions, those of the Fenner's series mostly lie in the area between the horizontal axis and the discrimination line, and those of the Bowen's series mostly lie in the area between the vertical axis and the discrimination line (Miyashiro 1975). When many volcanic rocks are plotted, the distribution of volcanic rocks is found to continue smoothly crossing the discrimination line (Fig. 7.8). The discrimination line seems not to be a natural boundary. But the volcanic rocks are sorted with this discrimination line to show how they appear in subsequent diagrams herein. All volcanic rocks below this discrimination line are assumed to be of Fenner's series and are

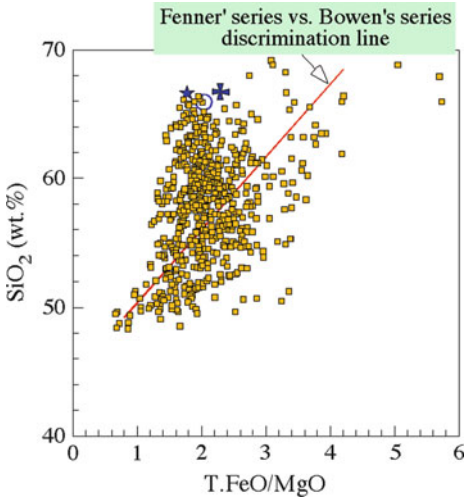

Fig. 7.8 Distribution on T.FeO/MgO-SiO_2 diagram of Quaternary volcanic rocks from Japan. Compositions of upper continental crust are from Taylor and McLennan (1985), *circle*; Shaw et al. (1986), *star*; Condie (1993), *cross*. The discrimination line is cited from Miyashiro (1975). Compositional data for volcanic rocks are from a lot of literature

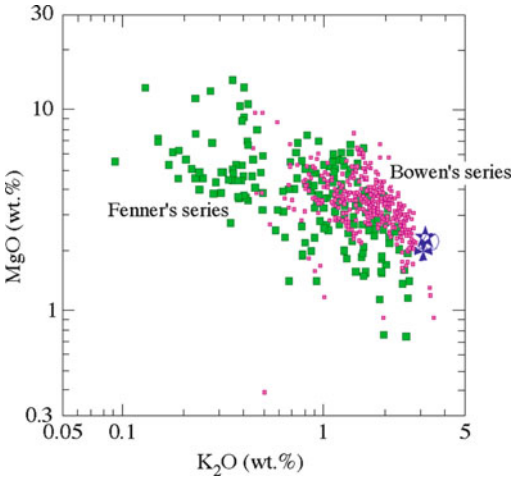

Fig. 7.9 Distribution on K_2O-MgO diagram of Fenner's and Bowen's series volcanic rocks. Data are the same as those in Fig. 7.8. *Green square*, Fenner's series volcanic rock; *pink small square*, Bowen's series volcanic rock. Compositions of upper continental crust are from Taylor and McLennan (1985), *circle*; Shaw et al. (1986), *star*; Condie (1993), *cross* (Modified from Yanagi and Yamashita (1994))

shown with green squares on the following diagrams. Similarly, all volcanic rocks above this line are assumed to be of the Bowen's series and are shown with small pink squares on the following diagrams.

Figure 7.9 is plotted in the same coordinate system as Fig. 7.6. The distributions of volcanic rocks of the Fenner's and Bowen's series are separated from each other in Fig. 7.6. This is because Masuda and Aoki (1979) intentionally collected typical samples of the two series and hence made the difference prominent. In Fig. 7.9, the distribution of volcanic rocks is continuous, and volcanic rocks of the Bowen's series distribute to the K_2O-rich side. All the low-K_2O volcanic rocks belong to the Fenner's series. These correspondences are correct, and well expected from crystallization differentiation in the open-system chamber. However, K_2O-rich volcanic rocks of the Fenner's series should be explained. The occurrence of these volcanic rocks is a reflection of the fact that water and K_2O should be sufficiently concentrated in magma of the open-system chamber before magma composition changes from that of the Fenner's series to that of the Bowen's series (see Fig. 7.8). As a result of this hydrous and K_2O enrichment, crystallization of magnetite arises sufficiently earlier, and then magma composition changes from the Fenner's to the Bowen's series. This is because the small SiO_2 increment accumulates step by step with the increase of the step.

The distribution density of fractionation lines, which show magma evolution in the refilled magma chamber, increases toward the right hand side of Fig. 7.6, then reaches its maximum, and suddenly becomes zero. On the other hand, when looking at volcanic rocks independently of their classification, from the left hand side to the right hand side of Fig. 7.9, the distribution of volcanic rocks is found to be sharply and diagonally demarcated on the K_2O-rich side. The distribution density of volcanic rocks increases toward this boundary, reaches a maximum and then suddenly becomes zero immediately after crossing this boundary. These characteristics of the distribution density of volcanic rocks (Fig. 7.9) are identical

to those of the distribution density of fractionation lines (Fig. 7.6). Since the chemical compositions of dacites from the last four steady-state stages at Shimabara Peninsula lie on this boundary line, it must surely represent chemical variation at steady state. Reported compositions of upper continental crust lie at the K_2O-rich tip of the boundary line. Therefore, it is evident that the distribution of Quaternary volcanic rocks from the Japanese Archipelago represents the entire story of magma evolution, from primitive compositions to the composition of the upper continental crust, and that this evolution is due to crystallization differentiation in the repeatedly refilled magma chamber.

Figure 7.10a shows SiO_2 and TiO_2 contents of Quaternary volcanic rocks. The distribution of these volcanic rocks is accounted for in the following explanation by crystallization differentiation in the refilled magma chamber.

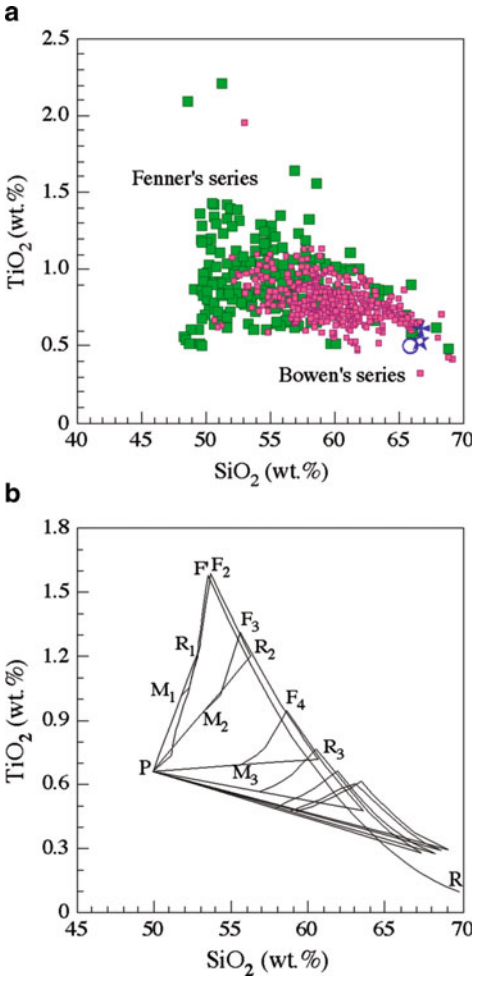

Fig. 7.10 Distribution on SiO_2-TiO_2 diagram of Fenner's and Bowen's series volcanic rocks. (**a**) Compositional data are the same as those in Fig. 7.8. *Green square*, Fenner's series volcanic rock; *pink small square*, Bowen's series volcanic rock. Reported compositions of upper continental crust are from Taylor and McLennan (1985), *circle*; Shaw et al. (1986), *star*; Condie (1993), *cross*. (**b**) Evolution of magma by fractional crystallization in a chamber that is repeatedly supplied with parental magma, based on results of a numerical calculation using Melts (Ghiorso and Sack 1995). *Point P* stands for a parental magma composition. *Line PF'R* shows magma evolution caused by fractional crystallization in a closed-system chamber. *Numerals* attached to M and R represent chemical steps. *Line* $M_{(n-1)}F_nR_n$ shows magma evolution caused by fractional crystallization at *i*th step. *Line* R_nM_n shows a compositional change caused by injection of parental magma at $(n + 1)$th step. See text for other details

A model calculation of magma evolution is inevitable, as in the case of K_2O and MgO contents, since the compositional evolution of magma in the refilled magma chamber is rather complicated. The numerical model of Ghiorso and Sack (1995) is employed here, since it includes the effect of water on the liquidus phase relation. Figure 7.10b shows magma evolution in the refilled magma chamber at 0.1 GPa, which was constructed by tracing the chemical variation in magma in the chamber step by step. This model is still being developed, and does not yet reach the level at which it withstands full quantitative examination. However, the results of the calculation are applicable to understanding the basics of magma evolution in the refilled magma chamber.

Point P in Fig. 7.10b represents the parental magma. Its dry major element composition is that of primitive arc basalt that was reported by Kushiro (1987). Water was added to the parental magma by 0.3 wt%. The oxygen fugacity was set by the quartz-fayalite-magnetite buffer. In the case of fractional crystallization in a closed-system chamber, the magma evolves along line PF'R. Line PF' represents magma evolution caused by fractional crystallization of silicate minerals. During this fractionation period, SiO_2 content remains almost constant, and TiO_2 content markedly increases. At point F' magnetite begins to crystallize. Then line F'R represents magma evolution caused by fractional crystallization of a set of silicate minerals and magnetite. SiO_2 content markedly increases and TiO_2 content decreases during this period.

In the case of magma evolution in the repeatedly refilled magma chamber, the parental magma P of a unit mass was added to the chamber after crystallization of half a mass of the mixed magma at each chemical step. Magma evolution by fractional crystallization at the first step starts at point P and arrives at point R_1. When magma in the chamber arrives at point R_1, the parental magma P of a unit mass is added to the residual magma R_1 to form mixed magma M_1. During this magma injection interval, magma composition changes from point R_1 to point M_1 along line R_1M_1. Evolution at the second step starts from mixed magma M_1, passing through point F_2, and finishes at the second residual magma R_2. Point F_n represents the composition at which magnetite starts crystallization at *n*th step. On mixing of the parental magma P and residual magma R_2, a range of mixed magmas along line R_2M_2 forms depending on the proportion of injected parental magma. At the third step, mixed magma M_2 evolves to residual magma R_3 through point F_3. Figure 7.10b shows these progressions until injection of the parental magma at the seventh step.

Figure 7.10b shows that varied magma compositions formed during evolution in the refilled magma chamber are distributed not only along the perimeter of a triangular form but also within its interior. At early steps, the increase in SiO_2 is suppressed and magma compositions trace the trends of the Fenner's series. At later steps, as a result of repetitive crystallization of magnetite, SiO_2 is concentrated step by step in the magma in the chamber, and magma composition comes to trace the trend of the Bowen's series. Such characteristics appear on magma compositions having SiO_2 more than 55 wt%. These observational facts match the characteristics of the distribution of volcanic rocks in Fig. 7.10a. In Fig. 7.10a, the reported

compositions of upper continental crust lie at the SiO_2-rich corner of the triangular distribution of the volcanic rocks. The average is at about 66 wt% SiO_2, and 0.6 wt % TiO_2. Results of the model calculation (Fig. 7.10b) show that the magma in the refilled magma chamber is evolving to this composition with increase in chemical step. Thus, using SiO_2 and TiO_2, the distribution of compositions of the Quaternary volcanic rocks also is well accommodated by fractional crystallization in the refilled magma chamber.

On diagrams of SiO_2 *versus* T.FeO, SiO_2 *versus* CaO, and SiO_2 *versus* Al_2O_3, volcanic rocks of both the Fenner's and Bowen's series are arranged linearly together. Reported compositions of the upper continental crust are at the SiO_2-rich tip of these lines.

Finally, the entire process of conversion of a primitive basaltic magma into magma compositions of the Bowen's series is presented. Parental magma P in Fig. 7.11 has the primitive magma composition of the Skaergaard Layered Intrusion. For the calculation, water was added to this parental magma at 0.5 wt%. Figure 7.11 shows the entire process of magma evolution in the refilled magma chamber. It is the result calculated step by step with the numerical model of Ghiorso and Sack (1995). The pressure was fixed at 0.1 GPa, and the oxygen fugacity was set according to the quartz-fayalite-magnetite buffer. The parental magma of a unit mass was added after half a mass of the mixed magma was crystallized at each chemical step. Violet thin lines show changes in magma composition by fractional crystallization, and green thick lines show changes in magma composition caused

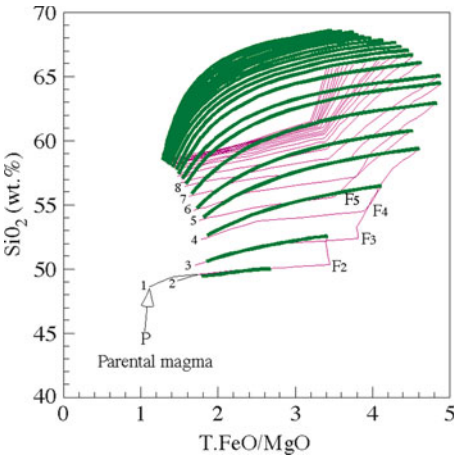

Fig. 7.11 Chemical evolution of magma by fractional crystallization in a chamber that is repeatedly supplied with parental magma, resulting from a numerical calculation using Melts (Ghiorso and Sack 1995). *Violet thin lines* represent magma evolution caused by fractional crystallization in the refilled chamber. *Green thick lines* represent compositional variations caused by repetitive parental magma injection. *P* stands for a parental magma composition. It is the primitive magma composition of the Skaergaard Layered Intrusion. *Numerals* indicate chemical steps. *Point Fn* represents a magma composition from which magnetite starts crystallization at *n*th step

by injection and mixing of the parental magma. Point F_n is the point at which a thin line sharply bends, and represents a magma composition at which magnetite starts crystallization at the *n*th step. In early steps, both fractionation and mixing lines have variation trends of the Fenner's series. The increment of SiO_2 at each step, however, accumulates because of the repetitive crystallization of magnetite, and finally, granitic magma compositions rich in SiO_2 are formed. At these later steps, the mixing lines have variation trends of the Bowen's series. In the case where the parental magma is richer in water and K_2O, SiO_2-rich magmas form earlier.

An important comment on the residual magma proportion should be added here. In the explanation presented so far, the proportion of residual magma in the refilled magma chamber has been postulated at less than 50% at each step. Magma evolution in major element compositions, however, depends on the proportion of residual magma at the end of each chemical step. In the case that only 5% of the mixed magma, for instance, crystallizes and 95% of the magma remains at the end of each step, it may be difficult for magnetite to crystallize in the refilled magma chamber.

7.3 Further Implications of Repeatedly Refilled Magma Chambers

7.3.1 Two-Layer Structure of the Continental Crust

Crystallization differentiation in the repeatedly refilled magma chamber now has been shown to transform primitive basaltic magma into magma with a composition of the upper continental crust. The explanation presented above for the origin of the continental crust is essential; however, it is insufficient for complete understanding. It is thus necessary to account for the origin of the two-layer structure of the continental crust.

For crystallization differentiation to continue in the refilled magma chamber, a system of combined upper and lower chambers is needed. If the supply of parental magma stops after a sufficient amount has been supplied, the magma in the upper chamber will remain as a granitic pluton (granodioritic pluton in the sense of petrography), and the lower chamber will disappear. Almost nothing of the lower chamber will remain after the parental magma supply has stopped. The plug between the upper and lower chambers remains as a layer of gabbroic cumulates. Its mineralogical composition is not homogeneous. As water and potassium are concentrated in the magma in the upper chamber, the primary field of plagioclase crystallization is narrowed around its chemical composition. As a result, pyroxenes crystallize from the mixed magma just after the injection of the parental magma, and form pyroxenites in the upper chamber. Therefore, the magma is enriched in plagioclase components. After that, plagioclase crystals crystallize abundantly to form plagioclase-rich gabbroic cumulates. This process repeats after any injection

of the parental magma into the upper chamber. Accordingly, the mineralogical composition cyclically varies in a vertical direction within the cumulate plug. Thus the plug comes to have a layered structure.

Lower crust fragments that have erupted with basaltic lava flows comprise abundant gabbros and some pyroxenites. Seismic reflection surveys commonly have shown layered structures of the lower crust. These observational data about the lower crust match well the petrological characteristics of the cumulate plug.

Thus, if continental crust is produced by crystallization differentiation in a system of combined upper and lower chambers, the continental crust will become a two-layer structure, with upper granitic and lower gabbroic cumulate layers.

7.3.2 *Abundant Andesites on the Surface, and Abundant Granitic Plutons in the Crust of Mature Island Arcs*

The surface area of mature island arcs is extensively covered by andesitic volcanic rocks, and their crust is occupied abundantly by granitic plutons. These facts need to be accounted for by the model.

Since magma temperatures are generally high, many pieces of evidence for magma mixing seem to quickly disappear. Such evidence, however, abundantly remains in volcanic rocks. This suggests that magma extrusions occur immediately after or simultaneously with injection of the parental magma.

Next, let us examine magma compositions. After SiO_2 content starts increasing in magma by crystallization differentiation in the repeatedly refilled magma chamber, a residual magma formed at the end of each chemical step quickly becomes dacitic in composition with increase in chemical step, because the partition coefficient of SiO_2 is large and close to 1. When the parental basaltic magma mixes with this residual dacitic magma at the beginning of each chemical step, naturally the mixed magma is andesitic in composition. There is no chance for the mixed magma to be basaltic except in the very early steps. Since the mixed magma is extruded to the surface several times during each injection of parental magma, and the chance of magma extrusion from the chamber during crystallization differentiation at any step is limited, it is natural for andesitic volcanic rocks to become overwhelmingly abundant at the surface. Therefore, it is possible to regard an arc volcano as a great pile of lava flows and pyroclastic rocks that record repetitive magma mixing occurring during the magma evolution.

Furthermore, we should redefine the Fenner's and Bowen's series, since volcanic rocks are now found to have been extruded mostly during magma mixing. This is because the definition of these series was made by supposing that volcanic rocks had been extruded during crystallization differentiation of magma, although that had not been evident. However, in the case that the magma in the chamber is enriched in SiO_2 by crystallization differentiation, a wide variation in SiO_2 content also appears during mixing when the parental magma is injected. In the case that the

T.FeO/MgO ratio of the magma in the chamber is enriched by crystallization differentiation, a wide variation in the T.FeO/MgO ratio also appears during mixing when the parental magma is injected. Therefore, we have continued to use the same terms for mixed magmas by classifying the former into the Bowen's series and the latter into the Fenner's series.

Now we consider that the refilled magma chamber is occupied by the andesitic mixed magma rich in both water and potassium after injection of the last mass of parental magma. Similarly to the previous steps, crystallization differentiation proceeds to form residual dacite magma, since its viscosity remains very low. Then, this residual dacite magma finally solidifies as a granitic pluton. The same thing happens for repeatedly refilled magma chambers at any site in the arc crust. Therefore, the upper crust becomes rich in granitic plutons.

7.3.3 Plate Subduction and the Bowen's Series

The repetitive supply of parental magma is important but insufficient to form magmas of the Bowen's series. The repetitive magma supply seems to be ubiquitous along oceanic ridges throughout the world. No volcanic rocks of the Bowen's series, however, are extruded from these oceanic ridges. This is because large portions of magma in the chamber gush out to the ocean floor. For the formation of magmas of the Bowen's series, it is necessary for water and alkali elements to be concentrated in magma in the chamber. If a large portion of the magma enriched in water and alkalis by crystallization differentiation is extruded when injection of the new parental magma occurs in the chamber, the cumulative enrichment of water and alkali elements cannot be realized. The enrichment degree reaches a maximum when the proportion of magma extruded from the chamber to the surface or to the ocean floor becomes zero. The coupled upper and lower chambers system can repeatedly accept parental magma with no magma extrusion. In addition to this, the physical environment in which the upper chamber lies should have the ability to greatly suppress magma extrusion. Ocean ridges commonly occur under tensional conditions. Open cracks form abundantly there, through which a great amount of magma gushes out from the chamber to the ocean floor. Open cracks, however, are hard to form in the thick arc crust under compressional environments. This makes it difficult for magma in the upper chamber to be extruded to the surface. This is the reason why magmas of the Bowen's series form at island arcs. There is no need for the subducted plate to lie beneath volcanoes that spew out magmas of the Bowen's series. Abundant volcanic rocks of the Bowen's series characterize both Mount Unzen and Mount Tara in Kyushu. However, there is no subducted, seismically active slab beneath them. The Philippine Sea plate subducts beneath Kyushu from the Nankai trough. The subducted slab increases its slope beneath the Aso caldera at about 100 km east of Mount Tara, and then disappears at a depth of 110–120 km (Hasegawa et al. 2009). Volcanic rocks of the Bowen's series at Mount Tara have already been found to have been derived from parental basaltic magma

characterized by having the same incompatible element abundances as those of hot-spot-type oceanic island basalts. Their formation does not depend on chemical composition of the parental magma, but rather on the physical environment in which the chamber lies.

There is a popular idea that the fact that arc magmas are generally rich in water and incompatible elements can be understood by connecting magma generation with dehydration reactions occurred in a subducting slab (e.g., Iwamori 1998; Hasegawa et al. 2009). This may be correct. But it is not always necessary to imagine that this enrichment is due to dehydration reactions. The enrichment is sufficiently achieved by crystallization differentiation in the repeatedly refilled magma chamber. In this case, the role of plate subduction causes convection in the mantle prism beneath an island arc. In turn, this convection causes the magma generation in the mantle, removes cumulates from the refilled magma chamber, carries them to the deep mantle, and finally generates compressive stresses in the arc crust. The compressive stresses in the crust are caused by two forces of mutually opposite directions. One is generated by the horizontal mantle-surface flow moving toward the aseismic front beneath the arc crust, and the other is generated in association with oceanic plate subduction.

7.3.4 Archean Continental Crust and the Open-System Magma Chamber

Next, we examine the time when crystallization differentiation in the repeatedly refilled magma chamber began to work in Earth's history. Condie (1993) published a list of chemical compositions of the upper continental crust of various ages. These major element compositions show that, except for K_2O contents, there are insignificant differences among them. A clear chronological variation appears in the K_2O/Na_2O ratio. It is low at 0.68–0.70 in upper continental crust formed before 2.5 billion years ago, and it is high at 0.84–0.92 in upper continental crust formed in the Proterozoic and the Phanerozoic. This reflects the abundant occurrence of K-feldspar-poor trondhjemites and tonalities in the Archean, and the predominant occurrence of K-feldspar-rich granites in the subsequent age.

Figure 7.12 shows results of calculations of the numerical model. The K_2O/Na_2O ratio increases step by step because of repetition of crystallization differentiation in the repeatedly refilled magma chamber. The parental magma used for the calculation is the primary magma of the Skaergaard Intrusion, to which water is added by 0.5 wt%. Other conditions have been presented previously. The K_2O/Na_2O ratio reaches 0.94 after 30× repetition of fractional crystallization, although it is low at 0.105 in parental magma. This is because K_2O is concentrated step by step in the magma, while the Na_2O that is a major component of plagioclase remains almost unchanged. Therefore, even if the magma becomes granitic in regard to SiO_2 content by crystallization differentiation in the refilled magma

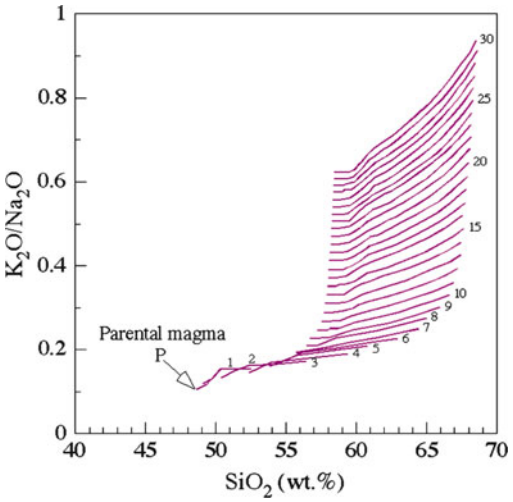

Fig. 7.12 Progressive increase in K_2O/Na_2O ratio of magma by fractional crystallization in a chamber that is repeatedly supplied with parental magma, resulting from a numerical calculation using Melts (Ghiorso and Sack 1995). *Point P* stands for a parental magma composition. It is the primitive magma composition of the Skaergaard Layered Intrusion. *Numerals* indicate chemical steps. *Violet lines* show magma evolution caused by fractional crystallization in the refilled chamber. All mixing lines between residual magmas and the parental magma are not shown to avoid complexity

chamber, it is rather poor in K_2O in the early steps, and becomes rich in K_2O at later steps.

Although they are low, the K_2O/Na_2O ratios in Archean crust are at relatively high levels that are not realized by a single fractional crystallization in the closed-system magma chamber. These high ratios, however, are easily achieved by crystallization differentiation in the open-system magma chamber (Fig. 7.12). This suggests that crystallization differentiation in the repeatedly refilled magma chamber started working early in the Archean. Even so, there may arise a question as to why the K_2O/Na_2O ratios are low in the Archean.

There are two explanations for the low ratios. One is that the period of repetitive magma supply may be assumed to have been too short to allow for enrichment of K_2O. Such an assumption, however, is not possible, because it is commonly accepted that the Archean mantle was higher in temperature, was more primitive, and hence was able to generate magma for a longer period of time. If so, then the open-system magma chamber must have probably stayed closer to the surface of the crust so as to release large amounts of heat at high rates. This leads to the second explanation.

While large portions of magma are extruded from the repeatedly refilled magma chamber, enrichment of K_2O is suppressed and K_2O/Na_2O ratio cannot rise. The extrusion rate depends on both the stress in the crust and thickness of the crust lying over the chamber. If the overlying crust is thin, it may be easily cracked, and the

volcanic vent may be short, and hence the magma may be easily extruded. As a result, the K_2O/Na_2O ratio remains low. The Kyushu-Palau Ridge is a thin-crust remnant arc separated from the Izu-Bonin Arc by the opening of the Shikoku basin. Trondhjemites were found there by Ishizaka and Yanagi (1975). Thick crust under compressional environments, like the crust of the Japanese Islands, is necessary for the formation of granitic plutons having high K_2O/Na_2O ratios. Thus, the low K_2O/Na_2O ratios of the Archean crust may suggest that the open-system magma chamber was at shallow levels of the crust. The fact that Archean crust also consists of upper and lower crustal components would not be understood easily, if crystallization differentiation in a system of coupled upper and lower chambers were rejected.

7.4 Roles of Water

Continental crust forms on Earth because water is available. If there were no water, then there would be no volcanic rocks of the Bowen's series and hence there would be no continental crust on Earth. Water drives early magnetite crystallization and hence, makes the formation of granitic magmas possible. Furthermore, water enables the magma to mix with other magmas of different compositions. As a result, it opens up the road for the development of granitic magmas.

Magma viscosities measured by Murase and McBirney (1973) indicate that the viscosity difference between dry basalt and dry andesite magmas is so great that they are unable to mix. Water, however, inhibits the polymerization of SiO_2 and greatly lowers magma viscosity. Murase (1962) reported that the effect is small in basaltic magmas and large in granitic magmas. The viscosity of the latter is lowered by about 10^6 poise if water is present. Since primary magma is generally low in water, and water is concentrated in magma by crystallization in the repeatedly refilled magma chamber, let us follow this line of thinking further. Viscosities of dry basalt magma at 1,220°C and water-saturated granitic magma at 900°C lie together at about 10^3 poise, and the difference is very small. Magma mixing in a wide compositional range is possible only in the case where sufficient water is available.

A difference in temperature between two magmas that are going to mix is also an important subject for investigation. When high temperature basaltic magma meets low temperature dacitic magma, the temperature of the former cannot easily fall because crystallization of the former liberates latent heat. Conversely, when dacite magma meets basaltic magma, if the former contains insignificant amounts of crystals and is heated, its temperature is quickly raised. However, the temperature of a dacitic magma with abundant phenocrysts cannot rise rapidly because phenocrysts absorb a great deal of heat as they melt and disintegrate. Granitic plutons and dacite lavas often contain abundant basic magmatic inclusions. This may represent the above circumstance, in which basaltic magma was not able to easily mix with dacitic and/or granitic magmas having abundant crystals. Magma mixing is a major subject for petrological investigation, since it is fundamentally important for understanding the origin of the wide chemical variations in igneous rocks.

References

Condie KC (1993) Chemical composition and evolution of the upper continental crust: contrasting results from surface samples and shales. Chem Geol 104:1–37

Gao S, Luo T-C, Zhang B-R, Zhang H-F, Han YW, Zhao Z-D, Hu Y-K (1998) Chemical composition of the continental crust as revealed by studies in East China. Geochim Cosmochim Acta 62:1959–1975

Ghiorso MS, Sack RO (1995) Chemical mass transfer in magmatic process IV. A revised and internally consistent thermodynamic model for the interpolation of liquid-solid equilibria in magmatic systems at elevated temperatures and pressures. Contrib Miner Petrol 119:197–212

Hasegawa A, Nakajima J, Uchida N, Okada T, Zhao D, Matsuzawa T, Umino N (2009) Plate subduction, and generation of earthquakes and magnas in Japan as inferred from seismic observations: an overview. Gond Res 16:370–400

Ishizaka K, Yanagi T (1975) Occurrence of plagiogranite in the older tectonic zone, southwest Japan. Earth Planet Sci Lett 27:371–377

Iwamori H (1998) Transportation of H_20 and melting in subduction zones. Earth Planet Sci Lett 160:65–80

Kuno H (1959) Origin of Cenozoic petrological provinces of Japan and surrounding areas. Bull Volcanol Ser 2(20):37–76

Kushiro I (1987) A petrological model of the mantle wedge and lower crust in the Japanese island arcs. In: Maysen BO (ed) Magmatic processes: physicochemical principles, vol 1, Special Publication. Geochemical Society, University Park, pp 165–181

Masuda Y, Aoki K (1979) Trace element variations in the volcanic rocks from the Nasu Zone, Northeast Japan. Earth Planet Sci Lett 44:139–149

Miyashiro A (1975) Classification characteristics, and origin of ophiolites. J Geol 83:249–281

Murase T (1962) Viscosity and related properties of volcanic rocks at 800 to 1400°C. J Fac Sci, Hokkaido Univ Ser 7 1:487–584

Murase T, McBirney AR (1973) Properties of some common igneous rocks and their melts at high temperatures. Geol Soc Am Bull 84:3563–3592

Ogata M (1993) Magmatic differentiation and growth history of Taradake volcano, Northwestern Kyushu, Japan. Ph. D. Thesis, Kyushu University, 140 p

Shaw DM, Cramer JJ, Higgins MD, Truscott MG (1986) Composition of the Canadian Precambrian shield and the continental crust of the earth. In: Dawson JB, Carswell DA, Hall J, Wedepohl KH (eds) The nature of the lower continental crust, vol 24, Geological Society Special Publication. Blackwell Scientific Publication, Oxford, pp 275–282

Sugimoto T (1999) Magmatic differentiation and evolution of a chamber system beneath the Unzen volcano. Ph. D. Thesis, Kyushu University, 141 p

Taylor SR, McLennan SM (1985) The continental crust: its composition and evolution. Blackwell Scientific Publication, Carlton, 312 p

Wager LR (1960) The major element variation of the Layered Series of the Skaergaard Intrusion and a re-estimation of the average composition of the hidden layered series and of the successive residual magmas. J Petrol 1:364–399

Wager LR, Brown GM (1967) Layered igneous rocks. W. H. Freeman, San Francisco, 588 p

Wedepohl KH (1995) The composition of the continental crust. Geochim Cosmochim Acta 59:1217–1232

Yagi K, Kawano Y, Aoki T (1963) Types of Quaternary volcanic activity in northeast Japan. Bull Volcanol 26:223–235

Yanagi T, Yamashita K (1994) Genesis of continental crust under island arc conditions. Lithos 33:209–223

Chapter 8
Volcanic Arcs and Outer Arcs

8.1 Granitic Plutons Associated with and Without Coeval Volcanic Rocks

Primitive magma has been found to finally solidify as a granitic pluton after transformation to dacitic magma of a chemical composition identical to the composition of the upper continental crust. This granitic pluton and the associated cumulate also have been found to form the two-layered continental crust. In addition, parental magma also has been found to evolve to volcanic rocks of mostly andesitic composition via extrusion from the chamber to the surface during this magmatic transformation. However, there is no need for the magma in the upper chamber to be extruded to the surface, because the coupled chambers form a reservoir system that can repeatedly and smoothly accept parental magma from the mantle with no extrusion of magma.

There are many granitic plutons with no coeval volcanic rocks around them. Among these, there may be cases where volcanic rocks have already disappeared due to erosion. The Osumi granitic pluton at the southern end of Kyushu Island is large (batholith scale) and young. It was emplaced in the Middle Miocene. However, there is no evidence for volcanic activity around this pluton. Miocene volcanic formations are located abundantly along the coast of the Japan Sea side of the Japanese Islands. Therefore, the lack of volcanic rocks does not mean that volcanic rocks have disappeared because of erosion. In southern Kyushu, there also are several granitic stocks that have no associated volcanic rocks. These examples from southern Kyushu indicate that there are cases where formation of granitic plutons occurs without formation of volcanic rocks. The problem is how to locate where such granitic plutons form. Results from an investigation searching for such sites in an island arc (Yanagi 1981) are presented below.

T. Yanagi, *Arc Volcano of Japan*, Lecture Notes in Earth Sciences 136,
DOI 10.1007/978-4-431-53996-4_8,

8.2 Topographic Configuration of an Island Arc

Before the search for granitic pluton formation sites is undertaken, we first explore the topographic configuration of an island arc.

The northeast Japan arc (Fig. 8.1) is a well-studied, typical island arc formed by subduction of the Pacific Plate. The topography of the northeast Japan arc reflects an ordinary arrangement of a trench, a deep seismic zone, an aseismic front, an outer arc, a volcanic front, and a volcanic arc. Figure 3.1 shows a schematic cross section of this topography. The Japan Trench is the site from which the Pacific Plate subducts into the mantle, and the seismic zone in the mantle beneath the northeast Japan arc represents the top surface of the slab subducting into the mantle (Hasegawa et al. 2009). The aseismic front is a physical boundary that lies at a depth range between 40 and 60 km in the mantle (Yoshii 1972; see Fig. 3.1). Seismic activity is extremely high in the mantle on the trench side, and is extremely low in the mantle on the continental side. On a topographic map of the Japanese Islands, the aseismic front extends from south to north along the coast on the Pacific

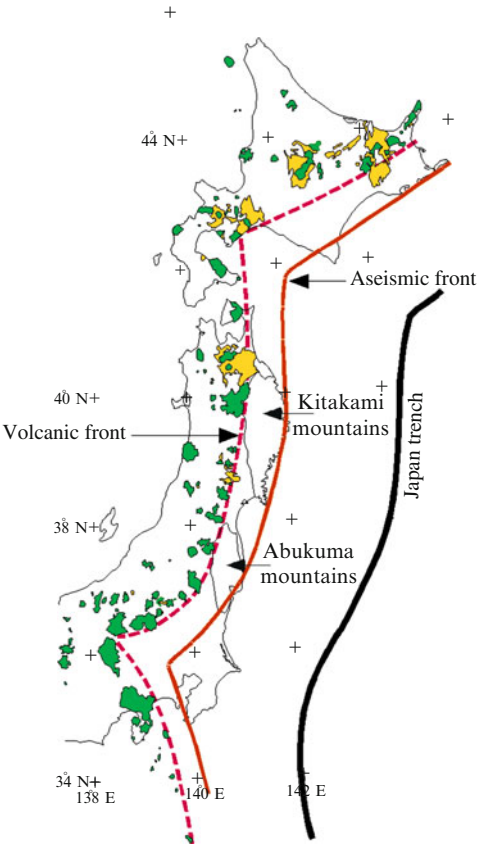

Fig. 8.1 Distribution of Quaternary volcanic rocks, and locations of volcanic front, aseismic front, outer arc, and trench in North and Northeast Japan. *Green area*, basaltic and andesitic volcanic rocks; *orange area*, dacitic and rhyolitic volcanic rocks. Ridge between the volcanic and aseismic fronts is an outer arc. It is represented by Abukuma and Kitakami mountains. The belt of volcanoes behind the volcanic front represents a volcanic arc (Modified from Yanagi (1981))

Ocean's side of the northeast Japan arc, and turns to the northeast off southern Hokkaido. It then continues to the northeast along the south coast of Nemuro Peninsula (Fig. 8.1). The outer arc is an uplifted ridge lying between the aseismic front and the volcanic front. The Abukuma and Kitakami Mountains are part of this outer arc. The zone of volcanic activity is demarcated by the volcanic front on its oceanic side. Volcanoes are abundant in the belt on the continental side of this front. However, there is no volcano in the belt on the oceanic side of this front. The volcanic arc is an elongated ridge of volcanic origin, and it lies in the volcanic belt.

Seismic activity in the crust is the highest between the aseismic front and the trench. However, it is very low in the crust of the outer arc (Hasegawa et al. 2009), although the outer arc is the nearest neighbor of the trench slope, which is the seismically most active area. Attenuation of seismic waves is strong and seismic wave velocities are slow in the mantle on the continental side of the aseismic front. Therefore, the mantle behind the aseismic front has been called the low-Q and low-V zones (Utsu 1971). Seismic waves passing through the mantle on the oceanic side of the aseismic front have ordinary velocities in ordinary mantle (Suzuki 1976). With regard to igneous activity in the island arc, terrestrial heat flow rate is very important. The rate is high (75–100 mW/m^2) in the volcanic belt. However, it decreases quickly after crossing the outer arc toward the trench, and is low (about 40 mW/m^2) in the trench area (Yoshii 1986; Tanaka et al. 2004). Regional variations in seismic activity and terrestrial heat flow rate are considered to be physical reflections of convection in the mantle prism beneath the island arc.

8.3 Two Types of Island Arcs of Different Topography

The ridge of an arc-trench system generally has a double configuration. One is a volcanic arc that represents the ridge margin on the continental side. The other is an outer arc that represents the ridge margin on the oceanic side. There are two types of arc-trench systems, and they differ in topography. The Kurile arc-trench system is characterized by a well-developed volcanic arc, and the Ryukyu arc-trench system is characterized by a well-developed outer arc.

Tanega-shima, Amami-ohshima, and Okinawa-jima lie on the outer arc of the Ryukyu arc-trench system. These are fairly large non-volcanic islands. Multistage marine terraces have commonly developed on these islands. According to Machida et al. (2001), the entire surface of Tanega-shima is covered by multi-stage marine terraces. The highest of them lies at 250–260 m above the sea level. Four low-relief surfaces at altitudes of 1,700–1,400 m on Yaku-shima are reported to be erosional remnants of multi-stage terraces. The fact that multi-stage terraces lie on all islands on the outer arc is strong proof for continued uplift of all islands lying on the outer arc of the Ryukyu arc-trench system. The uplift rate has been estimated at 0.6–0.9 mm/year and 0.7–0.8 mm/year at Tanega-shima and Yaku-shima, respectively.

The volcanic arc of the Ryukyu arc-trench system lies 60 km west of the outer arc. It extends for about 300 km from islands in the immediate south of Kyushu to the Tokara Islands. However, this system is quite different in island size compared with the Kurile arc, in that it is mainly represented by a chain of large volcanic islands, such as Kunashir, Iturup, Urup and Paramshir. The volcanic arc of the Ryukyu arc-trench system consists of very small volcanic islands of diameters less than 12 km. On the contrary, Kunashir, a volcanic island at the western end of the Kurile arc, has a length of about 100 km. Iturup, the next island east of Kunashir, has a length of about 200 km. Although very small in size, the Kurile arc-trench system also has an outer arc that is represented by Nemuro Peninsula and its eastward extension to the east of Hokkaido. This outer arc is at a germinating stage and lies below sea level for the most part. To clearly illustrate the topographic difference between the Kurile and the Ryukyu arc-trench system, Fig. 8.2 shows areal proportions of islands lying in each of the volcanic and the outer arc regions. Although the ridge of an arc-trench system consists of volcanic and outer arcs, Fig. 8.2 shows that the growth of these arcs is almost inversely related.

In the Izu-Bonin arc-trench system, the Izu Chain of Islands, extending from Izu-ohshima to Hachijo-jima, represent the volcanic arc. On the other hand, the Bonin Islands represent the outer arc lying about 100 km east of the volcanic arc. There is no clear outer arc in front of the Izu Chain of Islands. The volcanic arc behind the Bonin Islands is not well developed. Small submarine volcanoes arranged in a line represent the volcanic arc. The Izu-Bonin arc-trench system also provides an example in which volcanic and outer arc growth is inversely related.

The growth of a volcanic arc is understandable, because the arc is repeatedly supplied with magma from the mantle. However, it is very difficult to understand continuous uplift of islands on an outer arc, since there is no clear evidence for material accretion to the outer arc. If it is assumed that isostasy is maintained and that the uplift is caused by growth in thickness of crust, then the uplift of Tanega-shima by 250 m may mean growth in thickness of the crust by about 1.5 km.

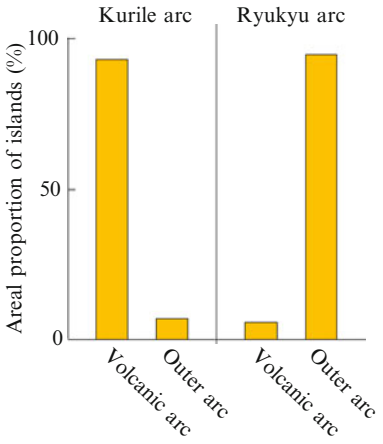

Fig. 8.2 Areal proportions of islands lying within volcanic and outer arcs (Modified from Yanagi (1981))

To understand what is contributing to this growth, it is better to examine geological constituents of volcanic and outer arcs of a slightly older age. In these older examples, the mechanisms for uplift of outer arcs may be revealed, since it seems probable that exhumed subsurface geology would indicate what was added to these arcs while they were growing.

Violent igneous activity occurred in both northeast Japan and southwest Japan during the Miocene. However, the styles of the igneous activities were quite different. In northeast Japan, violent volcanic activity and tectonic movement took place in a belt of 110 km wide behind the outer arc that was represented by the Kitakami and Abukuma Mountains (Fig. 8.3). Crustal subsidence began first at

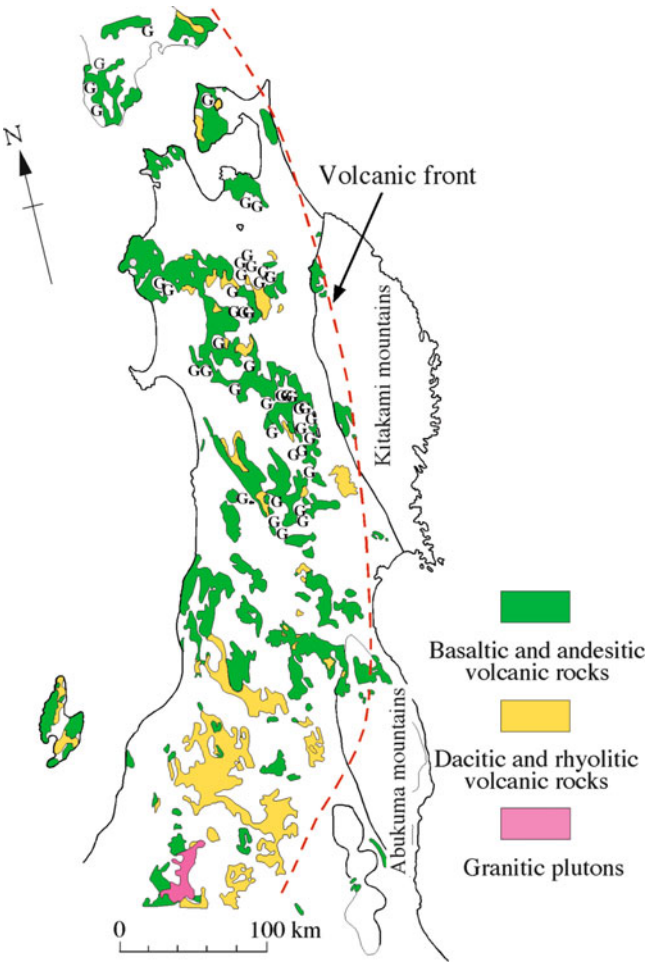

Fig. 8.3 Distribution of Miocene volcanic rocks and granitic plutons in Northeast Japan. *G* represents a small outcrop of granitic plutons. *Broken line* represents the Miocene volcanic front (Modified from Yanagi (1981))

the axial region and then expanded toward the Japan Sea side and resulted in formation of a large elongated sedimentary basin extending in the north-south direction. In other words, it ran in parallel with the present Japan trench. Thick sediments were deposited, and violent volcanic activity occurred there (Fig. 8.3). The volcanic activity commenced in the early Miocene and continued until the late Miocene. Then, crustal movement style turned from subsidence to uplift. Uplift began first in the axial region, and then expanded toward the Japan Sea side. During this time, small stocks of granitic plutons were emplaced sporadically in the elongated sedimentary basin (Fig. 8.3). Volcanic activity and uplift are still continuing even today, and have come to form the present topographic features of northeast Japan.

Contrasting this history, the Miocene volcanic activity in southwest Japan was so low and sporadical that it was hard to apply the concept of volcanic arc to this region (Fig. 8.4). Yet, Miocene granitic plutons are relatively abundant. They were emplaced in densely imbricated sedimentary rocks in the outer arc belt of southwest Japan (Fig. 8.4). These sedimentary rocks have tectonic and sedimentological features characteristic of an accretionary sedimentary prism formed at a trench. The granitic plutons show no evidence for volcanism around them. The Minami-osumi granitic pluton in southern Kyushu, the largest among them, also was emplaced in accreted sedimentary formations. It is a batholith with a surface area of 43 $\times$ 13 km^2. There is no evidence for volcanic activity around it.

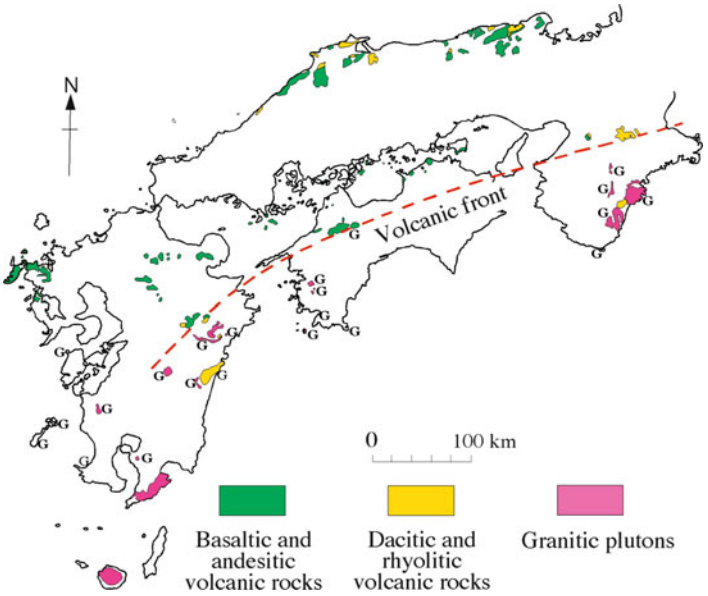

Fig. 8.4 Distribution of Miocene volcanic rocks and granitic plutons in Southwest Japan. *G* represents a small outcrop of granitic plutons. *Broken line* represents the Miocene volcanic front (Modified from Yanagi (1981))

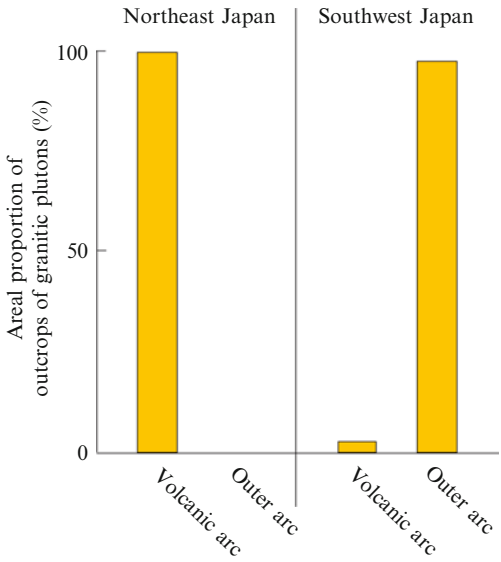

Fig. 8.5 Areal proportions of outcrops of Miocene granitic plutons in volcanic and outer arcs of Miocene Northeast and Southwest Japan arc-trench systems (Modified from Yanagi (1981))

Figure 8.5 shows a comparison in areal proportion of exposure surfaces of granitic plutons in northeast and southwest Japan. In northeast Japan, all the granitic plutons were emplaced as small stocks in the volcanic belts. To the contrary, in southwest Japan, most of granitic plutons were emplaced as stocks and a batholith in the outer arc belt. Some were extruded to the surface (e.g., Kumano acid igneous complex: Aramaki 1965) in the outer arc belt. This difference has something in common with the topographic difference between the Kurile and Ryukyu arc-trench systems. When a volcanic arc is fully grown, growth of the associated outer arc is much depressed, and when a volcanic arc is subdued, the associated outer arc is fully grown. This seems to correspond to the data showing that Miocene granitic plutons occur in a volcanic belt in northeast Japan where the volcanic activity was very high, and that Miocene granitic plutons occur in the outer arc belt in southwest Japan where the volcanic activity was very low. If this correspondence is correct, then the following idea emerges: the mechanism that supports uplift of the outer arc of the Ryukyu arc-trench system is the formation of new granitic magmas at depth beneath the outer arc crust.

8.4 Magma Chambers Beneath Volcanic and Outer Arcs

By assuming formation of upper continental crust in a repeatedly refilled magma chamber, growth mechanisms of volcanic and outer arcs can be examined. The key point is how the chamber is fixed in relation to the convecting mantle. It is necessary for the chamber location to be fixed, since the chamber owes its magma supply and cumulate removal to this convection, as shown in Fig. 3.1. Its location seems to be

determined by a combination between flow pattern at the top of the mantle and base topography of the solid crust.

The position of the top of mantle flow moving toward the aseismic front is considered first. Since the temperature at the top of the mantle beneath the Japanese Islands is high (900–1,000°C), and the melting point of the gabbroic lower crust is lower than that of the mantle, the viscosity of the lower crust in contact with the mantle top layer is considered to be lower than that of the mantle top layer. If this is the case, then the top surface of convective mantle flow will be considered to lie in the lower crust. Since geothermal temperature falls in the crust, from the high temperature of the top surface of the mantle to the ordinary temperature of the surface of the crust, it is certain that viscosity rises quickly in the crust. Hence, earthquake hypocenters concentrate in the central part of the crust, with very few located at depths of over 25 km. Therefore, the top surface of convective mantle flow is considered to lie at the lower part of the lower crust beneath the Japanese Islands.

There may be a few types of magma chambers with different magma supplies and mechanisms of chamber fixing against the flow. If magma generation is due to decompression melting in the mantle upwelling flow, the place where magma supply rate is highest must be at the uppermost portion of the upwelling flow. Since the top of the upwelling mantle flow reaches the elastic layer of crust, the magma chamber is considered to be formed at a concave portion of the base of the elastic crust. This concave portion originates by both melting from the accumulated primitive magma and erosion by the upwelling flow. These agents work together to form the magma chamber by eating into the lower arc crust, and then the chamber is fixed there. Subsequently this chamber develops into a system of coupled upper and lower chambers. In this case, the lower chamber is fixed by the elastic crust against the flow.

If the rate of magma supply is too low, or if the temperature of the lower crust is too low for magma to form a chamber by melting the base layer of the elastic crust, the magma carried to the top of the upwelling mantle flow may spread horizontally as a thin layer or layers, due to horizontal laminar flow in a basal layer of lower crust between the volcanic front and the aseismic front. Then, this thin magma layer is carried behind the aseismic front by horizontal flow, and finally it is squeezed. At this point, it accumulates to form a magma chamber where the flow begins to descend behind the aseismic front. Since the crust between the volcanic front and the trench is under highly compressive stresses, it is difficult for the magma to erupt to the surface to form a volcano. Crystallization differentiation continues in the refilled magma chamber behind the aseismic front, as long as upwelling beneath the volcanic front continues, and hence the magma supply continues to the chamber. Magma of the composition of upper continental crust finally forms in the chamber behind the aseismic front.

Besides these two types of chambers, there may be other types of chambers. There is no need for the flow between the volcanic front and the aseismic front to be uniform. The flow may converge and start descending in between the volcanic front and the aseismic front. In such cases, a magma chamber may form where the flow

starts descending. Horizontal flow toward the aseismic front may fluctuate up and down, due to ruggedness of the bottom surface of the elastic crust. When this takes place, magma may accumulate where downflow starts. Of these different types of chambers, the most stable and greatest number of chambers would be those formed at the top of the mantle upwelling flow and those formed behind the aseismic front. As will be described in the next section, the former supports growth of the volcanic arc while the latter supports growth of the outer arc.

8.5 Model for Alternative Growth of Volcanic and Outer Arcs

It has been found that a stable magma chamber forms alternatively at two sites. One is just above the upwelling flow, and the other is immediately behind the aseismic front. The genetic relation of these two chambers is considered next from the viewpoint of rate of magma supply.

In the case where a large amount of magma is supplied at a high rate, the crust may become thin owing to both tensional stresses and erosion due to upwelling flow. As a result, the crust subsides. This subsidence, in turn, results in formation of a sedimentary basin at the surface of the crust. Magma accumulates at a concave portion of the base of the crust. The concave portion originally may be formed by erosion due to upwelling flow. This chamber is repeatedly supplied with primitive magma, and then develops into the coupled chambers. Tensional cracks often form in the crust lying above the upwelling flow. Magma in the chambers beneath the sedimentary basin sometimes erupts through these cracks to form a volcanic arc. The magma in the upper chambers evolves to dacite of the composition of upper continental crust, and the eroded portion of the base of the crust is progressively filled with cumulate. As a result, the crust becomes thick, and tectonic movement of the crust turns from subsidence to uplift. Simultaneously, dacite magma in the upper chambers at various places in the sedimentary basin solidifies as granitic plutons. This scenario corresponds well with the history of the Miocene sedimentary basin in northeast Japan.

In the case where the rate of magma generation is low, the physical situation necessary for formation of a chamber may not be achieved at the base of the crust above the upwelling flow of the mantle. The slow rate of magma genesis is a reflection of slow upwelling rate in the mantle and/or of lower mantle temperatures. There may be a case where tensional stress is too weak in the overlying crust and erosion rate of the lower crust is too low. In such a case, magma carried to the top of the upwelling flow is transported by horizontal flow toward the aseismic front as thin magmatic layers. Then, they are squeezed and accumulate behind the aseismic front as the flow begins to descend. Since the magma does not remain in large volumes above the top of the upwelling flow, the volcanic arc does not grow. A magma chamber formed behind the aseismic front will develop if the successive magma supply continues. In this case, the magma evolves to dacite of the same composition as upper continental crust. It becomes a granitic pluton after

solidification. Due to both magma accumulation and cumulate formation behind the aseismic front, the overlying crust then is uplifted to form an outer arc. If the overlying crust is thick, like in continental crust, the uplift will form a coastal mountain range. If it is thin like oceanic crust, the uplift will be reflected as a chain of non-volcanic islands made mostly of densely imbricated sedimentary formations. Since the crust behind the aseismic front is under compressional stresses, open cracks are difficult to form. As a result, magma behind the aseismic front has almost no chance to erupt to form volcanoes. The crust around the aseismic front is made mostly of accretionary sedimentary complexes that often include some fragments of oceanic crust. This part of the crust may be formed due to retreat of the trench toward the ocean as a result of growth of the accretionary prism. The accretionary sedimentary complexes behind the aseismic front are exposed to high temperatures of magmas at rather low lithostatic pressures for a long time, and become regional metamorphic rocks. This scenario corresponds well to the history of the Miocene outer arc belt of southwest Japan. Since this outer arc belt topographically and geologically continues to the outer arc of the Ryukyu arc-trench system, it is understood that uplift of the islands in the outer arc is the topographic reflection of the formation of both dacitic magma and cumulate beneath this arc.

Based on the above reasoning, it seems likely that the alternative growth of volcanic and outer arcs depends on the rate of magma generation. Nonetheless, if the rate of magma generation is too high, there may be a case where the chamber beneath the volcanic arc cannot completely catch the entire volume of the supplied magma, and some may be carried to the aseismic front. In this case, the volcanic and outer arcs may grow simultaneously.

It is necessary to add some supplemental comments to the process of magma evolution that occurs behind the aseismic front. Until now, the surface of the horizontal flow from beneath a volcanic front to behind an aseismic front was assumed to lie in the lower layer of the lower crust. This is so in the case of thick crust like that of the Japanese Islands. In the case of a thin crust like oceanic crust, the mantle could not flow even at its top surface beneath such thin crust. In this case, the top surface of the convective flow lies within a surface layer of the mantle. Transport and accumulation of magma occurs within a surface layer that is several tens of kilometers thick. In this case, magma evolution in the chamber behind the aseismic front is restricted by the ambient peridotite that has abundant olivine crystals. Liquid compositions in chemical equilibrium with surrounding peridotite are already known through high pressure melting experiments. They are basaltic liquids under dry conditions, or andesitic liquids rich in MgO under hydrous conditions (Kushiro 1990). Such magmas may have a chance to erupt to the surface of islands on an outer arc of an embryonic arc-trench system, because the crust is so thin and uplift generates tensional stresses in the overlying crust. The occurrence of high-magnesian andesites on the Bonin Islands likely reflects this situation (see Lee et al. 2009).

8.6 Cretaceous Southwest Japan

At the end of this chapter, the geological correlation between the Cretaceous southwest Japan arc and the present northeast Japan arc is discussed.

The period between 120 and 50 million years ago was the time of the most violent igneous activity in the geological history of the Japanese Islands. Cretaceous volcanic activity is recorded as the Kanmon Group and its equivalent formations. These are volcanic successions with abundant andesitic materials, and are distributed in a belt that extends from north Kyushu to central Honshu in Japan for about 700 km (Fig. 8.2). In succession from the continental to the oceanic side, the geology on the Pacific Ocean side of this belt consists of Ryoke low P/T metamorphic belt with abundant granitic plutons, Sanbagawa high P/T metamorphic belt, and Jurassic and Cretaceous accretionary sedimentary complexes. Therefore, the Cretaceous trench is considered to have been present on the Pacific Ocean side of the volcanic belt.

The most representative volcanic rocks extruded from present arc volcanoes are andesites, and a boundary that limits the distribution of arc volcanoes toward the associated trench is a volcanic front. Therefore, the line that demarcates the distribution of the Kanmon Group and its equivalent formations toward the Pacific Ocean is a volcanic front in the Cretaceous. The broken line in Fig. 8.6 shows this Cretaceous volcanic front. It extends from north Kyushu to central Honshu for about 700 km. In addition to the Kanmon Group and its equivalents, Fig. 8.6 shows the Abu and Nouhi Groups and their equivalents, the San-in and Ryoke granitic plutons, the Ryoke low P/T metamorphic rocks, the Sanbagawa high P/T metamorphic rocks, and the Median Tectonic Line. The Abu and Nouhi Groups are volcanic successions made of dacitic to rhyodacitic lavas, pyroclastics, and related sediments. The Median Tectonic Line is the tectonic line that divides the geology of southwest Japan into an inner belt on the Japan Sea side and an outer belt on the Pacific Ocean side.

The thick volcanic successions comprising mainly dacitic materials are distributed on both sides of the Cretaceous volcanic front (Fig. 8.4). Granitic plutons have been intruded into these dacitic volcanic successions, and are widely distributed on both sides of the volcanic front within the inner belt of southwest Japan. However, their distribution is sharply demarcated by the Median Tectonic Line toward the Pacific Ocean (Fig. 8.4). Observing the geology from the north side of the islands toward the Median Tectonic Line, it can be seen that the dacitic volcanic successions quickly reduce in abundance and then disappear in a short distance after crossing the volcanic front, and conversely, granitic plutons rapidly increase in abundance. The zone between the point of this rapid increase of granitic plutons and the Median Tectonic Line almost corresponds to the Ryoke belt, which is characterized by an intimate association of the low P/T metamorphic rocks and granitic plutons, some of which are foliated.

This belt extends from north Kyushu to central Honshu in parallel with both the Cretaceous volcanic front and the Median Tectonic Line. The distance between the

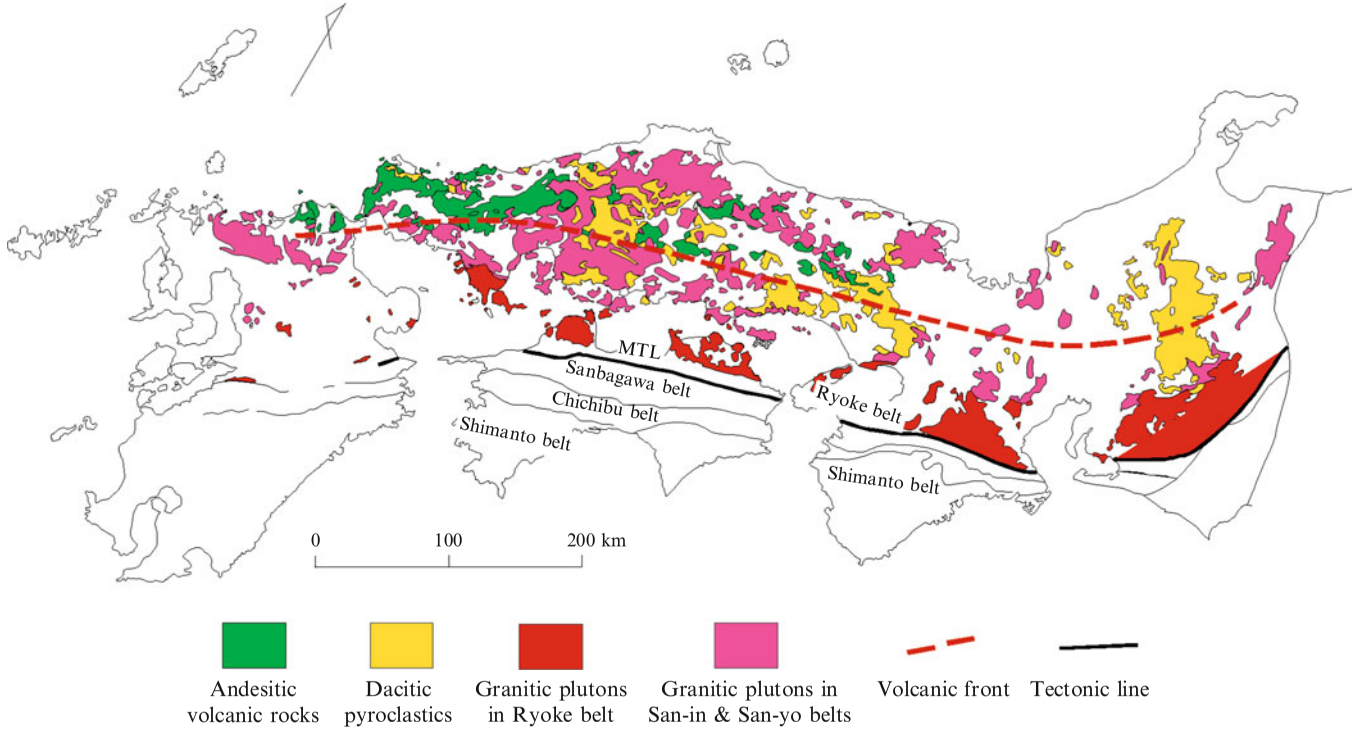

Fig. 8.6 Distribution of volcanic rocks and granitic plutons in Cretaceous Southwest Japan. *MTL* is Median Tectonic Line. Ryoke belt comprises Cretaceous low P/T metamorphic rocks and granitic plutons. Sanbagawa belt is made of high P/T metamorphic rocks. Chichibu belt represents Jurassic accretionary complexes, and Shimanto belt is made of Cretaceous and Paleogene accretionary complexes (Modified from Yanagi (1981))

volcanic front and the Median Tectonic Line is about 75 km. This distance is in accord with the distance between the volcanic front and the aseismic front in the present northeast Japan arc (Fig. 8.1). Therefore, based on the distance from the volcanic fronts, the Median Tectonic Line in southwest Japan corresponds in position to the aseismic front of Cretaceous time. The present aseismic front runs along the coastline on the Pacific Ocean side of the outer arc of the northeast Japan arc (Fig. 8.1). We have already discussed that the magma chamber forms behind the aseismic front, that the magma in the chamber evolves to dacite in composition, and that the accretionary sedimentary rocks around the chamber are metamorphosed to low P/T regional metamorphic rocks. Thus, the Ryoke low P/T metamorphic rocks and granitic plutons in the Ryoke belt behind the Median Tectonic Line are considered to represent the geology of an outer arc in the Cretaceous. In addition to this, the Median Tectonic Line seems to have been formed in order for the outer arc to be able to rise in response to development of granitic plutons. This would have separated outer arc crust from trench-side crust upon which fore-arc basins and the trench slope lie.

Based on the relationships so far presented between the model and arc topography and geology, it can be said that convection in the mantle prism beneath an island arc (Fig. 3.1) is one of the most fundamentally important requirements for understanding geological development of arc-trench systems. Furthermore, the Japanese Islands and the surrounding island arcs also can be said to represent diverse types and stages of development of arc-trench systems, and they present great opportunities to study how continental crust separates from the mantle.

References

Aramaki S (1965) Mode of emplacement of acid igneous complex (Kumano Acidic Rocks) in Southeastern Kii Peninsula. J Geol Soc Jpn 71:525–540 (In Japanese with English abstract)

Hasegawa A, Nakajima J, Uchida N, Okada T, Zhao D, Matsuzawa T, Umino N (2009) Plate subduction, and generation of earthquakes and magnas in Japan as inferred from seismic observations: an overview. Gond Res 16:370–400

Kushiro I (1990) Partial melting of mantle wedge and evolution of island arc crust. J Geophys Res 95:15929–15939

Lee C-T, Luffi P, Plank T, Dalton H, Leeman WP (2009) Constraints on the depths and temperatures of basaltic magma generation on Earth and other terrestrial planets using new thermobarometers for mafic magmas. Earth Planet Sci Lett 279:20–33

Machida H, Ota Y, Kawana T, Moriwaki H, Nagaoka S (2001) Kyushu/Ryukyu islands, topography of the Japanese islands, vol 7. Tokyo University Press, Tokyo, 355 p (In Japanese)

Suzuki S (1976) Lateral variation of P wave velocity in the upper mantle beneath Northeast Japan, as derived from travel time of earthquakes. Zisin (ii) 29:99–116 (In Japanese with English abstract)

Tanaka A, Yamano M, Yano Y, Sasada M (2004) Geothermal gradient and terrestrial heat flow database of the Japanese Islands and the circumference region. Chishistu (Geol) News, Geol Surv Japan 603:42–45 (In Japanese)

Utsu T (1971) Seismological evidence for anormalous structure of island arcs with special reference to the Japanese region. Rev Geophys Space Phys 9:839–890

Yanagi T (1981) Alternative magmatic process of continental growth in an island arc. Mem Fac Sci, Kyushu Univ Ser D 24:189–206
Yoshii T (1972) Features of the upper mantle around Japan as inferred from gravity anomalies. J Phys Earth 20:23–34
Yoshii T (1986) Basic geophysical data in the vicinity of the Japanese Islands. In: Taira T, Nakamura K (eds) Formation of Japanese islands. Iwanami, Tokyo, pp 102–107 (In Japanese)

Appendix

1. Basic equations used in Chap. 4 are presented here.

Equilibrium Partial Melting

C_{is}, C_{im}, and C_{ir} are concentrations of a minor element i in a solid source material, in the melt formed by partial melting from the source, and in the solid melting residue, respectively. D_i is a partition coefficient of the element i between the melt and the residue. It is defined as C_{ir}/C_{im}. F is a fraction of the melt produced by partial melting from the source material. When equilibrium is maintained between the melt and the coexisting residue, we have the following equation, since mass of the element is conserved:

$$C_{is} = C_{im}\{D_i(1-F)+F\}.$$

Fractional Crystallization

C_{ip}, C_{il}, and C_{ic} are concentrations of a minor element i in a parental liquid, in the residual liquid formed by fractional crystallization from the parent, and at the surface of the coexisting cumulate, respectively. The partition coefficient D_i is defined between the liquid and the cumulate surface and expressed as C_{ic}/C_{il}. F is a fraction of the residual liquid. When equilibrium is maintained between the liquid and the cumulate surface, we have the following equation, since mass of the element is conserved:

$$C_{il} = C_{ip}\,F^{(D_i-1)}$$

T. Yanagi, *Arc Volcano of Japan*, Lecture Notes in Earth Sciences 136,
DOI 10.1007/978-4-431-53996-4,

Crystallization in an Open-System Magma Chamber

C_{ip}, C_{il}, and C_{ic} are concentrations of a minor element i in a parental liquid, in the liquid in the chamber, and at the surface of the cumulate, respectively. The partition coefficient D_i is defined between the liquid and the cumulate surface and expressed as C_{ic}/C_{il}. In this case, the chamber is continuously, but very slowly supplied with the parental liquid, the crystallization continues in the chamber, and the cumulate is continuously removed from the chamber. When equilibrium is maintained between the liquid and the cumulate surface in the chamber, and the liquid mass in the chamber is kept constant, we have the following equation, since mass of the element is conserved:

$$\mathrm{R} = 1/D_i \log\left\{\left(C_{ip} - D_i \cdot C_{ip}\right)/\left(C_{ip} - D_i \cdot C_{il}\right)\right\},$$

where R is a ratio of the total mass of parental liquid supplied to the chamber compared with the liquid mass in the chamber.

Index